UNIVERSITÉ DE MONTRÉAL

COD "LOSS" IN ENHANCED BIOLOGICAL PHOSPHORUS REMOVAL SYSTEMS

REZA SALEHI

DÉPARTEMENT DES GÉNIES CIVIL, GÉOLOGIQUE ET DES MINES

ÉCOLE POLYTECHNIQUE DE MONTRÉAL

THÈSE PRÉSENTÉE EN VUE DE L'OBTENTION

DU DIPLÔME DE PHILOSOPHIAE DOCTOR

(GÉNIE CIVIL)

AVRIL 2016

UNIVERSITÉ DE MONTRÉAL

ÉCOLE POLYTECHNIQUE DE MONTRÉAL

Cette thèse intitulée :

COD "LOSS" IN ENHANCED BIOLOGICAL PHOSPHORUS REMOVAL SYSTEMS

présentée par : SALEHI Reza

en vue de l'obtention du diplôme de : Philosophiae Doctor

a été dûment acceptée par le jury d'examen constitué de :

M. BARBEAU Benoit, Ph. D., président

M. COMEAU Yves, Ph. D., membre et directeur de recherche

M. DOLD Peter L., Ph. D., membre et codirecteur de recherche

Mme DORNER Sarah, Ph. D., membre

M. PARKER Wayne, Ph. D., membre

DEDICATION

This thesis is dedicated to my family for their endless love, support and encouragement.

ACKNOWLEDGEMENTS

I express my deepest gratitude to my research supervisor, Professor Yves Comeau for his valuable support, useful advice, critical insight, continuous trust in me and his patience over the period of this research study.

I give my special thanks to my co-supervisor and the president of EnviroSim Associates Ltd., Peter Dold, for his encouragement, immense knowledge, valuable support and excellent guidance as well as his patience throughout this research.

I thank Professor Jalal Hawari and Dr. Marc-Andre Labelle for their help and valuable guidance.

Thanks also to Denis Bouchard, the technician in the environmental Lab for his endless assistance and technical support for my experimental system.

Melanie Bolduc, the technician in the environmental Lab, is thankfully acknowledged for her help with the laboratory procedures, safety concerns and ordering the chemicals needed over the period of this research.

I thank all my colleagues of the laboratory of Professor Yves Comeau for assistance and discussion over the period of this study. My research would not have been possible without their help.

Finally, thanks to my family who encouraged me to pursue my Ph.D. study in Canada and support me spiritually as always throughout this long period.

RÉSUMÉ

La validation des données observées provenant d'un procédé de traitement des eaux usées peut être réalisée en effectuant les bilans massiques en DCO et en azote. De faibles bilans massiques en DCO (environ 80%) ont été rapportés dans un certain nombre de cas pour les systèmes à boues activées incluant des zones non aérées.

L'objectif de cette recherche était d'évaluer rigoureusement les bilans de masse en DCO et en azote sous différentes conditions environnementales, consitutés de systèmes aérobie-aérobie (OX-OX), anoxie-aérobie (AX-OX) et anaérobie- aérobie (AN-OX), ce dernier étant utilisé pour la déphosphatation biologique des eaux usées et de proposer une explication à ce phénomène de faible bilan DCO.

Dans la première phase expérimentale (identifiée système OX-OX), un procédé de boues activées membranaire de taille laboratoire, constitué de deux réacteurs OX en série a été opéré à un temps de rétention des boues (TRB) de 10 jours et à une température de 20 °C à l'aide d'une eau usée synthétique contenant du citrate comme seule source de carbone. Des temps de rétention hydraulique (TRH) de 1,1 et 2,5 heures ont été appliqués pour le premier et le second réacteur, respectivement, et le rapport débit de recirculation sur celui de l'affluent (a) était de 4.5 L/L. De bons bilans massiques en DCO et en azote (101,4% et 101,3%, respectivement) ont été observés pour ce système.

Dans la deuxième phase expérimentale (identifiéesystème AX-OX), la condition du premier réacteur de la phase # 1 a été changée d'un état aérobie à un état anoxie. De plus, la concentration en DCO et d'azote de l'affluent a été d'ajustée pour s'assurer de maintenir une concentration de nitrate provenant de la recirculation dans le réacteur AX. Les données issues de cette phase ont présenté un bilan massique en DCO de 97%, ce qui est un peu inférieur à celui observé à la phase # 1 et un excellent bilan de masse d'azote d'environ 100%.

La troisième phase (identifiée système AN-OX) a été mise en place pour évaluer la possible perte de DCO en présence de conditions anaérobies. Par conséquent, le réacteur anoxie a été changé à des conditions anaérobies par ventilation de la phase gazeuse au-dessus du liquide avec de l'azote gazeux, et en diminuant la concentration d'azote de l'affluent et le débit de recirculation. Par rapport aux phases # 1 et 2, la concentration de phosphore de l'affluent a été augmentée de 20 à 50 mg P/L pour éviter toute limitation en phosphore pouvant résulter de la croissance des organismes accumulant le phosphore en excès de leurs besoins métaboliques, les

OAP. Cette phase a été divisée en deux phases principales # 3A et 3B selon le type de source de carbone utilisée. Le citrate, qui est une source de carbone fermentable, a été utilisé comme substrat pour la phase # 3A alors que la phase # 3B a été opérée à l'aide d'acétate, un substrat non fermentable.

Les données issues de la phase # 3A pour effectuer les bilans de masse ont été classées en sous-phases # 3A.1, 3A.2, 3A.3 et 3A.4 car il a été observé que les OAP on été actifs ou inactifs au cours de la phase # 3A.

Les phases # 3A.1 et 3A.3 fonctionnaient comme un système non déphosphatant avec des teneur en phosphore dans les boues d'environ 2,0% mg P/mg MVES (matières volatiles en suspension). Ces phases ont présenté un bilan massique en DCO entre 80% et 90%, et le bilan de masse d'azote était d'environ 100%.

Les phases # 3A.2 et 3A.4 fonctionnaient comme un système déphosphatant avec des teneur en phosphore dans les boues de 5% et 13% mg P/mg MVES, respectivement. Le bilan massique en DCO au cours de ces phases a varié entre 83% et 86% avec un bilan massique en azote de 100%. La principale raison pour la bonne élimination du phosphores dans la phase # 3A.4 était liée à une charge inférieure de oxygène et nitrate dans le réacteur AN par rapport à celle des phases # 3A.1 et 3A.3.

Lorsque la source de carbone a été changée de citrate à acétate (phase # 3B) les bilans massiques en DCO et en azote ont été d'environ 90% et 100%, respectivement, avec une teneur en phosphore dans les boues de 12% mg P/mg MVES.

Ces résultats suggèrent que la perte de DCO ne semble pas être reliée à l'élimination du phosphore. Les principaux mécanismes pouvant expliquer la perte de DCO observée pourraient être reliés à la fermentation résultant en la formation de composés volatils réduits sous conditions anaérobies dans le réacteur ou à l'intérieur de flocs microbiens. Ces composés incluent les acides gras volatils, l'hydrogène, l'anhydride sulfuré et le méthane qui pourraient être dégazés soit dans le réacteur non aéré ou à leur entrée dans le réacteur aérobie, un phénomène qu'il serait plus probable d'observer dans des réacteurs peu profonds tels qu'utilisés à l'échelle de laboratoire avec des transferts de gaz très inefficaces que dans des systèmes à pleine échelle.

Les résultats d'essais discontinus à différentes valeurs de pH ont révélé que l'aération et le mélange ont produit un dégazage négligeable d'acétate. La contribution de la production de méthane à la perte de DCO observée aété estimée à 0,05%. Le soufre a pu contribuer à une perte

de DCO (0,1-2,0%) lorsque le sulfate réduit dans le réacteur anaérobie n'a pas été réoxydé dans les conditions aérobies subséquentes. L'oxydation partielle du polyhydroxybutyrate-valérate (PHBV) qui pourrait survenir lors de la détermination analytique de la DCO a été démontrée négligeable. Les tentatives de mesure de la concentration d'hydrogène dissous dans le réacteur anaérobie ont indiqué que la production d'hydrogène n'a pas contribué à expliquer la perte de DCO observée (0 %). Les résultats d'essais discontinus ont montré que l'hydrogène a été facilement dégazé d'une colonne à bulles au laboratoire dans laquelle seulement 32% de la concentration théorique de saturation a pu être atteinte. Donc, l'hypothèse de la production d'hydrogène et dégazage demeure comme une cause potentielle pour expliquer une certaine perte de DCO. La perte de DCO en l'absence de source de carbone fermentable à l'affluent a été expliquée par le mécanisme de mort-régénération de la biomasse qui permet la production de substrat biodégradable pouvant être fermenté.

Cette recherche propose les équations requises pour effectuer le bilan massique en DCO sous différentes conditions environnementales.

Enfin, les résultats de cette recherche suggèrent que la perte de DCO proviendrait de la perte de substrats volatils et réduits produits par fermentation dans des systèmes à échelle laboratoire où la faible profondeur de liquide produit un artefact qui ne serait probablement pas observé de façon significative dans des réacteurs à pleine échelle.

ABSTRACT

Validation of observed data derived from a wastewater treatment process can be performed by conducting chemical oxygen demand (COD) and nitrogen (N) mass balances. Poor COD mass balances (about 80%) have been reported in a number of instances for activated sludge systems incorporating anaerobic zone.

The objective of this research was to evaluate rigorously the COD and N mass balances under different environmental conditions including aerobic-aerobic (OX-OX), anoxic-aerobic (AX-OX) and anaerobic-aerobic (AN-OX; as found in enhanced biological phosphorus removal (EBPR)) systems and to propose an explanation for this phenomenon.

In the first experimental phase (termed OX-OX system), a laboratory scale continuous flow system consisting of two OX reactors in series was operated at a sludge retention time (SRT) of 10 days and a temperature of 20 ^{o}C using a synthetic wastewater containing citrate as sole carbon source. A hydraulic retention time (HRT) of 1.1 and 2.5 hours applied for the first and second reactors, respectively, where the recycle-to-influent flow ratio (a) was 4.5 L/L. Good COD and N mass balances (101.4% and 101.3%, respectively) were observed on this system.

In the second experimental phase (termed AX-OX system), the condition of the first reactor of phase # 1 was switched from OX to AX. No more changes made compared to phase # 1 except that the influent COD and N concentrations were adjusted to provide enough nitrate concentration in the AX reactor. Data derived from this phase exhibited a COD mass balance of 97% which was a little lower than that observed in phase # 1 and an excellent N mass balance of approximately 100%.

The third phase (termed AN-OX system) was set up to evaluate the possible COD loss expected occurring in the presence of AN conditions. Therefore, the AX reactor was switched to AN conditions by flushing the head space with nitrogen gas, and by decreasing the influent nitrogen concentration and recycle flow rate. Compared to phases # 1 and 2, the influent phosphorus concentration was increased from 20 to 50 mg P/L to prevent any phosphorus limitation that could result from the growth of phosphate accumulating organisms (PAOs). This phase was divided into two main phases # 3A and 3B depending on type of carbon source used. Citrate which is a fermentable carbon source was used as substrate for phase # 3A whereas phase # 3B was operated using acetate, a non fermentable substrate.

The data derived from phase # 3A to perform the mass balances were categorized into sub-phases # 3A.1, 3A.2, 3A.3 and 3A.4 because it was observed that PAOs were active or non-active throughout phase # 3A.

Phases # 3A.1 and 3A.3 were operating as a non-EBPR system with sludge phosphorus content of about 2.0% mg P/mg VSS. These phases exhibited a COD mass balance ranging between about 80% and 90% where N mass balance averaged approximately 100%.

Phases # 3A.2 and 3A.4 were an EBPR system with a sludge phosphorus content of about 5% and 13% mg P/mg VSS. The COD mass balance during these phases ranged between 83% and 86% with a nitrogen mass balance of 100%. The main reason for good phosphorus removal in phase # 3A.4 was related to a lower oxygen and nitrate loading to the AN reactor compared to that in phases # 3A.1-3A.3.

When carbon source was changed from citrate to acetate (phase # 3B), the COD and N mass balances averaged about 90% and 100%, respectively, with a sludge phosphorus content of 12% mg P/mg VSS.

These findings suggested that the COD mass balance did not seem to be connected with phosphorus removal. The main possible mechanisms contributing to the observed COD loss was hypothesized to be due to fermentation resulting in the formation of reduced volatile compounds formed under AN conditions in the reactor or within microbial flocs (volatile fatty acids, methane, hydrogen sulfide, hydrogen) that are stripped either in the non aerated reactor or upon entering the OX reactor, a phenomenon expected more in shallow lab scale reactors with very inefficient gas transfer than full scale systems.

Batch tests results at different pH values revealed that aeration and mixing induced stripping of acetate was negligible. The contribution of methane production to the observed COD loss was as small as 0.05%. Sulfur was shown to contribute to the COD loss (0.1-2.0%) when the anaerobic sulfate reduced was not reoxidized under aerobic conditions. Partial oxidation of polyhydroxybutyrate-valerate (PHBV) that may occur under the COD test conditions was found to be negligible. Attempts to measure dissolved hydrogen concentration in the AN reactor indicated that hydrogen production did not contribute to explain the observed COD loss (0%). The result of a batch showed that hydrogen was easily stripped in a hydrogen bubble lab scale column in which no more than 32% of the saturation concentration could be achieved. Therefore, the hypothesis of hydrogen production and stripping remains as a likely potential cause to

explain some COD loss. Death-regeneration phenomenon was hypothesized as a possible explanation for some COD loss even in the absence of a fermentable influent carbon source because the consequence of death-regeneration is the production of biodegradable substrate that can be fermented.

This research proposes an useful equation to perform the COD mass balance under different environmental conditions. The results of this research suggest that COD loss from laboratory scale systems may be enhanced due to the shallow depth resulting in this phenomenon being a lab scale artefact that may not be observed in full scale deep reactors.

TABLE OF CONTENTS

LIST OF TABLES

LIST OF FIGURES

LIST OF SYMBOLS AND ABBREVIATIONS

a	Aerobic mixed liquor recycle ratio with respect to Q_{inf} (L/L)
AD	Anaerobic digestion process
ADM1	Anaerobic digestion model no. 1
AN	Anaerobic
AnS	Anaerobic stabilization
AO	Anaerobic-aerobic process
A^2O	Anaerobic-anoxic-aerobic process
APHA	American Public Health Association
ATP	Adenosine triphosphate
AX	Anoxic
Bardenpho	Barnard-denitrification-phosphorus process
BEPR	Biological excess phosphorus removal
BOD	Biochemical oxygen demand (mg O_2/L)
C_A*	Concentration of compound A in the bulk liquid in equilibrium with that in the bulk gas phase (mol/L)
$C_{A,i}$	Concentration of compound A at the liquid-gas interface (mol/L)
$C_{A,liquid}$	Concentration of compound A in the bulk liquid (mol/L)
COD	Chemical oxygen demand (mg COD/L)
D_A	Diffusivity coefficient of compound A ($cm^2.s^{-1}$)
DO	Dissolved oxygen concentration (mg O_2/L)
DO_{inf}	Influent DO concentration (mg O_2/L)
$DO_{mid,R1}$	DO concentration at midpoint during OUR test in reactor R1 (mg O_2/L)
$DO_{mid,R2}$	DO concentration at midpoint during OUR test in reactor R2 (mg O_2/L)
$DO_{sat.,clean\ water}$	Saturation DO concentration in clean water (mg O_2/L)
$DO_{sat.,used}$	Saturation DO concentration in the mixed liquor (mg O_2/L)
EBPR	Enhanced biological phosphorus removal
EPA	Environmental Protection Agency
F1	Influent organic solution
F2	Influent mineral solution
F3	Influent calcium-distilled water

$FCOD_{INPUT}$	Mass rate of total COD entering the system (mg COD/d)
$FCOD_{OUTPUT}$	Mass rate of total COD in the streams leaving the system plus total COD oxidized across the system (mg COD/d)
$FCOD_{oxid}$	Mass rate of total COD oxidized across the system (mg COD/d)
FID	Flame ionization detector
$FN_{NO3,denit}$	Mass rate of nitrate denitrified (mg N/d)
$FN_{NO3,inf}$	Influent nitrate mass rate (mg N/d)
$FN_{NO2,inf}$	Influent nitrite mass rate (mg N/d)
$FN_{NO3,input\ R1}$	Mass rate of nitrate entering reactor R1 (mg N/d)
$FN_{NO3,output\ R1}$	Mass rate of nitrate leaving reactor R1 (mg N/d)
$FN_{NO3,eff}$	Effluent nitrate mass rate (mg N/d)
$FN_{NO3,prod}$	Mass rate of nitrate produced (mg N/d)
$FN_{NO3,WAS}$	Mass rate of nitrate in the sludge wastage (mg N/d)
$FN_{NO2,eff}$	Nitrite effluent mass rate (mg N/d)
$FN_{NO2,WAS}$	Mass rate of nitrite in the sludge wastage (mg N/d)
$FN_{TKN,eff}$	Effluent TKN mass rate (mg N/d)
$FN_{TKN,inf}$	Influent TKN mass rate (mg N/d)
$FN_{TKN,WAS}$	Mass rate of TKN in the sludge wastage (mg N/d)
$FN_{TN,INPUT}$	Mass rate of TN entering the system (mg N/d)
$FN_{TN,OUTPUT}$	Mass rate of TN leaving the system (mg N/d)
FO_{air}	Mass rate of oxygen transferred to the reactor R2 (g O_2/L)
FO_{nit}	Mass rate of oxygen consumed for nitrification (mg COD/d)
$FO_{NO3,denit}$	Mass rate of oxygen equivalent of nitrate denitrified (mg COD/d)
FO_{OUR_B}	Mass rate of oxygen utilized by biomass (mg COD/d)
$FO_{OUR_{meas}}$	Measured OUR mass rate (mg COD/d)
$FO_{surface}$	Mass rate of oxygen entering reactor from the liquid surface (mg COD/d)
$FO_{streams\ entering\ R1}$	Mass rate of oxygen entering reactor R1 through the influent/recycle streams (mg COD/d)
$FO_{SO4\ reduc}$	Mass rate of oxygen equivalent of sulfate reduced (mg COD/d)
$FO_{sulfide\ oxid}$	Mass rate of oxygen consumed for sulfide oxidation (mg COD/d)
$FP_{TP,eff}$	Effluent TP mass rate (mg P/d)

$FP_{TP,inf}$	Influent TP mass rate (mg P/d)
$FP_{TP,WAS}$	Sludge wastage TP mass rate (mg P/d)
FS_{eff}	Mass rate of effluent soluble COD (mg COD/d)
FS_{WAS}	Mass rate of soluble COD in the sludge wastage (mg COD/d)
$FS_{T,eff}$	Effluent total COD mass rate (mg COD/d)
$FS_{T,inf}$	Influent total COD mass rate (mg COD/d)
$FS_{T,WAS}$	Mass rate of the total COD in the sludge wastage (mg COD/d)
$FSO_{4,input\ R1}$	Mass rate of sulfate entering reactor R1 (mg S/d)
$FSO_{4,output\ R1}$	Mass rate of sulfate leaving reactor R1 (mg S/d)
$FSO_{4\ reduc}$	Mass rate of sulfate reduced (mg S/d)
FX_{eff}	Mass rate of particulate COD in the effluent (mg COD/d)
FX_{WAS}	Mass rate of particulate COD in sludge wastage (mg COD/d)
$f_{va,aa}$	Fraction of valerate from amino acids in the ADM1
$f_{ac,aa}$	Fraction of acetate from amino acids in the ADM1
$f_{ac,su}$	Fraction of acetate from sugars in the ADM1
$f_{bu,aa}$	Fraction of butyrate from amino acids in the ADM1
$f_{bu,su}$	Fraction of butyrate from sugars in the ADM1
$f_{H2,aa}$	Fraction of H_2 from amino acids in the ADM1
$f_{H2,su}$	Fraction of H_2 from sugars in the ADM1
$f_{pro,aa}$	Fraction of propionate from amino acids in the ADM1
$f_{pro,su}$	Fraction of propionate from sugars in the ADM1
f_P	Organic phosphorus-to-VSS ratio in the sludge wastage (mg P/mg VSS)
f_{VT}	VSS-to-TSS ratio (mg VSS/mg TSS)
f_{CV}	Particulate COD-to-VSS ratio (mg COD/mg VSS)
GC	Gas chromatography
H_A	Henry's law constant of compound A (at.L. mol^{-1})
HFM	Hollow fiber membrane
HRT	Hydraulic retention time (h)
J_A	Volumetric mass transfer rate of compound A ($mol.L^{-1}.h^{-1}$)
JHB	Johannesburg process
k_La_{meas}	Oxygen mass transfer coefficient in clean water (h^{-1})

k_La_{used}	Oxygen mass transfer coefficient in the mixed liquor (h^{-1})
KHP	Potassium hydrogen phthalate
LCFA	Long chain fatty acids
MBR	Membrane bioreactor
MUCT	Modified UCT process
MWW	Municipal wastewater
N	Nitrogen
NADH	Reduced nicotinamide-adenine dinucleotide
NBS	New Brunswick Scientific
$N_{NO3,eff}$	Effluent nitrate concentration (mg N/L)
$N_{NO3,WAS}$	Sludge wastage nitrate concentration (mg N/L)
$N_{NO3,R1}$	Nitrate concentration in the reactor R1 (mg N/L)
$N_{NO3,R2}$	Nitrate concentration in the reactor R2 (mg N/L)
$N_{NO2,eff}$	Effluent nitrite concentration (mg N/L)
$N_{NO2,WAS}$	Sludge wastage nitrite concentration (mg N/L)
$N_{TKN,inf}$	Influent TKN concentration (mg N/L)
$N_{TKN,eff}$	Effluent TKN concentration (mg N/L)
$N_{TKN,WAS}$	Sludge wastage TKN concentration (mg N/L)
o-PO_4	Orthophosphate (mg P/L)
OTE	Oxygen transfer efficiency (%)
OUR_B	Biomass oxygen uptake rate (mg $O_2.L^{-1}.h^{-1}$)
OUR_{meas}	Measured oxygen uptake rate (mg $O_2.L^{-1}.h^{-1}$)
OX	Aerobic
P	Phosphorus
$P_{TP,eff}$	Effluent TP concentration (mg P/L)
$P_{TP,inf}$	Influent TP concentration (mg P/L)
$P_{TP,WAS}$	Sludge wastage TP concentration (mg P/L)
PAO	Phosphate accumulating organisms
PHA	Polyhydroxyalkanoates
PHB	Polyhydroxybutyrate
PHBV	Polyhydroxybutyrate valerate

Phoredox	Phosphorus reduction-oxidation process
PHV	Polyhydroxyvalerate
PP	Polyphosphate
Pres	Pressure (mmHg)
$p_{A,gas}$	Partial pressure of compound A in the bulk gas (atm)
$p_{A,i}$	Partial pressure of compound A at the liquid-gas interface (atm)
Q_{air}	Influent air flow rate (L/min)
Q_{eff}	Effluent flow rate (L/d)
Q_{inf}	Influent flow rate (L/d)
Q_r	Recycle flow rate (L/d)
Q_{WAS}	Sludge wastage flow rate (L/d)
R1	Reactor # 1
R2	Reactor # 2
RAS	Return activated sludge
RPC	Research and production council
rpm	Revolutions per minute
SBR	Sequencing batch reactor
$SO_{4,eff}$	Effluent sulfate concentration (mg S/L)
$SO_{4,inf}$	Influent sulfate concentration (mg S/L)
$SO_{4,R1}$	Sulfate concentration in the reactor R1 (mg S/L)
$SO_{4,R2}$	Sulfate concentration in the reactor R2 (mg S/L)
SRO	Sulfate reducing organisms
SRT	Sludge retention time (d)
S_{aa}	Amino acids concentration in the ADM1
S_{ac}	Acetate concentration in the ADM1
S_B	Soluble readily biodegradable substrate
S_{bu}	Butyrate concentration in the ADM1
S_{CH4}	Methane concentration in the ADM1
S_{eff}	Effluent soluble COD concentration (mg COD/L)
S_{fa}	Long chain fatty acids concentration in the ADM1
S_{H2}	Hydrogen concentration in the ADM1

S_{pro}	Propionate concentration in the ADM1
S_{su}	Monosaccharide concentration in the ADM1
$S_{T,inf}$	Influent total COD concentration (mg COD/L)
$S_{T,r}$	Total COD concentration in the recycle stream (mg COD/L)
$S_{T,R1}$	Total COD concentration in the reactor R1 (mg COD/L)
$S_{T,WAS}$	Sludge wastage total COD concentration (mg COD/L)
S_U	Soluble unbiodegradable organics
S_{va}	Valerate concentration in the ADM1
S_{WAS}	Soluble COD concentration in sludge wastage (mg COD/L)
T	Temperature (^oC)
ThOD	Theoretical oxygen demand (mg O_2/L)
TKN_{inf}	Influent total Kjeldahl nitrogen (mg N/L)
TN	Total nitrogen (mg N/L)
TP	Total phosphorus (mg P/L)
TSS	Total suspended solids (mg TSS/L)
UCT	University of Cape Town process
VCs	Volatile compounds
VFAs	Volatile fatty acids
VIP	Virginia initiative plant process
V_R	Reactor volume (L)
VSS	Volatile suspended solids (mg VSS/L)
vvm	Gas flow per unit of liquid volume per minute ($L.L^{-1}.min^{-1}$)
WAS	Waste activated sludge
WRRF	Water resource recovery facility
w_{O2}	Oxygen mass fraction in air (%g/g)
X_B	Slowly biodegradable substrate
X_C	Composite concentration in the ADM1
X_{ch}	Carbohydrates concentration in the ADM1
X_{eff}	Effluent particulate COD concentration (mg COD/L)
X_H	Active heterotrophic biomass
X_I	Unbiodegradable organics

X_{li}	Lipids concentration in the ADM1
X_{pr}	Proteins concentration in the ADM1
X_U	Particulate unbiodegradable organics
X_{WAS}	Particulate COD concentration in sludge wastage (mg COD/L)
Y_{aa}	Yield of amino acids uptake in the ADM1
Y_{ac}	Yield of acetate uptake in the ADM1
Y_{bu}	Yield of butyrate uptake in the ADM1
Y_{fa}	Yield of LCFAs uptake in the ADM1
Y_{H2}	Yield of H_2 uptake in the ADM1
Y_{OBS}	Observed yield coefficient (gCOD/g COD or g VSS/g COD)
Y_{pro}	Yield of propionate uptake in the ADM1
Y_{su}	Yield of sugars uptake in the ADM1
Y_{va}	Yield of valerate uptake in the ADM1
α	k_La correction factor
β	DO_{sat} correction factor
ρ_{air}	Air density (g/L)

LIST OF APPENDICES

CHAPTER 1 INTRODUCTION

1.1 Introduction

Enhanced biological phosphorus removal (EBPR) process is a modification of the activated sludge process in which activated sludge biomass is subjected to an alternating anaerobic (AN)-aerobic (OX) condition. An AN condition is one in which neither dissolved oxygen (DO) nor nitrite (NO_2^-)/nitrate (NO_3^-) are present while DO is present as an electron acceptor in the OX one. EBPR process is preferred over the chemical phosphorus removal processes in which the excess sludge enriched with the chemical precipitates leading to extra costs for the sludge treatment.

The efficiency of an EBPR process is linked to the growth of polyphosphate accumulating organisms (PAOs) that can uptake volatile fatty acids (VFAs) (present in the wastewater or generated through fermentation reaction) under AN condition. These organisms are capable of accumulating phosphorus in amounts greater than that typically required for the nutritional growth. Phosphorus content captured in the sludge of enhanced cultured EBPR system operated by Wentzel et al. (1989) ranged between 0.32 to 0.38 g phosphorus per g volatile suspended solids (VSS).

Research on the EBPR process became an interesting topic for environmental engineers from the moment the results of Lan et al. (1983) towards phosphorus removal in an AN-OX system revealed an indirect disappearance of chemical oxygen demand (COD) under AN conditions. Later, it was reported that the oxygen requirement in the OX reactor which was preceded by an AN reactor was approximately 30% less than that for a conventional activated sludge system (Bordacs and Tracy, 1988). These findings stimulated the thinking of researchers to pay serious attention to the COD mass balance on activated sludge systems.

Evaluation of COD mass balance on different types of activated sludge system (strictly OX and unaerated-OX conditions) operated in a range of operational parameters and wastewater characteristics conducted by Barker and Dold (1995). Their findings revealed that the OX and AX-OX systems present COD mass balances close to 100% while it ranged between about 80% (with municipal wastewater as substrate) and 90% (with acetate) for the systems incorporating AN reactors. This means that up to 20% of the daily mass of influent COD cannot be accounted

for in the sludge wastage/effluent or in the mass of COD oxidized across the system (termed COD "loss"). The authors suggested that the reason for the COD loss was the release of gaseous fermentation products from the system under OX condition.

Investigation of COD loss in laboratory and pilot plant scale EBPR systems performed by Randall et al. (1992) showed that a COD loss ranging between 0% and about 50% depending on the nature and strength of substrate. They stated that the possible mechanism explaining the COD loss while using dextrose as substrate was connected with metabolism by fermenting organisms (not PAOs). Although most of authors suggested that the observed COD loss occurring under AN condition was associated with the fermentation reactions, negligible amount of hydrogen has been reported either in the mixed liquor or in the off-gas of the AN reactor (Erdal et al., 2005; Wable and Randall, 1992; Wable and Randall; 1994).

A major consequence of COD loss in activated sludge system is a reduction in both sludge production and oxygen requirements (Barker and Dold, 1996). Since operating costs for activated sludge system is potentially connected with sludge production and oxygen requirements, understanding the mechanism and potential causes of COD loss would make it possible to design the activated sludge processes in the way leading to a decrease in operating costs.

1.2 Body of the thesis

The second chapter presents a literature review on phosphorus removal process followed by anaerobic digestion (AD) processes and gas transfer in biological systems. In addition, it provides a comprehensive overview of the findings of researchers associated with the COD and nitrogen (N) mass balances on the activated sludge systems operated under either aerated (OX) or un-aerated (AX/AN) conditions using various substrates. This chapter also presents the factors influencing the COD mass balance and the possible mechanisms contributing to the COD loss which has been under investigation by researchers for many years. The last part of Chapter 2 deals with theoretical considerations including equations needed to perform COD, nitrogen (N) and phosphorus (P) mass balances for phases of this research. The hypotheses and objectives are presented in Chapter 3.

The materials and methods chapter (Chapter 4) specifies the composition of the synthetic wastewater used, experimental equipments, configuration and system operation. It is then followed by the measurement techniques for determination of the parameters required.

Results and discussion are given in Chapter 5 which is followed by Chapter 6 presenting the conclusions and recommendations.

A time schedule describing when operation of each phase started and when the mass balances performed provided in Appendix A. The Appendix B presents the data set and detailed calculations of COD, N and P mass balances. The list of equations/reactions is given in Appendix C.

CHAPTER 2 LITERATURE REVIEW

2.1 Phosphorus removal process

Phosphorus (P) is a common nutrient in wastewater and should be eliminated or diminished prior to discharge to water bodies, especially freshwater ones, because of eutrophication problems. It is non-volatile and cannot be removed from the wastewater through transferring to the gaseous phase. Therefore, it should be initially converted to a particulate form (Cheremisinoff, 1994).

The first strategies were established based on the addition of the chemical coagulants such as lime, alum or ferric chloride. This method (termed chemical phosphorus removal), can remove up to 95% of phosphorus but it suffers the two main disadvantages of high costs of coagulants and production of large amount of sludge (Johansson, 1994; Brett, 1997). Enhanced biological phosphorus removal (EBPR) offers an alternative and more "ecological" approach.

A distinction first needs to be made between aerobic (OX), anoxic (AX) and anaerobic (AN) conditions because EBPR processes are typically configured as an AN-OX (AO) or AN-AX-OX (A^2O) reactor system. The distinction between AX and AN conditions is not made by microbiologists but is made by environmental engineers.

- An OX condition is one in which dissolved oxygen (DO) is present as an electron acceptor.
- An AX condition is one in which nitrite or nitrate (NO_2^- or NO_3^-) is present but DO is absent.
- An AN condition is one in which neither DO nor NO_2^-/NO_3^- are present. AN condition favor the activity of EBPR, sulfate reducing, fermenting and methanogenic organisms.

An AN reactor may exhibit mainly AN condition activities but may also have some AX/OX condition activities due to influent or sludge recirculation adding some DO or oxidized nitrogen. Such varied conditions may take place in the bulk liquid or inside biological flocs or granules.

2.1.1 Enhanced Biological Phosphorus Removal (EBPR)

EBPR activities were first reported by Srinath et al. (1959). They observed that the sludge taken from OX reactor contained an excessive amount of phosphorus which was higher than for nutritional requirements. This process later was called the EBPR process. Experimental observations from full scale water resource recovery facilities (WRRFs) and batch tests showed phosphorus release under AN and uptake under OX conditions (Levin and Shapiro, 1965). They

also suggested that phosphorus uptake was distinctly a biological process because in the presence of inhibitors such as 2,4-dichlorophenoxyacetic acid (a pH greater than 9), phosphorus was not taken up. It was proposed that one of the necessary requirements was the presence of an AN reactor in which the return sludge and wastewater are fed (Barnard, 1974; 1975 and Nicholls, 1975). On the basis of this proposition, various configurations for EBPR process have been experimentally examined and implemented in WRRFs around the world. An initial study regarding the direct relation between phosphorus release and uptake was done by Rensink (1981) and then biochemical models were developed (Comeau et al., 1986; Wentzel et al., 1986; Mino et al., 1987).

In the AN reactor, volatile fatty acids (VFAs) are taken up by phosphate accumulating organisms (PAOs) in the form of polyhydroxyalkanoates (PHAs) resulting in phosphorus release in the bulk liquid. Then, in the OX reactor, PAOs utilize the accumulated PHAs for growth and to store phosphate as polyphosphates intracellularly. Since phosphorus uptake rate in OX reactor is greater than the release in the AN reactor, phosphorus is removed from the system through the sludge wastage (Mino et al., 1998; Yang et al., 2013; Oehmen et al., 2007; Kristiansen et al., 2013; Muszynski et al., 2013). A schematic diagram of the metabolic process taking place in AN and OX/AX conditions by PAOs is illustrated in Figure 2.1.

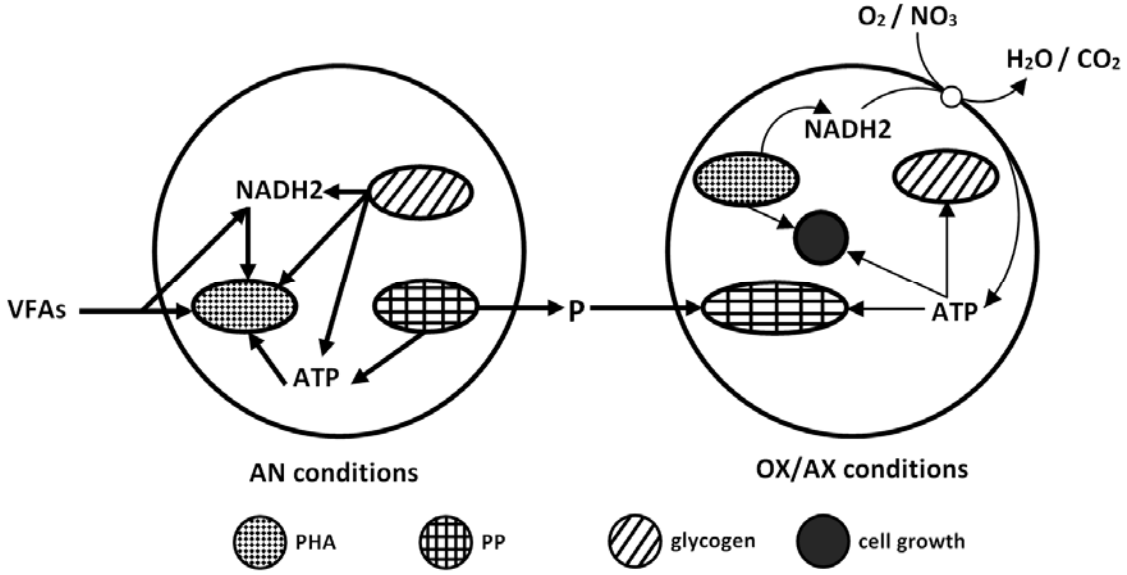

Figure 2-1: Metabolic processes occurring in AN and OX/AX conditions by PAOs (adapted from Yuan et al., 2012).

Note: VFAs: volatile fatty acids; NADH2: reduced nicotinamide-adenine dinucleotide;

ATP: adenosine triphosphate; PP: polyphosphate.

2.1.2 EBPR process configurations

A simple configuration for an EBPR process is composed of two reactors in series followed by a final clarifier. The first reactor is operated under AN condition and the second one is an OX reactor. The activated sludge from the final clarifier is returned to the AN reactor (termed AO system, Figure 2.2).

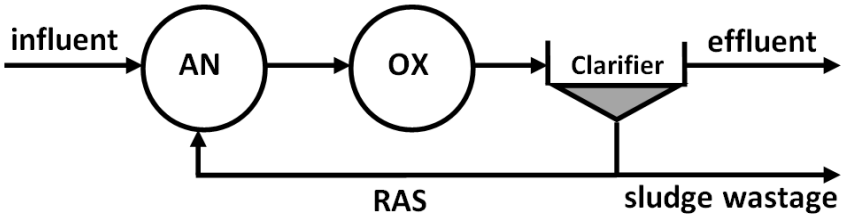

Figure 2-2: EBPR process (AO system) (adapted from van Haandel and van de Lubbe, 2007).

Note: RAS: return activated sludge

Since nitrification takes place in the OX reactor, introduction of NO_3^- in the AN reactor is unavoidable. Consequently, phosphorus removal efficiency is negatively affected because the availability of readily biodegradable matter for PAOs growth is reduced.

Various configurations for biological phosphorus removal have been developed in order to minimize the introduction of NO_3^- in AN reactor (Figure 2.3). A review of the different configurations (such as phosphorus reduction oxidation (Phoredox), Barnard-denitrification-phosphorus (Bardenpho), PhoStrip, Johannesburg (JHB), Virginia initiative plant (VIP), University of Cape Town (UCT), modified UCT (MUCT), etc.) can be found in Comeau (1990).

In this study, an AO system for biological phosphorus removal was used. Since OX reactor was a membrane bioreactor (MBR), no final clarifier was used and activated sludge recirculated from the OX to the AN one.

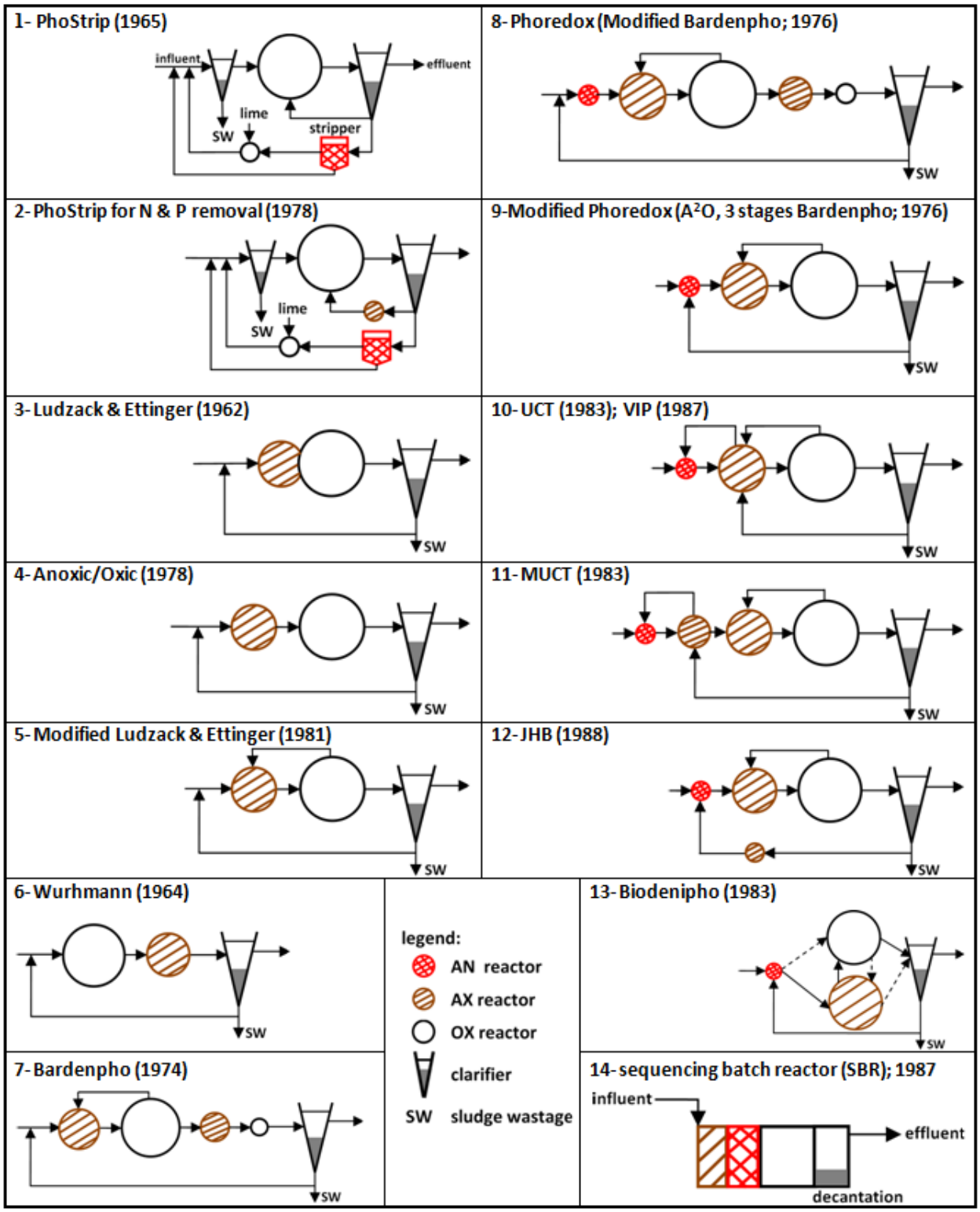

Figure 2-3: EBPR process configurations (adapted from Comeau, 1990)

2.1.3 Sludge phosphorus content

Sludge phosphorus content in activated sludge processes is ranged typically between 0.015 and 0.020 g P per g volatile suspended solids (VSS) (Cretu and Tobolcea, 2005). A number of experimental observations showed that the sludge phosphorus content varies between 0.08 and 0.20 g P per g VSS depending on the type of carbon source, influent chemical oxygen demand (COD) to total phosphorus (TP) ratio and the operation conditions (Appeldoorn et al., 1992; Mino et al., 1998; Wang et al., 2002b). The sludge of enhanced cultured EBPR systems operated by Wentzel et al. (1989), however, contained as much as 0.32 to 0.38 g P per g VSS. A value of 0.38 g P per g VSS for the aerobic sludge of enhanced sequencing batch reactor (SBR) system was also reported by Copp (1998).

2.2 Anaerobic digestion (AD) processes

Under AN conditions, a wide variety of microorganisms are involved in breaking down the organic matter into soluble substances and gases such as methane (CH_4), carbon dioxide (CO_2), hydrogen (H_2) and hydrogen sulfide (H_2S) through steps that are categorized as follows.

2.2.1 Disintegration

Disintegration is a non-biological process in which the cell walls are physically or chemically broken down to release intracellular substances. The end products of this stage are carbohydrates, proteins, lipids and particulate/soluble unbiodegradable organics (Figure 2.4, stage A). The description of the symbols used in Figure 2.4 is presented in Table 2.1 (adapted from Batstone et al., 2002).

2.2.2 Hydrolysis

High molecular weight organics produced by disintegration cannot be directly utilized by microorganisms. Thus, hydrolysis (Figure 2.4, stage B) is needed to break them down into soluble compounds such as monosaccharides, amino acids and long chain fatty acids (LCFAs) that are further processed by acidogenic bacteria (Mitchell and Gu, 2010). According to the death-regeneration concept proposed by Dold et al. (1980), heterotrophic biomass (X_H) is split into slowly biodegradable (X_B) and inert (X_I) substances where X_B is then hydrolyzed into readily biodegradable matter (S_B) (Figure 2.5).

2.2.3 Acidogenesis/acetogenesis

The acidogenesis process is performed by a group of microorganisms that are identified as acidogens by which monosaccharides and amino acids are converted to VFAs (such as acetate, propionate, butyrate and valerate) and H_2. Since VFAs, except acetate, cannot be utilized by methanogenic bacteria, acetogenesis is the next stage to transform the VFAs to acetate (Figure 2.4, stage C/D) (Stams, 1994; Schink, 2002). H_2 production in AD processes results from both the acidogenesis and the acetogenesis stages.

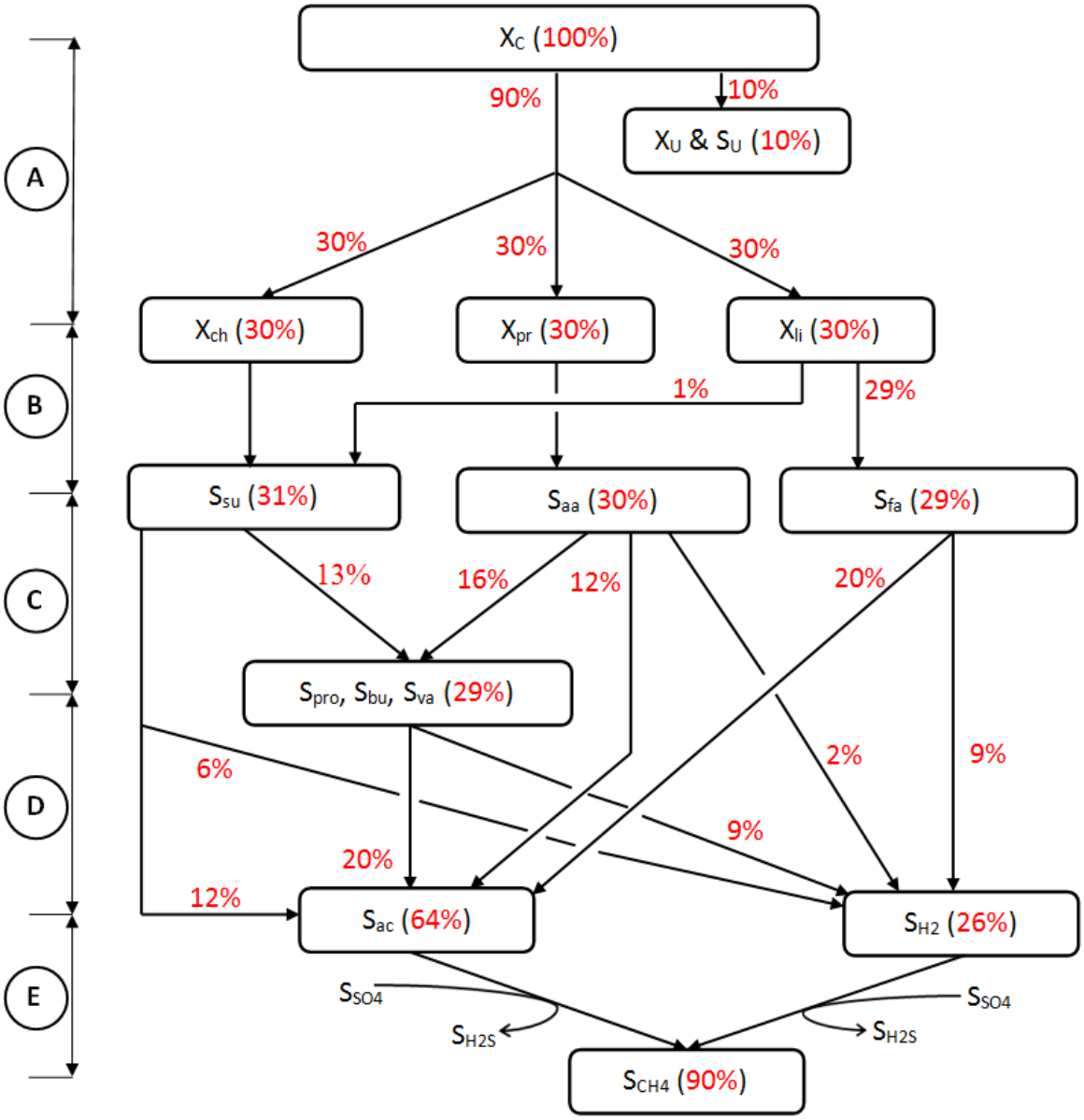

Figure 2-4: Anaerobic conversion of complex organic matter

(adapted from Batstone et al., 2002).

Note: The percentages are regarded as approximate values

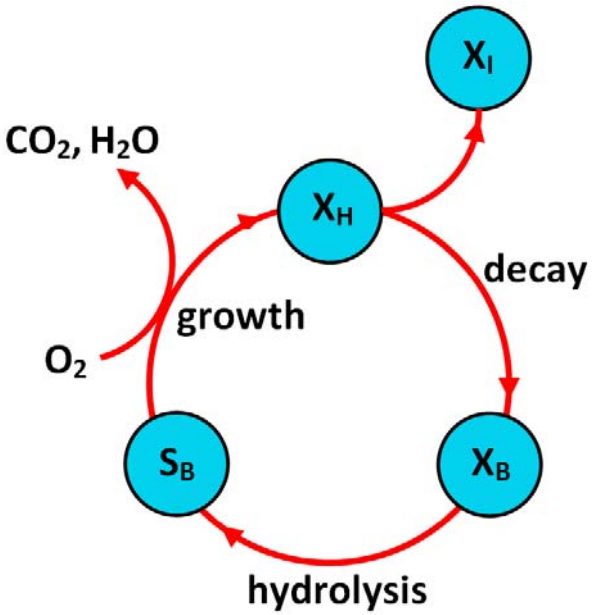

Figure 2-5: Death-regeneration concept for the activated sludge process

(adapted from Dold et al., 1980)

Table 2-1: Description of symbols used in Figure 2.4 (adapted from Batstone et al., 2002)

Compound		Conversion stage	
Symbol	Description	Symbol	Description
X_C	Composite	A	Disintegration
X_U	Particulate unbiodegradable organics	B	Hydrolysis
S_U	Soluble unbiodegradable organics	C	Acidogenesis
X_{ch}	Carbohydrates	D	Acetogenesis
X_{pr}	Proteins	E	Methanogenesis/Sulfidogenesis
X_{li}	Lipids		
S_{su}	Monosaccharides		
S_{aa}	Amino acids		
S_{fa}	LCFAs		
S_{pro}	Propionate		
S_{bu}	Butyrate		
S_{va}	Valerate		
S_{ac}	Acetate		
S_{H2}	Hydrogen		
S_{CH4}	Methane		
S_{SO4}	Sulfate		
S_{H2S}	Hydrogen sulfide		

According to the AD model no. 1 (ADM1), the processes resulting in H_2 production are listed in Table 2.2 and schematically illustrated in Figure 2.6.

H_2 can be generated either directly from the degradation of monosaccharides/amino acids/LCFAs or indirectly via the degradation of VFAs produced (Figure 2.6). Since acetate is not fermented to H_2, it is not shown in Figure 2.6.

The description of symbols used in Table 2.2 and Figure 2.6 are presented in Table 2.3 which also presents the values suggested for stoichiometric coefficients of components generated through H_2 production using different types of substrate.

Table 2-2: ADM1 matrix (only processes resulting in H_2 production presented; adapted from Batstone et al., 2002)

Component i →	S_{su}	S_{aa}	S_{fa}	S_{va}	S_{bu}	S_{pro}	S_{ac}	S_{H2}
↓ **Process**	(g COD/l)	(g COD/l)	(g COD/l)	(g COD/l)	(g COD/l)	(g COD/l)	(g COD/l)	(g COD/l)
Monosaccharides uptake	-1				$(1-Y_{su}) \times f_{bu,su}$	$(1-Y_{su}) \times f_{pro,su}$	$(1-Y_{su}) \times f_{ac,su}$	$(1-Y_{su}) \times f_{H2,su}$
Amino acids uptake		-1		$(1-Y_{aa}) \times f_{va,aa}$	$(1-Y_{aa}) \times f_{bu,aa}$	$(1-Y_{aa}) \times f_{pro,aa}$	$(1-Y_{aa}) \times f_{ac,aa}$	$(1-Y_{aa}) \times f_{H2,aa}$
LCFAs uptake			-1				$0.70 \times (1-Y_{fa})$	$0.30 \times (1-Y_{fa})$
Valerate uptake				-1		$0.54 \times (1-Y_{va})$	$0.31 \times (1-Y_{va})$	$0.15 \times (1-Y_{va})$
Butyrate uptake					-1		$0.80 \times (1-Y_{bu})$	$0.20 \times (1-Y_{bu})$
Propionate uptake						-1	$0.57 \times (1-Y_{pro})$	$0.43 \times (1-Y_{pro})$

Si : concentration of soluble compound (i);

su: Monosaccharides; aa: Amino acids; fa: LCFAs; va: valerate;

bu: butyrate; pro: propionate; ac: acetate; H_2: hydrogen

Table 2-3: Values suggested for stoichiometric coefficients of components associated with H_2 production processes according to ADM1 (adapted from Batstone et al., 2002)

Symbol	Description	Value	Units
$f_{bu,su}$	fraction of butyrate from sugars	0.13	g COD/g COD
$f_{pro,su}$	fraction of propionate from sugars	0.27	g COD/g COD
$f_{ac,su}$	fraction of acetate from sugars	0.41	g COD/g COD
$f_{H2,su}$	fraction of H_2 from sugars	0.19	g COD/g COD
$f_{va,aa}$	fraction of valerate from amino acids	0.23	g COD/g COD
$f_{bu,aa}$	fraction of butyrate from amino acids	0.26	g COD/g COD
$f_{pro,aa}$	fraction of propionate from amino acids	0.05	g COD/g COD
$f_{ac,aa}$	fraction of acetate from amino acids	0.40	g COD/g COD
$f_{H2,aa}$	fraction of H_2 from amino acids	0.06	g COD/g COD
Y_{su}	yield of sugars uptake	0.10	g COD/g COD
Y_{aa}	yield of amino acids uptake	0.08	g COD/g COD
Y_{fa}	yield of LCFAs uptake	0.06	g COD/g COD
Y_{va}	yield of valerate uptake	0.06	g COD/g COD
Y_{bu}	yield of butyrate uptake	0.07	g COD/g COD
Y_{pro}	yield of propionate uptake	0.04	g COD/g COD
Y_{ac}	yield of acetate uptake	0.05	g COD/g COD
Y_{H2}	yield of H_2 uptake	0.06	g COD/g COD

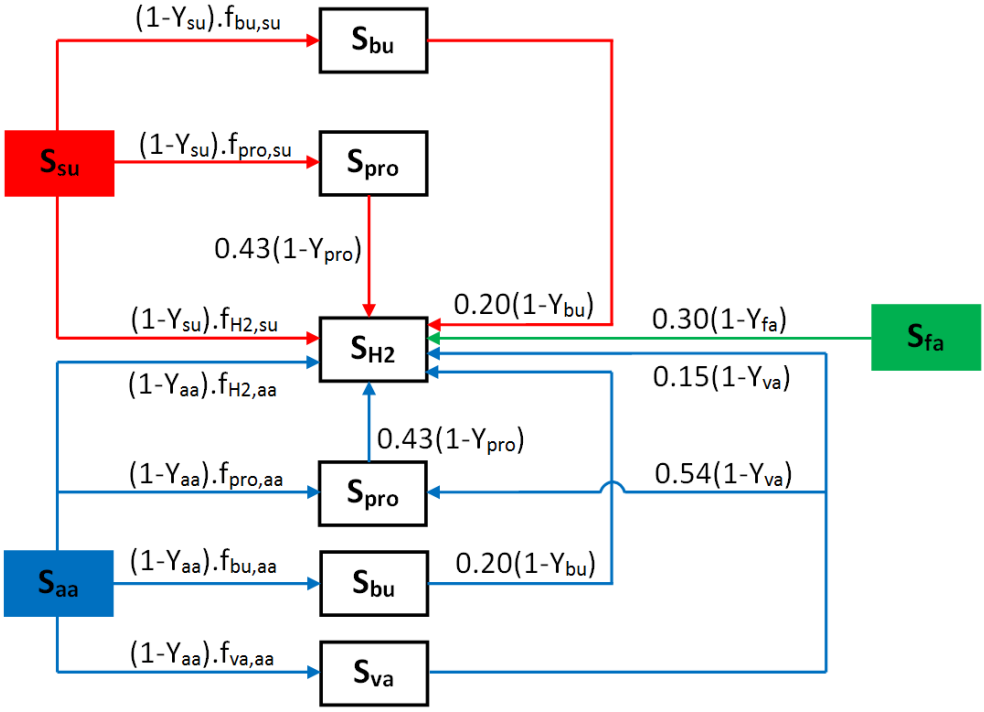

Figure 2-6: Schematic illustrating the different conversion pathways that involve in H_2 production through AD processes (adapted from Batstone et al., 2002)

The following yields can be calculated from the values reported in Table 2.3 and Figure 2.6.

- yield of H_2 produced from 1 g COD-propionate = $0.43 \times (1\text{-}Y_{pro}) = 0.41$ g COD-H_2

- yield of H_2 produced from 1 g COD-butyrate = $0.20 \times (1\text{-}Y_{bu}) = 0.19$ g COD-H_2

- yield of H_2 produced from 1 g COD-valerate = $0.15 \times (1\text{-}Y_{va}) + 0.54 \times (1\text{-}Y_{va}) \times 0.43 \times (1\text{-}Y_{pro})$ = 0.35 g COD-H_2

- yield of H_2 produced from 1 g COD-amino acids = $(1\text{-}Y_{aa}) \times f_{H2,aa} + (1\text{-}Y_{aa}) \times f_{va,aa} \times 0.15 \times (1\text{-}Y_{va}) + (1\text{-}Y_{aa}) \times f_{bu,aa} \times 0.20 \times (1\text{-}Y_{bu}) + ((1\text{-}Y_{aa}) \times f_{pro,aa} + (1\text{-}Y_{aa}) \times f_{va,aa} \times 0.54 \times (1\text{-}Y_{va})) \times 0.43 \times (1\text{-}Y_{pro}) = 0.19$ g H_2-COD

- yield of H_2 produced from 1 g COD-sugars = $(1\text{-}Y_{su}) \times f_{H2,su} + (1\text{-}Y_{su}) \times f_{bu,su} \times 0.20 \times (1\text{-}Y_{bu}) + (1\text{-}Y_{su}) \times f_{pro,su} \times 0.43 \times (1\text{-}Y_{pro}) = 0.29$ g COD-H_2

- yield of H_2 produced from 1 g COD-LCFA = 0.30 × (1-Y_{fa}) = 0.28 g COD-H_2

2.2.4 Methanogenesis

Methanogenesis in the last stage of the AD processes (Figure 2.4, stage E). Methanogens are anaerobic microorganisms consuming acetate and H_2 produced through acidogenesis and acetogenesis, respectively, and converting them to CH_4. About 70% of the CH_4 produced comes from the acetoclastic process and the rest from the hydrogenotrophic process (using H_2 and CO_2) (Batstone et al., 2002).

2.2.5 Sulfate reduction

Sulfate (SO_4^{2-}) is present in domestic wastewater at an average concentration of 10 mg SO_4^{2-}-S/L (Tchobanoglous et al., 2003) but industries that use sulfuric acid in their processes can increase this concentration in municipal wastewaters (MWW) to 100 mg SO_4^{2-}-S/L (Singh and Viraraghavan, 1998). Sulfate removal from wastewater can be achieved by precipitation with barium salts, for example, but the most common and economical method is by sulfate reduction. Sulfate reducing organisms (SRO) utilize SO_4^{2-} as electron acceptor and generate sulfide. The electrons needed for SO_4^{2-} reduction are provided from an organic substrate such as acetate and H_2 (Figure 2.4, stage E).

2.2.5.1 Fate of reduced sulfur produced by SRO

The reduced sulfur forms in a SO_4^{2-} reducing process are hydrogen sulfide (H_2S), bisulfide (HS^-) and sulfide ion (S^{2-}). H_2S dissociates into HS^- and S^{2-} according to the equilibrium reactions (2.1) and (2.2) (Chen, 1970).

$$H_2S \leftrightarrow H^+ + HS^- \qquad pKa1 = 6.97 \text{ to } 7.06 \quad (\text{at } 25°C) \tag{2.1}$$

$$HS^- \leftrightarrow H^+ + S^{2-} \qquad pKa2 = 12.35 \text{ to } 15.0 \quad (\text{at } 25°C) \tag{2.2}$$

The dominance of sulfide species in solution containing sulfide depends on the pH. For example, at a pH value of 7.4, 28% of total sulfide is in the H_2S form and the portion remaining (72%) is as HS^- with less than 0.001% being as S^{2-} (Li and Lancaster, 2013).

The produced sulfide is subjected to reactions of precipitation, emission and re-oxidation as schematically illustrated in Figure 2.7.

Sulfide precipitation by metal salts

The dissolved sulfide can react with metal salts such as ferrous ion (Fe^{2+}) to form a ferrous sulfide (FeS) precipitate according to reaction (2.3). This reaction is used as a strategy to prevent the emission of H_2S in sewer systems (Nielsen et al., 2008) and in anaerobic digesters.

$$Fe^{2+} + HS^{-} \rightarrow FeS\downarrow + H^{+} \quad (2.3)$$

- *Sulfide emission/oxidation*

H_2S may be stripped from the liquid into the gas phase due to mechanical mixing and aeration. Sulfide can be re-oxidised to SO_4^{2-} by aeration.

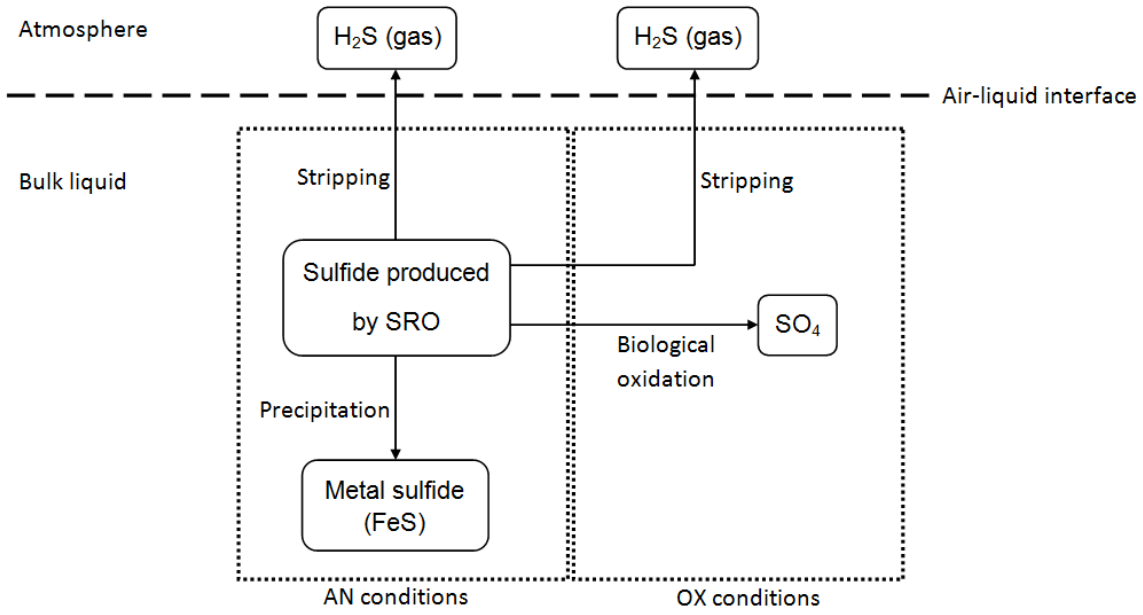

Figure 2-7: Schematic illustration of the fate of sulfide produced by SRO

(adapted from Zhang et al., 2008)

2.3 Gas transfer in biological processes

Mass transfer is the net movement of molecules from one phase to another according to a concentration gradient. In a gas-liquid system, gas molecules can cross the interface until

equilibrium conditions are attained which is when the rate of transfer of gas molecules from the gas to liquid phase equals to that from the liquid to gas phase (Figure 2.8).

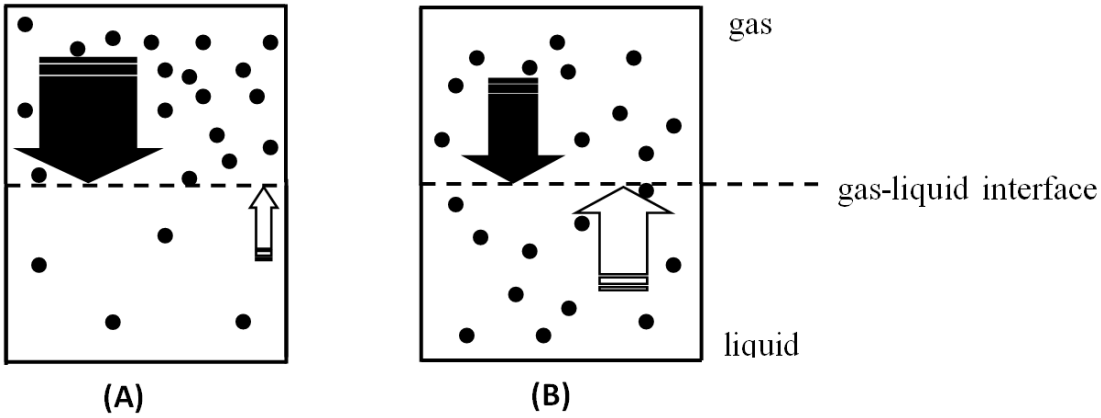

Figure 2-8: Schematic representation of the movement of gas molecules in a liquid-gas system with (A) unsaturated liquid phase and (B) saturated liquid phase (adapted from von Sperling, 2007)

Oxygen transfer into solution by aeration represents a significant part of the operating costs of WRRFs, notably due to the limited capacity of water to dissolve oxygen. Conversely, in an anaerobic digester, degassing of volatile compounds (VCs), such as CH_4, CO_2 and H_2S, is a central part of the process.

A schematic diagram illustrating the profile of concentrations for transfer from the liquid to gas phase assuming that the rate of mass transfer is controlled by the resistance of the liquid film shown in Figure 2.9. In this case, the transfer of gas molecules from liquid to gas phase is a three-step process. The first step is the transport of gas molecules from the bulk liquid to the liquid-film and then crossing the liquid film to arrive at the liquid-gas interface. The third step involves the transfer from the liquid-gas interface to the bulk gas. The K_La represented in Figure 2.9 is the overall liquid mass transfer coefficient which depends on parameters such as agitation at the liquid-gas interface, temperature, nature of gas, liquid viscosity (Treybal, 1980). Similar reactions can take place to a lower extent, in the AN zone of an activated sludge process.

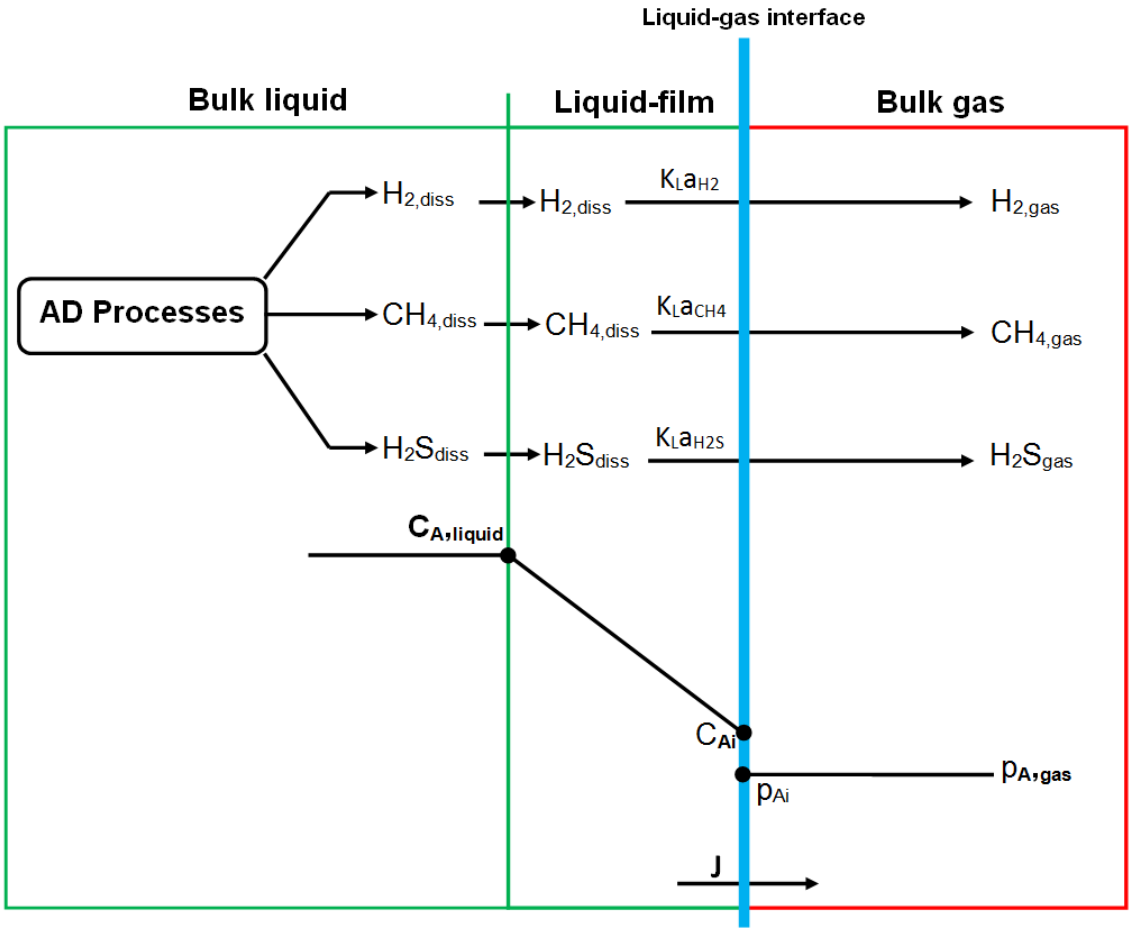

Figure 2-9: Conceptual representation of liquid-gas mass transfer steps in an AN reactor assuming the transfer rate is controlled by the liquid-film resistance (adapted from Kraemer and Bagley, 2007; Beckers et al., 2015).

Note: subscripts 'i' and 'diss' refer to 'liq-gas interface' and 'dissolved', respectively.

The volumetric mass transfer rate of a compound (A) can be calculated as the product of the volumetric mass transfer coefficient and the driving force of the concentration in the bulk liquid as shown in Equation (2.4) (Treybal, 1980).

$$J_A = k_L a_A \times \left(C_{A,liquid} - C_{A,i}\right) = K_L a_A \times \left(C_{A,liquid} - C_A^*\right) \quad (2.4)$$

Based on Henry's law, Equation (2.4) can be written as Equation (2.5).

$$J_A = K_L a_A \times \left(C_{A,liquid} - \frac{p_{A,gas}}{H_A}\right) \quad (2.5)$$

where,

J_A: volumetric mass transfer rate of compound A (mol l^{-1} h^{-1})

$k_L a_A$: liquid-film mass transfer coefficient of compound A (h^{-1})

$K_L a_A$: overall mass transfer coefficient of compound A based on liquid phase concentration (h^{-1})

$C_{A,liquid}$: concentration of compound A in the bulk liquid (mol/L)

C_A^*: concentration of compound A in the bulk liquid in equilibrium with that in the bulk gas phase (mol/l)

$C_{A,i}$: concentration of compound A at the liquid-gas interface (mol/L)

$p_{A,gas}$: partial pressure of compound A in the bulk gas (atm)

H_A: Henry's constant of compound A (at. l/mol)

The $K_L a$ value for VCs, for example H_2, is given by Equation (2.6) (Beckers et al., 2015).

$$K_L a_{H2} = K_L a_{O2} \times \left(\frac{D_{H2}}{D_{O2}}\right)^{0.5} \quad (2.6)$$

where,

D_{H2}: H_2 diffusivity coefficient in the liquid phase (cm^2/s)

D_{O2}: O_2 diffusivity coefficient in the liquid phase (cm^2/s)

$K_L a_{H2}$: overall liquid mass transfer coefficient of H_2 (h^{-1})

$K_L a_{O2}$: overall liquid mass transfer coefficient of O_2 (h^{-1})

The diffusivity coefficients (D) and Henry's law constants (H) for H_2, CH_4 and H_2S are listed in Tables 2.4 and 2.5.

Table 2-4: Diffusivity coefficient (D) of some VCs in water (adapted from Lide, 2003)

Compound	$D/10^{-5}$						Units
	10 °C	15 °C	20 °C	25 °C	30 °C	35 °C	
H_2	3.62	4.08	4.58	5.11	5.69	6.31	cm^2/s
CH_4	1.24	1.43	1.62	1.84	2.08	2.35	cm^2/s
H_2S				1.36			cm^2/s
O_2		1.67	2.01	2.42			cm^2/s

Table 2-5: Henry's law constant (H) of some VCs in water (calculated from Coker, 2007)

Compound	$H \times 10^{-3}$						Units
	10 °C	15 °C	20 °C	25 °C	30 °C	35 °C	
H_2	63.4	66.2	68.7	70.8	72.6	74.1	atm
CH_4	28.5	32.1	35.7	39.2	42.7	46.0	atm
H_2S	0.38	0.43	0.48	0.54	0.60	0.67	atm
O_2	32.6	36.3	40.0	43.6	47.1	50.5	atm

2.3.1 VCs stripping by diffused aeration in an OX reactor

Stripping is generally defined as the removal of VCs from a liquid medium. It can be done by applying mechanical agitation or/and introducing a sparging gas through the liquid. In a biological wastewater treatment process, air is pumped into subsurface bubble diffusers or introduced by mixing using surface aerators to provide oxygen required for microorganisms metabolism. If an OX zone is preceded by an AN one, a portion of VCs produced by anaerobic processes may be transferred to the OX zone and then stripped due to agitation and aeration.

The stripping rate of a VC in an OX zone is influenced by the following factors (Bielefeldt and Stensel, 1999).

1) Aeration flux

2) Turbulence created using mechanical agitation (speed of mixing)

3) pH (in the case of H_2S) and temperature

4) Liquid depth

5) Overall mass transfer coefficient of the VC

6) Henry's law constant and diffusivity of the VC in liquid

The fraction of a VC that can be stripped in a diffused aeration completely mixed reactor is given by Equation (2.7) (Bielefeldt and Stensel, 1999).

$$\text{Fraction of VC stripped} = 1 - [1 + \frac{Q_{air}H}{Q_l} \times \left[1 - \exp\left(-\frac{K_L a_{VC}.h.A}{Q_{air}H}\right)\right]]^{-1} \quad (2.7)$$

where,

Q_{air}: diffused air flow rate (m^3/h)

Q_l: flow rate of liquid stream containing VC (m^3/h)

H: Henry's constant of VC (unitless)

$K_L a_{VC}$: overall mass transfer coefficient of VC (h^{-1})

h: liquid depth (m)

A: reactor surface area (m^2)

2.4 COD mass balance

In WRRFs, the degree of organic matter pollution can be reported in COD units. Validation of observed data obtained from a wastewater treatment process can be achieved by conducting a COD mass balance.

The general form of COD mass balance in an activated sludge system under steady state conditions (accumulation term is zero) is *the daily mass of COD entering the system must either leave or oxidized within the system*. The following data set is needed to perform a COD mass balance for a continuous flow system under steady state conditions:

- influent, effluent, sludge wastage and recycle flow rates
- reactors volume
- total COD concentration of the influent, effluent and sludge wastage as well as the mass of COD oxidized across the system
- oxygen uptake rate (OUR) and oxygen mass transferred from the open reactors surface

- concentration of NO_3^- and NO_2^- in the influent and in each reactor
- DO concentration in the streams entering the system
- DO concentration in the OX reactors
- temperature and correction factors of alpha (α) and beta (β) and
- SO_4^{2-} concentration in the influent and effluent of each reactor.

2.4.1 Reported COD and N mass balances

OX systems

It has been reported that COD and N mass balances for OX systems are close to 100%. A summary of the COD and N mass balance results for the laboratory scale OX systems (Schroeter et al., 1982; McClintock et al., 1988) are described below.

- *Schroeter et al. (1982) system*:

Eight laboratory scale systems under fully OX conditions using domestic wastewater as influent with a COD concentration of about 500 mg COD/L were carried out. They varied the SRT from 3 to 20 days at temperatures of 12 and 20 ^oC. The COD and N mass balances performed on those results by Barker and Dold (1995) indicated that COD and N mass balances were close to 100%, averaging 99.7 for COD and 99.6% for N, respectively (Table 2.6).

Table 2-6: COD and N mass balance results in OX system (data from Schroeter et al., 1982)

System	Type	Substrate	SRT (day)	COD mass balance (%)		N mass balance (%)	
				12°C	20°C	12°C	20°C
OX	Lab-scale	Domestic wastewater (500 mg COD/L)	3	99.6	100.4	100.2	100.5
			3	99.7	100.2	100.2	99.5
			8	99.6	99.9	100.2	97.5
			20	99.4	98.4	99.2	99.4

Note**:** reported in Barker and Dold (1995).

- *McClintock et al. (1988) systems:* Five parallel laboratory scale single OX systems at different SRTs of 1.5, 3, 6, 10 and 15.2 days using bactopeptone as substrate were conducted. Using these results, an average N mass balance of 101.2% was calculated by Barker and Dold (1995). The COD mass balance has not been reported due to lack of OUR data.
- *Arkley and Marais (1981) systems:* Barker and Dold (1995) also examined the COD and N mass balances of those systems. Operational data, COD and N mass balance results are listed in Table 2.7.

Table 2-7: COD and N mass balance results of Arkley and Marais (1981) systems (calculated by Barker and Dold, 1995)

System	Type	Substrate	SRT (day)	COD mass balance (%)		N mass balance (%)	
				avg	std	avg	std
OX	Lab-scale	MWW	20	94.2	1.6	97.3	3.4
OX-OX	Lab-scale	MWW	20	96.6	1.4	101.6	1

Note: avg: average; std: standard deviation; MWW: Municipal wastewater.

AX, AX-OX and OX-AX systems

COD and N mass balance results for AX, AX-OX and OX-AX systems exhibited a significant variation in the COD mass balance from 70 to 95% while N mass balance ranged between 95 and 99% (Barker and Dold, 1995).

COD and N mass balance results of Smyth (1994), Power et al. (1992), McClintock et al. (1988) and Arkley and Marais (1981) systems are presented in Table 2.8. Excess NO_3^- was supplied to ensure the un-aerated reactor was under AX conditions. For example, NO_3^- concentration in the un-aerated reactor of Arkley and Marais (1981) system was about 14 mg NO_3^--N/L.

Table 2-8: Summary of COD and N mass balance results in AX-OX, OX-AX and AX systems

Process	Type	Feed	SRT (d)	AX zone volume fraction (%)	COD balance (%)	N balance (%)	Reference
(AX-OX)[1]	Lab-scale	MWW	20	70	70-85 (without alum) 75-95 (with alum)	N/R	Power et al. (1992)[2]
AX-OX	Lab-scale	MWW	20	40	97	110	Arkley and Marais (1981)[3]
OX-AX	Lab-scale	MWW	20	40	98	99	
AX	-	MWW	7.9, 9.6	100	85	N/R	Smyth (1994)[2]
AX	Lab-scale	bactopeptone	1.5-15.1	100	86-95	95-98	McClintock et al. (1988)[3]

Note:

[1] AX-OX operated to study chemical phosphorus removal using alum

[2] Referenced studies in Copp (1998)

[3] Referenced studies in Barker and Dold (1995)

N/R: not reported

AN-OX systems

Evaluation of COD and N mass balances for the systems incorporating AN reactors (such as AO, Bardenpho, UCT, etc) performed by Randall et al. (1992) and Barker and Dold (1995). According to their findings, N mass balance was close to 100% while COD mass balance ranged between 52 and 100%. In the other word, up to approximately 50% of the daily mass of input COD is disappeared across the system (termed COD "loss").

2.4.2 COD "loss"

The general form quoted for COD "loss" in an activated sludge system at steady state conditions is in the portion of mass of COD entering the system which is not accounted for in the mass of COD leaving and COD oxidized across the system. The terms of COD entering and leaving the system are directly measured while COD oxidized needs to be calculated. A detailed formulation for the term of COD oxidized at different conditions (OX, AX and AN) and system configurations is presented later in this chapter.

This section presents the COD "loss" results reported in the previous experiments included (Wentzel et al., 1989; 1990 and Randall et al., 1992). It also briefly summarizes their system configurations, SRT and type of substrates used.

2.4.2.1 Reported COD "loss"

- *Wentzel et al. (1989; 1990) systems*

The COD "loss" calculated from Wentzel et al. (1989; 1990) systems is presented in Table 2.9. A number of different systems included Phoredox, JHB, UCT, MUCT and Bardenpho in small size were studied, for example the volume of reactors in the UCT system was 2 liters. Acetate and MWW used as substrate. The COD and N mass balances ranged from 76.5 to 91.1% for COD and from 96.0 to 103.3% for N, respectively. The authors stated "This "loss" of COD apparently is associated with the fermentation processes occurring in the anaerobic zone of BEPR systems treating municipal wastewater".

Table 2-9: COD "loss" results adapted from Wentzel et al. (1989; 1990) (calculated by Barker and Dold, 1995)

Process	Substrate	SRT (d)	N mass balance (%)		COD mass balance (%)	
			avg	std	avg	std
Phoredox	MWW	3 and 4	99.8	8.7	76.5	10.8
JHB	MWW	5	103.3		81.3	
UCT	MWW	6, 8, 10	101.2	5.9	75.2	10.1
	acetate	10	103.1		91.1	
MUCT	MWW	15, 20, 21	97.2	3.8	79.2	8.6
Bardenpho	acetate	7.5, 10, 20	96.0	7.5	90.5	1.7

- *Randall et al. (1992) systems*

COD "loss" for a laboratory scale AO and UCT systems (either laboratory or pilot plant scale) evaluated by Randall et al. (1992). The volume of reactors was in the range of 1.7 - 25 L for the laboratory scale systems and approximately 220 L for the pilot plant UCT one. The systems operated with different substrates (such as dextrose, acetate, raw and settled MWW) and SRT ranged between 5 and 18 days. They reported a COD "loss" up to approximately 50%.

A detailed description of the operational data and COD "loss" results obtained is presented in Table 2.10.

The following points summarize their results:

- The COD "loss" obtained using synthetic substrate was significant, ranged from 23 to 48% with dextrose (25% of influent COD) as substrate. When dextrose replaced with acetate (37% of influent COD), the COD "loss" was in the range of 0-10%. It was concluded that the magnitude of COD "loss" was influenced by the nature of the readily biodegradable organic substrate.

- The COD "loss" only observed in a significant amount when the influent COD was greater than 212 mg COD/L. They stated that COD "loss" occurred only for COD in excess of that needed for bio-P processes.

- The authors claimed that the principal mechanism attributed to the observed COD "loss" was likely due to metabolism by non-PAOs (such as fermenting organisms).

Table 2-10: COD "loss" results in AO and UCT systems (Randall et al. 1992)

# Study	System	AN zones volume fraction (%)	Total volume[c] (L)	Substrate	Influent COD (mg COD/L)	SRT (d)	T (^{o}C)	COD "loss" (%)
1	AO[a]	31	6.5	Nutrient broth (69.4%) Dextrose (25%) Yeast extract (5.6%)	529-548	5, 6,10	N/R	23-48
2	UCT	32	15.5	Nutrient broth (67.8%) Dextrose (27%) Yeast extract (5.1%)	610 and 620	12, 18	20	23-27
				Nutrient broth (58.8%) Acetate (36.7%) Yeast extract (4.4%)	640	13	20	0-10
3	UCT	20	2170	Raw MWW	190-313	5-10	13-26	0-26
4	UCT[b]	25	50.4	Settled MWW	190, 262 and 320	5	10, 15, 20	8 -18
					170, 219 and 228	15	10, 15, 20	12-27

Note:

[a] nitrification inhibited by 2-imidazolidinethione

[b] reactors subdivided using vertical baffles to promote plug-flow regime

[c] clarifier volume was not considered

N/R: not reported

2.5 Parameters affecting COD mass balance

2.5.1 OUR measurement and open reactor surface

OUR is a crucial parameter to calculate the COD mass balance on systems incorporating an OX zone and it should be properly quantified. It has been reported that the oxygen consumption rate on a sample taken from the mixed liquor of an OX reactor is significant lower than the rate determined directly in that reactor (Marais and Ekama, 1976; Mueller and Stensel, 1987).

The results of COD mass balance reported for an OX laboratory scale system of Schroeter et al. (1982) revealed that a high turbulence at the open reactor surface can affect the COD mass balance if this oxygen mass transferred is ignored. The COD mass balance of 81.7% was reported in the presence of high turbulence but when the turbulence was reduced by using a smaller stirrer paddle, the COD mass balance was raised to 99.7% (Barker and Dold, 1995).

2.5.2 Denitrification stoichiometry

In systems incorporating an un-aerated zone, a portion of the mass of COD oxidized under un-aerated conditions is attributed to the mass of NO_3^- denitrified. The assumption of 2.86 mg O_2/mg NO_3^--N as oxygen equivalent to NO_3^- denitrified would be fine if NO_3^- were completely denitrified to N_2. In case of intermediate species production (such as NO_2^-, NO and N_2O), the conversion factor would be lower and the assumption of 2.86 mg O_2/mg NO_3^--N would result in an error in COD mass balance calculation.

2.5.3 Temperature and feed COD source

The effect of temperature on COD "loss" in activated sludge systems was evaluated by Erdal et al. (2005). They operated two pilot plant scale UCT systems at different temperatures of 5 ± 1 and 20 ± 1°C at an SRT of 10 days. They also operated a pilot plant scale AO system at a temperature of 20 ± 1°C and an SRT of 10 days.

Acetate was used as carbon source for all three systems. Their findings indicated that COD "loss" was not observed for the UCT system operated at temperatures of 5 ± 1°C. The COD "loss" for both systems operated at temperatures of 20 ± 1°C was about 10%. The reported COD "loss" ranged between 3 and 15% for the UCT system operated at temperatures of 20 ± 1°C. The authors performed the mass balance of PHA and glycogen, and observed different biochemical

metabolisms of storage and consumption as well as diverse bacterial communities. According to balancing of reducing equivalents, the amount of NADH required for re-synthesis of glycogen at 5°C was significantly less than that in the system operated at 20°C. They mentioned that there was a relation between EBPR storage mechanisms and the COD "loss" in the systems incorporating an AN zone. They stated "Since AnS (anaerobic stabilization) values were measured consistently, there must be other mechanisms responsible from anaerobic stabilization aside from the possible contribution of the fermentation reaction".

The experimental data from the EBPR systems conducted by Wentzel et al. (1989; 1990) was evaluated to investigate COD mass balances (Barker and Dold, 1995). It was reported that the COD mass balance on a mixed culture system treating MWW was only 78% while using acetate as carbon source, the COD mass balance was close to an average of 91%. It was suggested that the disappearance of COD could likely be attributed to fermentation processes taking place in the AN process.

The reported COD "loss" on a laboratory scale UCT-EBPR using glucose as influent was much higher than with acetate (Randall et al., 1987). These authors also reported a COD "loss" between 23 and 27% on a UCT system using nutrient broth and dextrose.

2.6 Possible causes of COD "loss"

As indicated above, a number of researchers reported that a fraction of the daily mass of influent COD could not be accounted for in the effluent or sludge wastage streams and in the mass of COD oxidized on the systems incorporating an AN reactor (Lan et al., 1983; Ramadori et al., 1985; Brannan, 1986; Randall et al., 1987, 1992; Wable and Randall, 1992; Barker and Dold, 1995; Erdal et al., 2005). This COD "loss" has been debated since 1983. The hypothesized mechanisms to explain some COD loss in the AN-OX systems are summarized in Table 2.11 and discussed below.

Table 2-11: Hypothesized mechanisms contributing to the COD loss in AN-OX systems

Mechanism		Reference
Partial oxidation of polyhydroxybutyrate-valerate (PHBV) under the conditions of the COD test (with dichromate at 150 °C for 2 hours)		1
Volatile compounds production in the AN reactor, and stripping either in the AN or the subsequent OX reactor	Methane	1, 2, 3, 4 and 5
	Hydrogen	1, 3, 4 and 5
Aerating and mixing induced stripping of volatile fatty acids		1 and 3
Anaerobic sulfate reduction		1 and 2

1: This research study; **2**: Randall et al., 1992; **3**: Wable and Randall, 1992;

4: Erdal et al., 2005; **5**: Wable and Randall, 1994.

2.6.1 Experimental error and COD test limitation

The measured value for the output COD of a biological process which is comprised of sludge wastage COD, effluent COD and COD oxidized, has some degree of experimental error. Some species may be recalcitrant and may not be completely oxidized by the COD dichromate reagent during the digestion period of 2 hours at 150 ^{o}C. Since these species have an associated COD, it could be a potential cause of the underestimation of the output COD resulting in a COD imbalance.

2.6.2 H_2 production and stripping

The COD "loss" in the systems incorporating an AN reactor was attributed to fermentation processes taking place in the AN zone (Randall et al., 1987). Significant differences in COD "loss" values were observed when fermentable substrates (glucose, nutrient broth and dextrose) were used compared to using acetate as substrate (Randall et al., 1992). The possibility of fermentation taking place in AN reactor when the EBPR system was fed with MWW as influent, as reported by Erdal et al. (2005) and Barker and Dold (1995; 1996).

H_2 can be produced via fermentation by facultative anaerobic bacteria using fermentable substrates. Therefore, its production and stripping could be a possible explanation of COD

"loss". Due to its low solubility in water (1.6 mg H_2/L at 20°C), it can easily be stripped from shallow laboratory scale reactors equipped with a mixer. The following points summarize the results of a number reports regarding H_2 production in systems that include an AN zone.

- A batch experiment using sludge taken from an AN-OX system was operated to quantify the amount of H_2 production (Erdal et al., 2005). They could not confirm the presence of H_2 in gaseous samples.
- The analysis of off-gases from AN reactor showed negligible H_2 production (Wable and Randall, 1992). In another study, a vacuum stripping method was applied to obtain gases dissolved in the anaerobic mixed liquor (Wable and Randall, 1994). The gaseous samples were analyzed for H_2 and CH_4. They reported that only 0.1% or less of the COD "loss" was explained by H_2 production and stripping. The detection limit of the instrument used to measure H_2 was 0.001 mg/L.

Attempts of researchers regarding COD "loss" associated with H_2 production in AN-OX systems resulted in inconclusive findings. Nevertheless, since low levels of H_2 are produced during fermentation, H_2 may be produced but not detected depending on the detection limit of the instrument used. H_2 produced could easily be stripped from the mixed liquor due to the low solubility of 1.6 mg H_2/L in water and because laboratory scale AN reactors are very shallow, resulting in much gas stripping.

2.6.3 CH_4 production and stripping

CH_4 is produced under anaerobic conditions and has a COD of 4 mg COD per mg CH_4 according to reaction (2.8).

$$CH_4 + 2\,O_2 \rightarrow CO_2 + 2\,H_2O \qquad (2.8)$$

The CH_4 production in an AN-OX system operated at 20°C should not be significant as methanogens are not expected to survive the exposure to OX conditions since they are obligate anaerobes. However, low oxygen-tolerant methanogenic bacteria have been reported and this possible mechanism should not be neglected (Barker and Dold, 1995).

The analysis of anaerobic gas by GC exhibited that the combined production of CH_4, H_2 and carbon monoxide (CO) was reported to only explain an insignificant portion of COD "loss" (Wable and Randall, 1992). Later in 1994, their findings revealed that CH_4 production and

stripping could be an explanation of COD "loss" in AN-OX system depending on the type of substrate. They reported that almost 19% of COD "loss" was explained by CH_4 production when the system was operated using formate but no more than 0.8% in the absence of formate (Wable and Randall, 1994). The authors claimed that one possible explanation for these results was the presence of only species of methanogenic bacteria that utilize formate (not acetate). The other possibility was that methanogenic bacteria were not able to compete with PAOs for acetate.

No CH_4 was detected in batch tests conducted with sludge taken from AN-OX systems operated at 5 and 20°C (Erdal et al., 2005).

2.6.4 VFAs production and stripping either in the AN or OX reactor

Another possible mechanism of COD "loss" is the volatilization of VFAs such as acetic acid produced via fermentation in AN reactor that would be stripped in the subsequent OX zone (Barker and Dold, 1995). This mechanism was considered unlikely as these readily biodegradable components should have be removed from solution prior to the aerated zone (Wable and Randall, 1992).

2.6.5 Sulfate reduction in AN reactor

SO_4^{2-} reduction occurs under strict AN conditions and the SO_4^{2-} to oxygen conversion factor is of 2.0 mg O_2/mg SO_4^{2-}-S. An average concentration of 10 mg SO_4^{2-}-S/L was reported for domestic wastewaters (Tchobanoglous, 2003). Thus, SO_4^{2-} reduction could contribute to explain a fraction of the COD "loss".

2.7 The importance of COD "loss"

One of the by-products arising from biological wastewater treatment is sludge. Sludge management may represent up to 60% of the total operating costs of a WRRF (Perez-Elvira et al., 2006; Canales et al., 1994; Campos et al., 2009). Similarly, aeration may represent up to 50% of the operating costs of a WRRF.

Since the activated sludge systems incorporating AN zone for the purpose of phosphorus removal showed a significant COD "loss", it can result in a reduction in sludge production and oxygen requirement for stabilization of organic matter. Therefore, understanding the mechanism

and potential causes of COD "loss", would make it possible to design the activated sludge processes in the way leading to a decrease in operating and possibly capital costs.

2.8 Theoretical considerations

Performing COD mass balance on a system needs a comprehensive data set as listed in section 2.4.

This section provides an equation to evaluate the COD, N and P mass balances on a two-reactor (R1 and R2) system where R2 is an OX reactor preceded by either an un-aerated (AX or AN) or an OX one.

2.8.1 COD mass balance calculation

COD mass balance on a system is generally expressed according to Equation (2.9).

$$\text{COD mass balance (\%)} = (\text{FCOD}_{\text{OUTPUT}}/\text{FCOD}_{\text{INPUT}}) \times 100 \quad (2.9)$$

$\text{FCOD}_{\text{INPUT}}$ is the mass rate of total COD entering the system given by Equation (2.10).

$$\text{FCOD}_{\text{INPUT}} = S_{T,\text{inf}} \times Q_{\text{inf}} \quad (2.10)$$

where,

$S_{T,\text{inf}}$: influent total COD concentration (mg COD/L)

Q_{inf}: influent flow rate (L/d)

The term of $\text{FCOD}_{\text{OUTPUT}}$ in Equation (2.9) is the mass rate of total COD in the streams leaving the system (effluent and sludge wastage) plus the mass rate of total COD oxidized in the system. It can be determined using Equation (2.11).

$$\text{FCOD}_{\text{OUTPUT}} = \text{FS}_{\text{eff}} + \text{FX}_{\text{eff}} + \text{FS}_{\text{WAS}} + \text{FX}_{\text{WAS}} + \text{FCOD}_{\text{oxid}} \quad (2.11)$$

where,

FS_{eff}: effluent soluble COD mass rate (mg COD/d)

FX_{eff}: effluent particulate COD mass rate (mg COD/d)

FS_{WAS}: mass rate of soluble COD in the sludge wastage stream (mg COD/d)

FX_{WAS}: mass rate of particulate COD in sludge wastage stream (mg COD/d)

$FCOD_{oxid}$: mass rate of the total COD oxidized in the system (mg COD/d)

When soluble and particulate COD concentrations in the sludge wastage as well as sludge wastage flow rate are known, FS_{WAS} and FX_{WAS} are given by Equations (2.12) and (2.13).

$$FS_{WAS} = S_{WAS} \times Q_{WAS} \quad (2.12)$$

$$FX_{WAS} = X_{WAS} \times Q_{WAS} \quad (2.13)$$

where,

S_{WAS}: soluble COD concentration in sludge wastage (mg COD/L)

X_{WAS}: particulate COD concentration in sludge wastage (mg COD/L)

Q_{WAS}: sludge wastage flow rate (L/d)

Similarly,

$$FS_{eff} = S_{eff} \times Q_{eff} \quad (2.14)$$

$$FX_{eff} = X_{eff} \times Q_{eff} \quad (2.15)$$

S_{eff}: effluent soluble COD concentration (mg COD/L)

X_{eff}: effluent particulate COD concentration (mg COD/L)

Q_{eff}: effluent flow rate (L/d)

An illustration of the components contributing to the COD mass balance calculation on a system is presented in Figure 2.10.

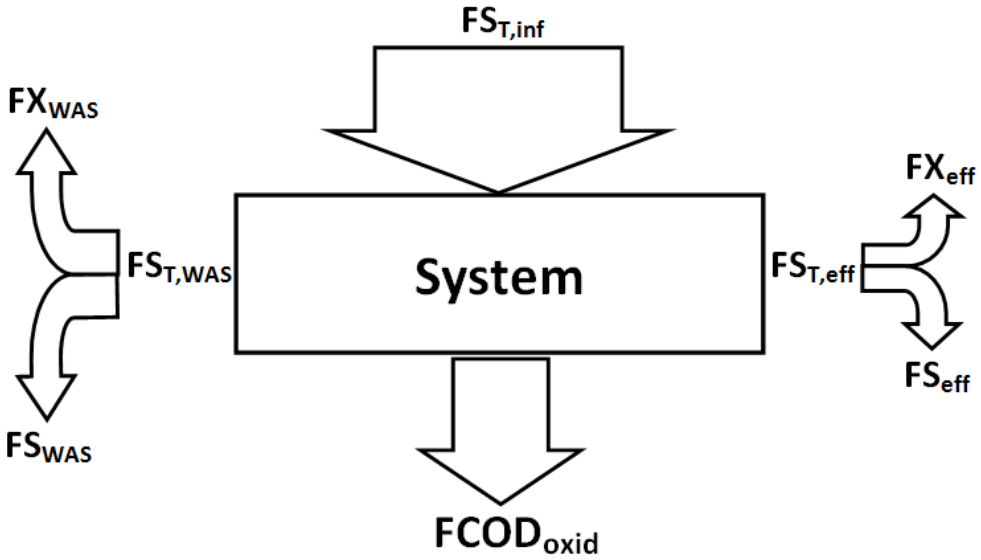

Figure 2-10: Conceptual illustration of the COD mass balance components

Note: "F", "S", "X" and "S_T" refer to "mass rate", "soluble COD conc." and "particulate COD conc." and "total COD conc.", respectively.

$S_{T,inf}$, S_{WAS}, X_{WAS}, S_{eff} and X_{eff} can be directly measured using Hach method whereas $FCOD_{oxid}$ depends on the type and the amount of electron acceptor consumed in the system. The following section provides an equation developed to determine $FCOD_{oxid}$ in each reactor of a two-reactor system under different conditions.

2.8.1.1 Evaluation of $FCOD_{oxid}$ in a two-reactor system

Consider two reactors (R1 and R2) in series configuration (Figure 2.11) where R2 is an OX membrane bioreactor (MBR) preceded by R1 one which is either an OX or an un-aerated (AX or AN) reactor.

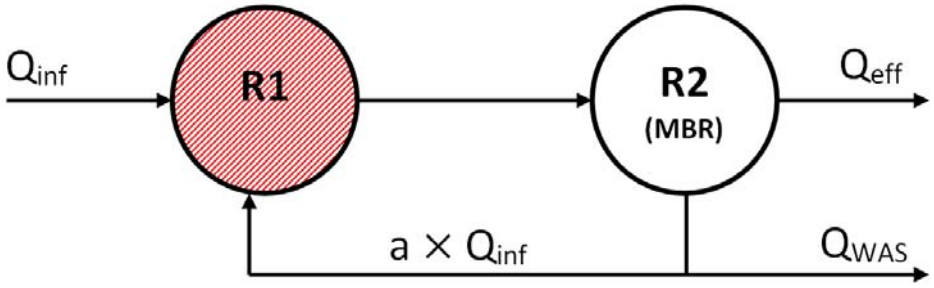

Figure 2-11: Typical schematic diagram of the system used in this study.

Note: a: aerobic mixed liquor recycle ratio with respect to Q_{inf}

To derive an equation for determination of $FCOD_{oxid}$, cases # 1-3 are considered as follows:

- *Case # 1: R1 is an OX reactor*

$FCOD_{oxid}$ in reactor R1 (and similarly for reactor R2) is computed from FO_{OURB} (it is discussed in section 2.8.1.2) after subtracting the mass rate of oxygen needed for nitrification (Equations 2.16 and 2.17).

$$FCOD_{oxid} = FO_{OUR_B} - FO_{nit} \quad (2.16)$$

$$FO_{OUR_B} = FO_{OUR_{meas}} + FO_{surface} + FO_{streams\ entering\ R1} \quad (2.17)$$

where,

FO_{OUR_B}: mass rate of oxygen utilized by biomass (mg COD/d)

FO_{nit}: mass rate of oxygen consumed for nitrification (mg COD/d)

$FO_{OUR_{meas}}$: measured OUR (mg COD/d)

$FO_{surface}$: mass rate of oxygen entering reactor R1 from the liquid surface (mg COD/d)

$FO_{streams\ enting\ R1}$: mass rate of oxygen entering reactor R1 through the influent/recycle streams (mg COD/d)

- *Case # 2: R1 is an AX reactor*

$FCOD_{oxid}$ in reactor R1 is given by Equation (2.18).

$$FCOD_{oxid} = FO_{NO3,denit} + FO_{surface} + FO_{streams\ entering\ R1} \quad (2.18)$$

where,

$FO_{NO3,denit}$: mass rate of oxygen equivalent of NO_3^- denitrified (mg COD/d)

$FCOD_{oxid}$ in reactor R2 can be calculated by using Equations (2.16) and (2.17).

- *Case # 3: R1 is an AN reactor*

Compared to case # 2, the oxygen equivalent of SO_4^{2-} reduced (in reactor R1) and oxygen consumed for sulfide oxidation (in reactor R2) should be considered in the calculation of $FCOD_{oxid}$ (Equations 2.19 and 2.20).

$$FCOD_{oxid,R1} = FO_{NO3,denit} + FO_{stream\ enting\ R1} + FO_{SO4\ reduc} \quad (2.19)$$

$$FCOD_{oxid,R2} = FO_{OUR_{meas}} + FO_{surface} + FO_{streams\ entering\ reactor} - FO_{nit} - FO_{sulfide\ oxid} \quad (2.20)$$

where,

$FO_{SO4\ reduc}$: mass rate of oxygen equivalent of sulfate reduction (mg COD/d)

$FO_{sulfide\ oxid}$: mass rate of oxygen consumed for sulfide oxidation (mg COD/d)

2.8.1.2 Derivation of an equation for FO_{OURB}

The general word statement for the DO mass balance on a continuous flow complete-mix reactor (as shown in Figure 2.12) is given by expression (2.21).

$$[\text{Rate of accumulation}] = [\text{Rate of input from flow}] + [\text{Rate of input through surface}] - [\text{Rate of depletion by biomass}] - [\text{Rate of output from flow}] \quad (2.21)$$

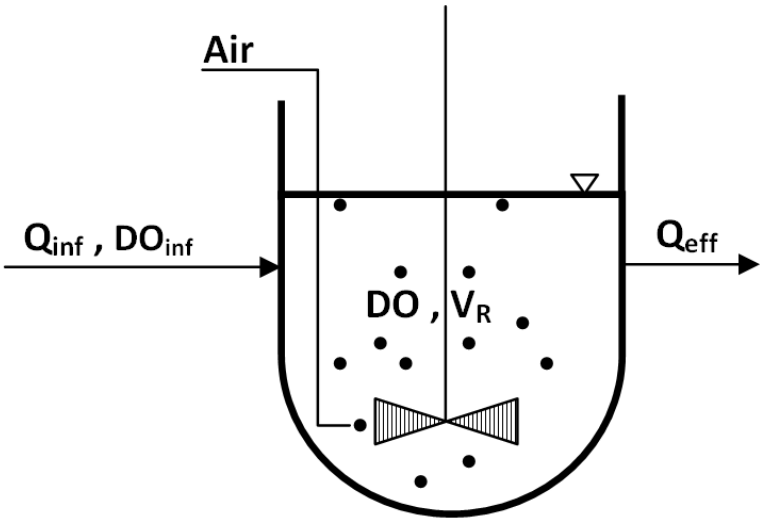

Figure 2-12: Diagrammatic sketch of a continuous complete-mix reactor

The expression (2.21) is simplified by symbolic representation given by Equation (2.22).

$$V_R \times (dDO/dt) = Q \times DO_{inf} + [k_L a_{used} \times (DO_{sat.,used} - DO) \times V_R] - (OUR_B \times V_R) - (Q \times DO) \quad (2.22)$$

where,

Q: flow rate (L/h)

V_R: volume (L)

DO_{inf}: influent DO concentration (mg COD/L)

DO: DO concentration in the reactor at time t (mg COD/L)

DO_{sat}: saturation DO concentration (mg COD/L)

OUR_B: biomass OUR (mg O_2 l^{-1} h^{-1})

k_La: oxygen mass transfer coefficient (h^{-1})

dDO/dt: slope of the straight line plotted from the decline of DO concentration against time while the aeration stopped (mg O_2 l^{-1} h^{-1})

-dDO/dt: OUR_{meas} in mg O_2 l^{-1} h^{-1} units

When Equation (2.22) is solved for OUR_B, it yields Equation (2.23).

$$OUR_B = OUR_{meas} + \frac{Q}{V_R} \times (DO_{inf} - DO) + k_L a_{used} \times (DO_{sat.,used} - DO) \quad (2.23)$$

and,

$$FO_{OUR_B} = 24 \times V_R \times OUR_B \quad (2.24)$$

where,

The $k_La_{\ used}$ and $DO_{sat.used\ at\ T}$ are represented by Equations (2.25) through (2.27).

$$k_La_{used} = \alpha \times k_La_{meas} \quad (2.25)$$

$$DO_{sat.used\ at\ T} = \beta \times DO_{sat.clean\ water\ at\ T} \quad (2.26)$$

$$DO_{sat.clean\ water\ at\ T} = DO_{sat.clean\ water\ at\ 20C} \times 51.6/(31.6 + T) \quad (2.27)$$

where,

α: k_La correction factor

β: DO_{sat} correction factor

T: temperature (^oC)

The alpha value of 0.7 and beta of 0.9 are the typical values that can be used for a broad diversity of industrial and municipal wastewaters (U.S.EPA., 1979).

By applying Equations (2.23) and (2.24), a general expression for FO_{OURB} in reactors R1 and R2 (cases # 1-3) can be written by Equations (2.28) through (2.34), respectively (Table 2.12).

Table 2-12: Equations developed for FO_{OURB} determination in R1 and R2 reactors illustrated in Figure 2.11 (cases #1-3)

# reactor	# case	$\mathbf{FO_{OUR_B}}$	equation
R1	1	$24 \times V_{R1} \times [OUR_{meas,R1} + \frac{Q_{inf}}{V_{R1}} \times (DO_{inf} - DO_{mid,R1}) + \frac{Q_{inf} \times a}{V_{R1}} \times (DO_{R2} - DO_{mid,R1}) + k_L a_{used,R1} \times (DO_{sat.,used} - DO_{mid,R1})]$	2.28
	2	Equation (2.28) where, $OUR_{meas,R1} = DO_{mid,R1} = 0$	2.29
	3	Equation (2.28) where, $OUR_{meas,R1} = DO_{mid,R1} = k_L a_{used,R1} = 0$	2.30
R2	1, 2, 3	$24 \times V_{R2} \times [OUR_{meas,R2} + \frac{Q_{inf} \times (1+a)}{V_{R2}} \times (DO_{R1} - DO_{mid,R2}) + k_L a_{used,R2} \times (DO_{sat.,used} - DO_{mid,R2})]$ case # 2 and 3: $DO_{R1} = 0$	2.31
R1R2	1	summation of equations (2.28) and (2.31)	2.32
	2	summation of equations (2.29) and (2.31)	2.33
	3	summation of equations (2.30) and (2.31)	2.34

Note: DO_{mid}: DO concentration at the middle point between the high and low levels of DO used for OUR measurement (mg O_2/l)

2.8.1.3 Determination of $FO_{NO3,denit}$

To estimate the conversion factor for the oxygen equivalent of NO_3^- denitrified under AX condition, it is assumed that denitrification process is occurred in a four-step reaction as described by expression (2.35) (Payne, 1981; Schepers and Raun, 2008; Koren et al., 2000).

$$NO_3^- \rightarrow NO_2^- \rightarrow NO \rightarrow N_2O \rightarrow N_2 \quad (2.35)$$

State # A: NO_3^- is only converted to NO_2^-:

The half reaction for reduction of NO_3^- to NO_2^-, and oxygen to water are given by reactions (2.36) and (2.37).

$$^1/_2\, NO_3^- + H^+ + e^- \rightarrow {}^1/_2\, NO_2^- + {}^1/_2\, H_2O \quad (2.36)$$

$$^1/_4\, O_2 + H^+ + e^- \rightarrow {}^1/_2\, H_2O \quad (2.37)$$

From reaction (2.36) and (2.37), the transfer of one electron needs the reduction of 0.25 mole oxygen or 0.5 mole NO_3^-. Considering the molecular weight of oxygen (32 mg/mmol) and nitrogen (14 mg/mmol) gives NO_3^- - to - O_2 conversion factors of 1.14 mg O_2/mg NO_3^--N.

State # B: NO_3^- is directly converted to NO without NO_2^- accumulation:

The half reaction for reduction of NO_2^- to NO is described by reaction (2.38).

$$NO_2^- + 2\, H^+ + e^- \rightarrow NO + H_2O \quad (2.38)$$

Combing the reactions (2.36) and (2.38) produces the reaction (2.39).

$$^1/_3\, NO_3^- + {}^4/_3\, H^+ + e^- \rightarrow {}^1/_3\, NO + {}^2/_3\, H_2O \quad (2.39)$$

Considering the reactions (2.37) and (2.39), the transfer of one electron needs the reduction of 0.25 mole oxygen or approximately 0.33 mole NO_3^- resulting in NO_3^- - to - O_2 conversion factor of 1.73 mg O_2/mg NO_3^--N.

State # C: NO_3^- is completely converted to N_2O without either NO_2^- or NO release:

The half reaction for reduction of NO to N_2O is presented by reaction (2.40).

$$2\,NO + 2\,H^+ + 2\,e^- \rightarrow N_2O + H_2O \quad (2.40)$$

The net reaction of NO_3^- reduction to N_2O is produced by combining the reactions (2.36), (2.38) and (2.40):

$$^1/_4\,NO_3^- + {}^5/_4\,H^+ + e^- \rightarrow {}^1/_8\,N_2O + {}^5/_8\,H_2O \quad (2.41)$$

Referring reactions (2.37) and (2.41), 0.25 mole oxygen or NO_3^- requires the transformation of one electron equivalent that gives NO_3^- - to - O_2 conversion factor of 2.29 mg O_2/mg NO_3^--N.

State # D: NO_3^- is completely converted to N_2 without any intermediates production:

The half reaction for reduction of N_2O to N_2 is given by reaction (2.42).

$$N_2O + 2\,H^+ + 2\,e^- \rightarrow N_2 + H_2O \quad (2.42)$$

Combining reactions (2.36), (2.38), (2.40) and (2.42) results in the reduction of NO_3^- to N_2 in the absence of intermediates production (reaction 2.43).

$$^1/_5\,NO_3^- + {}^6/_5\,H^+ + e^- \rightarrow {}^1/_{10}\,N_2 + {}^3/_5\,H_2O \quad (2.43)$$

Similarly, as mentioned above,

$$^1/_4\,\text{mole}\ O_2 \equiv {}^1/_5\,\text{mole}\ NO_3^-$$

Therefore, the conversion factor for the oxygen equivalent of NO_3^- reduced is 2.86 mg O_2/mg NO_3^--N.

Referring *<u>case # 2 and 3</u>*, when NO_3^- is completely converted to N_2, the mass rate of NO_3^- denitrified ($FO_{NO3,denit}$) in mg COD/d is described by Equation (2.44).

$$FO_{NO3,denit} = 2.86 \times FN_{NO3,denit} \quad (2.44)$$

where, $FN_{NO3,denit}$ is the mass rate of NO_3^- denitrified in mg NO_3^--N/d and can be calculated by Equations (2.45) through (2.47).

The mass rate of NO_3^- entering and leaving reactor R1:

$$FN_{NO3,input\,R1} = a \times Q_{inf} \times N_{NO3,R2} \quad (2.45)$$

$$FN_{NO3,output\ R1} = (1 + a) \times Q_{inf} \times N_{NO3,R1} \quad (2.46)$$

Consequently,

$$FN_{NO3,denit} = a \times Q_{inf} \times N_{NO3,R2} - (1 + a) \times Q_{inf} \times N_{NO3,R1} \quad (2.47)$$

where,

$N_{NO3,R1}$: NO_3^- concentration in the reactor R1 (mg NO_3^--N/L)

$N_{NO3,R2}$: NO_3^- concentration in the reactor R2 (mg NO_3^--N/L)

$FN_{NO3,input\ R1}$: mass rate of NO_3^- entering reactor R1 (mg NO_3^--N/d)

$FN_{NO3,output\ R1}$: mass rate of NO_3^- leaving reactor R1 (mg NO_3^--N/d)

$FN_{NO3,denit}$: mass rate of NO_3^- denitrified in the reactor R1 (mg NO_3^--N/d)

Substituting Equation (2.47) into Equation (2.44) results in Equation (2.48).

$$FO_{NO3,denit} = 2.86 \times [a \times Q_{inf} \times N_{NO3,R2} - (1 + a) \times Q_{inf} \times N_{NO3,R1}] \quad (2.48)$$

2.8.1.4 FO_{nit} calculation

Nitrification is a biological process in which ammonia is oxidized to NO_2^- by *Nitrosomonas* bacteria according to reaction (2.49). Then, NO_2^- produced is oxidized by *Nitrobacter* given by reaction (2.50).

$$2\,NH_4^+ + 3\,O_2 \xrightarrow{Nitrosomonas} 2\,NO_2^- + 4\,H^+ + 2\,H_2O \quad (2.49)$$

$$2\,NO_2^- + O_2 \xrightarrow{Nitrobacter} 2\,NO_3^- \quad (2.50)$$

Combining reactions (2.49) and (2.50) results in the net reaction of nitrification described by reaction (2.51).

$$2\,NH_4^+ + 4\,O_2 \rightarrow 2\,NO_3^- + 4H^+ + 2\,H_2O \quad (2.51)$$

From reaction (2.51), 2 mmol NH_4^+ needs 4 mmol O_2 to generate 2 mmol NO_3^-. Equivalently, 4.57 mg O_2 is consumed to oxidize 1 mg NH_4^+-N or to produce 1 mg NO_3^--N. Consequently, FO_{nit} in an OX system can be calculated by Equation (2.52).

$$FO_{nit} = 4.57 \times FN_{NO3,prod} \quad (2.52)$$

where,

$FN_{NO3,prod}$: mass rate of NO_3^- produced (mg NO_3^--N/d)

When the OX system is preceded by an un-aerated reactor either AX or AN (*cases # 2 & 3*), the mass of NO_3^- denitrified in the un-aerated reactor must be considered. Thus, Equation (2.52) is written as Equation (2.53).

$$FO_{nit} = 4.57 \times (FN_{NO3,prod} + FN_{NO3,denit}) \quad (2.53)$$

Considering Figure 2.11, a general expression for FO_{nit} in reactors R1 and R2 (cases # 1-3) is presented in Table 2.13.

Table 2-13: Equations developed for FO_{nit} determination in R1 and R2 reactors illustrated in Figure 2.11 (cases #1-3)

# reactor	**# case**	**FO_{nit}**	**equation**
R1	1, 2 & 3	$4.57 \times [(1 + a) \times Q_{inf} \times N_{NO3,R1} - a \times Q_{inf} \times N_{NO3,R2}]$ case # 2 & 3: $FO_{nit} = 0$	2.54
R2	1, 2 & 3	$4.57 \times [\, Q_{eff} \times N_{NO3,eff} + Q_{WAS} \times N_{NO3,WAS} + a \times Q_{inf} \times N_{NO3,R2} - (1 + a) \times Q_{inf} \times N_{NO3,R1}]$	2.55
R1R2	1	$4.57 \times [\, Q_{eff} \times N_{NO3,eff} + Q_{WAS} \times N_{NO3,WAS}]$	2.56
	2 & 3	$4.57 \times [\, Q_{eff} \times N_{NO3,eff} + Q_{WAS} \times N_{NO3,WAS} + FN_{NO3,denit}]$	2.57

Note**:** assuming that the influent NO_3^- concentration is zero

2.8.1.5 Determination of $FO_{sulfate\ reduc}$ and $FO_{sulfide\ oxid}$

The half reaction for sulfate reduction to sulfide is expressed by reaction (2.58).

$$^1/_8\,SO_4^{2-} + {}^{19}/_{16}\,H^+ + e^- \rightarrow {}^1/_{16}\,H_2S + {}^1/_{16}\,HS^- + {}^1/_2\,H_2O \qquad (2.58)$$

From reaction (2.37) and (2.58), 0.25 mmole O_2 or 0.125 mmol SO_4^{2-} requires the transformation of one electron equivalent. Considering the molecular weight of oxygen and sulfur (32 mg/mmol) gives SO_4^{2-} - to - O_2 conversion factor of 2 mg O_2/mg SO_4^{2-}-S.

Referring *case # 3,* the mass rate of sulfate reduced ($FO_{sulfate\ reduc.}$) in reactor R1, in mg COD/d units, is given by Equation (2.59).

$$FO_{SO_4,reduc} = 2 \times FSO_{4\,reduc} \qquad (2.59)$$

where, $FSO_{4\,reduc}$ is mass rate of SO_4^{2-} reduced in mg SO_4^{2-}-S/d units and can be calculated by Equations (2.60) through (2.62).

mass rate of SO_4^{2-}-S entering reactor R1:

$$FSO_{4\,input\,R1} = Q_{inf} \times SO_{4\,inf} + a \times Q_{inf} \times SO_{4\,R2} \qquad (2.60)$$

mass rate of SO_4^{2-}-S leaving reactor R1:

$$FSO_{4\,output\,R1} = (1 + a) \times Q_{inf} \times SO_{4\,R1} \qquad (2.61)$$

Thus, the mass rate of SO_4^{2-}-S reduced in reactor R1 is expressed by Equation (2.62):

$$FSO_{4\,reduc} = (Q_{inf} \times SO_{4\,inf} + a \times Q_{inf} \times SO_{4\,R2}) - (1 + a) \times Q_{inf} \times SO_{4\,R1} \qquad (2.62)$$

The mass of sulfide oxidized in reactor R2 is described by Equation (2.63).

$$\text{mass rate of sulfide oxidized (mg S/d)} = (1 + a) \times Q_{inf} \times (SO_{4\,R2} - SO_{4\,R1}) \qquad (2.63)$$

where,

$SO_{4\,R1}$: SO_4 concentration in the reactor R1 (mg SO_4-S/L)

$SO_{4\,R2}$: SO_4 concentration in the reactor R2 (mg SO_4-S/L)

Since 2 mg O_2 is consumed to oxidize 1 mg sulfide, therefore:

$FO_{sulfide\ oxid.}$ is given by Equation (2.64).

$$FO_{sulfide\ oxid} = 2 \times [(1 + a) \times Q_{inf} \times (SO_{4\ R2} - SO_{4\ R1})] \quad (2.64)$$

where,

$FO_{sulfide\ oxid}$: mass rate of sulfide oxidized (mg COD/d)

2.8.2 N mass balance calculation

Total nitrogen (TN) enters a system gives a measure for TKN (summation of ammonia and organic N), NO_2^- and NO_3^-.

In a nitrifying system, a major fraction of the influent TKN is converted to NO_2^-/NO_3^-. A portion of NO_3^- is then converted to nitrogen gas (N_2) if nitrifying system incorporates denitrifying zone. The amount of N_2 leaving the system can be determined by conducting a NO_3^- mass balance around the denitrifying zone. A fraction of the influent TKN is also removed via biomass synthesis and sludge wasting.

The components contributing to perform N mass balance on a process including nitrifying and denitrifying zones (only system boundary shown) are presented on Figure 2.13 and described below.

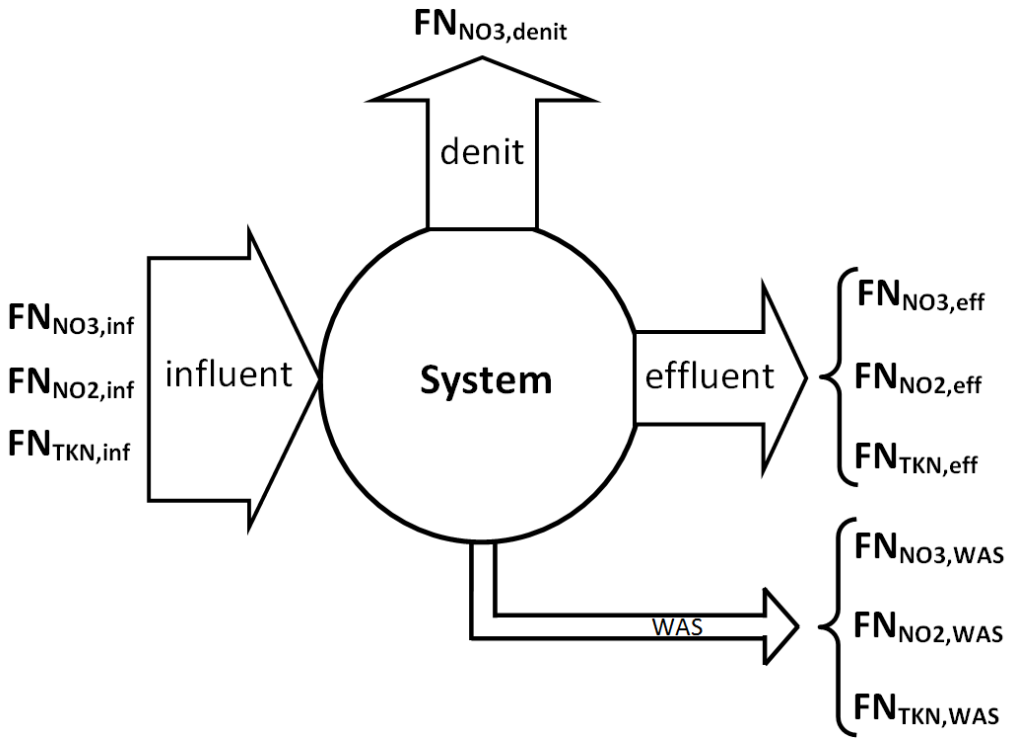

Figure 2-13: Components contributing to N mass balance calculation

(c.f. text for the notations)

$FN_{TKN,inf}$: mass rate of influent TKN (mg N/d)

$FN_{NO3,inf}$: influent NO_3^- mass rate (mg NO_3^--N/d)

$FN_{NO2,inf}$: influent NO_2^- mass rate (mg NO_2^--N/d)

$FN_{NO3,WAS}$: mass rate of NO_3^- in the sludge wastage (mg NO_3^--N/d)

$FN_{NO2,WAS}$: mass rate of NO_2^- in the sludge wastage (mg NO_2^--N/d)

$FN_{TKN,WAS}$: mass rate of TKN in the sludge wastage (mg N/d)

$FN_{NO3,eff}$: effluent NO_3^- mass rate (mg NO_3^--N/d)

$FN_{NO2,eff}$: effluent NO_2^- mass rate (mg NO_2^--N/d)

$FN_{TKN,eff}$: effluent TKN mass rate (mg N/d)

$FN_{NO3,denit}$: mass rate of NO_3^- denitrified (mg NO_3^--N/d)

$FN_{TKN,inf}$ is the product of influent TKN concentration (mg N/L) and the influent flow rate (L/d) given by Equation (2.65).

$$FN_{TKN,inf} = N_{TKN,inf} \times Q_{inf} \quad (2.65)$$

The TN entering the system (termed $FN_{TN,INPUT}$) equals $FN_{TKN,inf}$ if the influent NO_2^- and NO_3^- concentration is zero.

Similarly,

$$FN_{TKN,WAS} = N_{TKN,WAS} \times Q_{WAS} \quad (2.66)$$

$$FN_{NO3,WAS} = N_{NO3,WAS} \times Q_{WAS} \quad (2.67)$$

$$FN_{NO2,WAS} = N_{NO2,WAS} \times Q_{WAS} \quad (2.68)$$

$$FN_{TKN,eff} = N_{TKN,eff} \times Q_{eff} \quad (2.69)$$

$$FN_{NO3,eff} = N_{NO3,eff} \times Q_{eff} \quad (2.70)$$

$$FN_{NO2,eff} = N_{NO2,eff} \times Q_{eff} \quad (2.71)$$

where,

$N_{TKN,WAS}$: sludge wastage TKN concentration (mg N/L)

$N_{NO3,WAS}$: sludge wastage NO_3^- concentration (mg NO_3^--N/L)

$N_{NO2,WAS}$: sludge wastage NO_2^- concentration (mg NO_2^--N/L)

$N_{TKN,eff}$: effluent TKN concentration (mg N/L)

$N_{NO3,eff}$: effluent NO_3^- concentration (mg NO_3^--N/L)

$N_{NO2,eff}$: effluent NO_2^- concentration (mg NO_2^--N/L)

Q_{WAS}: wastage flow rate (L/d)

Q_{eff}: effluent flow rate (L/d)

TN leaving the system (Equation 2.72) termed $FN_{TN,OUTPUT}$ in mg N/d units is the summation of the Equations (2.66) through (2.71) as well as the $FN_{NO3,denit}$ discussed earlier (Equation 2.47).

$$FN_{TN,OUTPUT} = FN_{TKN,WAS} + FN_{NO3,WAS} + FN_{NO2,WAS} + FN_{TKN,eff} + FN_{NO3,eff} + FN_{NO2,eff} + FN_{NO3,denit} \quad (2.72)$$

Thus, N mass balance (%) is given by Equation (2.73).

$$\text{N mass balance (\%)} = (FN_{TN,OUTPUT}/FN_{TN,INPUT}) \times 100 \quad (2.73)$$

2.8.3 P mass balance calculation

Since phosphorus is a non-volatile compound, the mass of total phosphorus (TP) enters a system should be accounted for in the mass of TP leaving the system through effluent and sludge wastage streams (Figure 2.14). Therefore, P mass balance is given by Equation (2.74).

$$\text{P mass balance (\%)} = \left[\left(FP_{TP,eff} + FP_{TP,WAS}\right)/FP_{TP,inf}\right] \times 100 \quad (2.74)$$

where,

$FP_{TP,eff}$: effluent TP mass rate (mg P/d)

$FP_{TP,WAS}$: mass rate of TP in the sludge wastage (mg P/d)

$FP_{TP,inf}$: influent TP mass rate (mg P/d)

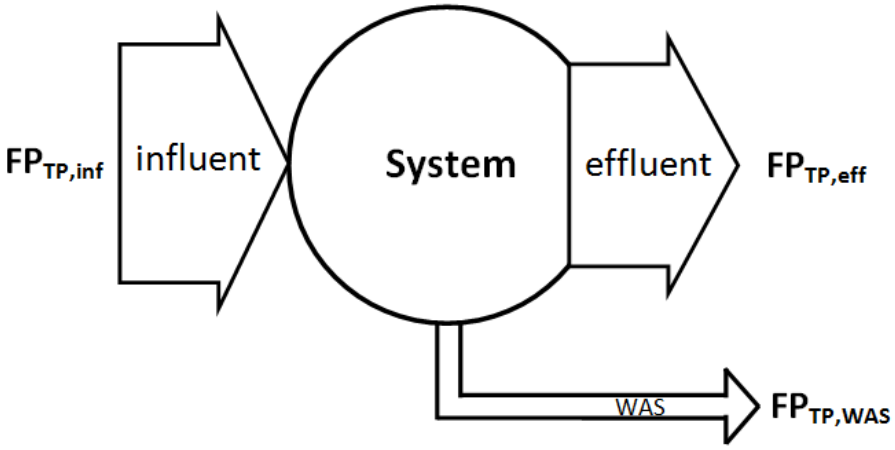

Figure 2-14: P mass balance components

(c.f. text for the notations)

The $FP_{TP,eff}$ is given by the product of effluent flow rate and effluent total phosphorus (TP) concentration (Equation 2.75).

$$FP_{TP,eff} = Q_{eff} \times P_{TP,eff} \quad (2.75)$$

Similarly,

$$FP_{TP,WAS} = Q_{WAS} \times P_{TP,WAS} \quad (2.76)$$

$$FP_{TP,inf} = Q_{inf} \times P_{TP,inf} \quad (2.77)$$

where,

Q_{eff}: effluent flow rate (L/d)

Q_{WAS}: sludge wastage flow rate (L/d)

Q_{inf}: influent flow rate (L/d)

$P_{TP,eff}$: effluent TP concentration (mg P/L)

$P_{TP,WAS}$: TP concentration in the sludge wastage (mg P/L)

$P_{TP,inf}$: influent TP concentration (mg P/L)

CHAPTER 3 HYPOTHESES AND OBJECTIVES

3.1 Hypotheses

COD loss in EBPR systems is due to fermentation processes producing reduced volatile compounds under anaerobic condition that are lost to the atmosphere by stripping either in the anaerobic or the subsequent aerobic zone. These volatile compounds are most likely hydrogen, possibly methane, hydrogen sulfide and possibly volatile fatty acids. Such anaerobic condition can be found in a reactor that is unaerated in the absence of nitrate/nitrite (AN reactor) or in their presence (AX reactor) but also in an OX reactor but inside thick enough flocs that would result in a gradient of dissolved oxygen or of nitrate such that an anaerobic condition would occur.

3.2 Originality justification

Prior studies have documented the loss of COD in EBPR systems but none has managed to quantify rigorously the mechanisms by which this loss of COD occurs.

3.3 Main objective

The main objective of this research was to quantify the COD loss in an EBPR system in which an OX reactor was preceded by a non aerated reactor that is either an AX or an AN reactor. With the goal of associating with the understanding the COD loss, this research conducted based on the specific objectives described below.

3.4 Specific objectives

To evaluate the COD loss in the EBPR process, a laboratory experimental study carried out mainly in three phases, which can be identified as follows:

Phase # 1: To assess the COD mass balance in OX – OX reactors in series configuration

Phase # 2: To evaluate the COD mass balance using an OX reactor preceded by an AX reactor

Phase # 3: To evaluate the COD loss using an OX reactor preceded by an AN reactor.

Phase # 3 was divided into two main sub-phases # 3A and 3B depending on the type of carbon source used. Citrate and acetate was used for phase # 3A and 3B, respectively.

CHAPTER 4 MATERIALS AND METHODS

This chapter provides a detailed description of the synthetic wastewater used, experimental equipments, configuration and system operation as well as the procedure of sampling and analysis of the samples. A time schedule describing when operation of each phase started and when the mass balances performed is provided in Appendix A.

4.1 Synthetic wastewater

A synthetic wastewater was used as a feed containing the requirements for growth of microorganisms. The chemical composition of stock solutions and the amount of each component are listed in Tables 4.1 and 4.2.

Table 4-1: Chemical composition and amount of each component in the stock solutions

	# Phase/concentration							
Component	Phase # 1	Phase # 2	Phase # 3					Units
			3A.1	3A.2	3A.3	3A.4	3.B	
solution (F1)								
$C_6H_5Na_3O_7.2H_2O$	7.80	3.90	3.60	3.80	3.80	3.90	-	g/L
$C_2H_3NaO_2.3H_2O$	-	-	-	-	-	-	3.90	g/L
$C_5H_7NO_2P_{1/12}$	0.03	0.03	0.03	0.03	0.03	0.03	0.03	g/L
$NaHCO_3$	0.40	3.80	0.40	0.40	0.40	0.40	0.90	g/L
solution (F2)								
$(NH_4)_2SO_4$	0.10	0.10	0.10	0.10	0.10	0.10	0.10	g/L
NH_4Cl	0.60	1.80	0.32	0.32	0.32	0.32	0.32	g/L
KH_2PO_4	0.33	0.33	0.80	0.80	0.80	0.80	0.80	g/L
$MgCl_2.6H_2O$	0.28	0.80	0.80	0.80	0.80	0.80	0.80	g/L
$C_{10}H_{14}N_2O_8Na_2.2H_2O$	0.07	0.07	0.07	0.07	0.07	0.07	0.07	g/L
KCl	-	0.40	0.10	0.10	0.10	0.10	0.10	g/L
solution (F3)								
$CaCl_2.2H_2O$	0.10	0.12	0.12	0.12	0.12	0.12	0.12	g/L

Note: A distinction made between phases # 1, 2 and 3As and 3B in sections 4.6.1 through 4.6.3.2.

Table 4-2: Chemical composition and amount of each component in the trace elements stock solution

Component	Quantity	Units
$Fe(NH_4)_2(SO_4)_2.6H_2O$	8.00	g/L
H_3BO_3	0.55	g/L
$CuSO_4.5H_2O$	0.20	g/L
KI	0.65	g/L
$MnSO_4.H_2O$	0.40	g/L
$Na_2MoO_4.2H_2O$	0.25	g/L
$ZnSO_4.7H_2O$	0.45	g/L
$CoCl_2.6H_2O$	0.50	g/L
$Al_2(SO_4)_3.(14\text{-}18)H_2O$	0.50	g/L
$NiSO_4.6H_2O$	0.20	g/L

Stock solutions were prepared using distilled water. The stock solution F1 contained carbon source, yeast extract and sodium bicarbonate. In phases # 1 and 2, citrate was used as carbon source while citrate and acetate (separately) examined in phase # 3 (citrate for phase # 3A and acetate for phase # 3B). Stock solution F2 contained macro nutrients (such as N, P, magnesium (Mg^{2+}), potassium (K^+) and SO_4^{2-}), and solution F3 was calcium-distilled water.

The weight of the chemical components to prepare the solutions was determined using a laboratory-analytical balance (Model E02140, Ohaus Explorer). The solutions were made up in 4-L Erlenmeyer flasks (KIMAX ®, KIMBLE, No. 26500, stopper No. 10) and stirred by agitator plate (No. cat. 11-500-78, Fisher Scientific) using magnetic stirrer bar to bring them in a proper solution.

Because trace elements (Cu, Zn, Fe, etc.) were not present in distilled water, a trace elements stock solution (Table 4.2) was prepared and 0.5 mL of it added per 1 L solution F2 (except for phases # 3A.3, 3A.4 and 3B).

In phases # 3A.3, 3A.4 and 3B, the amount of trace element solution increased from 0.5 to 2.0 mL per 1 L of the solution F2 to examine the possibility of sulfide precipitation (mainly FeS and Cu_2S) in the presence of SRO activities.

The solutions were transferred into three 10-L carboys (Nalgene™, Polypropylene Heavy-Duty). The carboys contained solutions F1and F2 were autoclaved at 120 ^oC for 45 minutes with a

SANYO Labo Autoclave (MLS-3780). It should be pointed that a volume of 24 L feed was prepared every two days.

4.2 Start-up sludge

The start-up sludge was taken from Saint-Hyacinthe WRRF, Quebec. Prior to use, the sludge was sieved using a 60 μm mesh to remove the solid particles (trash, debris).

4.3 System set-up

A continuous flow system involved two reactors in series (termed R1 and R2) carried out dividing into three main phases as follows:

- Phase # 1 (OX-OX): Each of the two reactors was operated under OX conditions. The synthetic wastewater used in this phase contained citrate as carbon source.
- Phase # 2 (AX-OX): Reactor R2 remained under OX conditions while reactor R1 was switched from OX to AX conditions. The same carbon source as phase # 1 was used for this phase.
- Phase # 3 (AN-OX): Reactor R2 was operated under OX conditions as phases # 1 and # 2 whereas reactor R1 was switched from AX to AN conditions by decreasing the influent ammonia and recycle flow rate. In this phase, citrate and acetate were separately used as carbon sources which both are readily biodegradable. Citrate could be fermented under AN conditions while acetate is non-fermentable.

In each phase, the objective was to evaluate the COD, N mass balances. Phase # 3 was divided into sub-phases # 3A.1, 3A.2, 3A.3, 3A.4 and 3B (it is discussed later).

A timeline showing the duration of each phase and experimental activities is provided in Appendix A.

4.4 Reactors system

Two cylindrical reactors (R1 and R2) in series configuration were used. The installation was constructed in the laboratory. The construction materials for reactors R1 and R2 were glass and plexiglas, respectively. Reactor R1 had an external coil (Nalgene tubing, 180 PVC, ¼ in ID × 3/8 in OD) and reactor R2 was a double jacket. The working volume and additional information regarding reactors dimensions is described in Table 4.3.

Table 4-3: Working volume and dimension of the reactors used in this study

Reactor	# Phase	Working volume		Liquid depth		Length: Diameter
		value	units	value	units	
R1	1 & 2	3.0	L	19.5	cm	3.3 : 1.0
R1	3	2.5	L	20.4	cm	2.0 : 1.0
R2	1, 2 & 3	7.0	L	22.3	cm	1.8 : 1.0

First, each reactor (R1 and R2) was operated under OX conditions, termed phase # 1. Reactor R2 was equipped with two modules of hollow fiber (HF) membrane (Zenon ZW-1 module), named complete mixed membrane bioreactor (MBR). Since the effluent was drawn through the membrane, no final clarifier used. To reduce the fouling difficulty, the membrane was modified as shown in Figure 4.1. It could be useful to maintain the membrane branches in movement and promote shear over its surface to minimize clogging.

Figure 4-1: HF Membrane

(right: ZW-1 module, left: modified ZW-1 module used);
length of fibers = 10 cm; flux = 0.1-0.5 $L.min^{-1}.m^{-2}$.

Some characteristics of HF membrane (Zenon ZW-1) are given in Table 4.4. Complete mixing in both reactors was provided by mechanical mixers (Stir-Pak dual shaft mixer, cole parmer, model 04555-25) positioned close to the reactors' bottom. A movable plate

connected to a motor was designed at the top of the MBR. A small hole was made in center of that plate in which the rod of mixer extended. The membrane modules were mounted on that plate to facilitate cleaning of the membrane modules by switching on the motor leading to moving up the plate. A Rushton turbine impeller with six vertical blades was used for mixing (Figure 4.2). A constant mixer speed of 100 and 175 rpm was maintained for reactor R1 and R2, respectively.

Table 4-4: Characteristics of HF membrane (Zenon ZW-1 module)

Parameter	Value		Units
module dimensions	length	diameter	cm
	17.5	5.8	
nominal pore diameter	0.08		µm
effective membrane surface area	0.047		sq m
operating transmembrane pressure	0.07-0.55		bar
operating pH range	5-9		
maximum feed suspended solids	25000		mg/L
Flux	0.1-0.5		$L.min^{-1}.m^{-2}$

Figure 4-2: Rushton turbine impeller with six vertical blades used in this study

(outside diameter: 5.0 and 7.5 cm for reactors R1and R2, respectively)

In phase # 2, AX-OX system, no changes were made to the reactor construction and configuration but only the condition in reactor R1 was switched from OX to AX by turning off the aeration and some changes in the feed composition that will be discussed later.

In phase # 3, AN-OX system, the reactor R1 used in phases # 1 and 2 was replaced with a New Brunswick Bioflo 110 reactor made up of glass with a total and working volume of 3 and 2.5 L, respectively. It was possible to seal it properly while feeding and mixing were provided. A Magmotor drive equipped with a Rushton turbine impeller with six vertical blades was used to keep the biomass in suspension. The side of the reactor was covered with aluminum foil to keep the light out. A schematic diagram of the system used in phase # 3 of this study is illustrated in Figure 4.3.

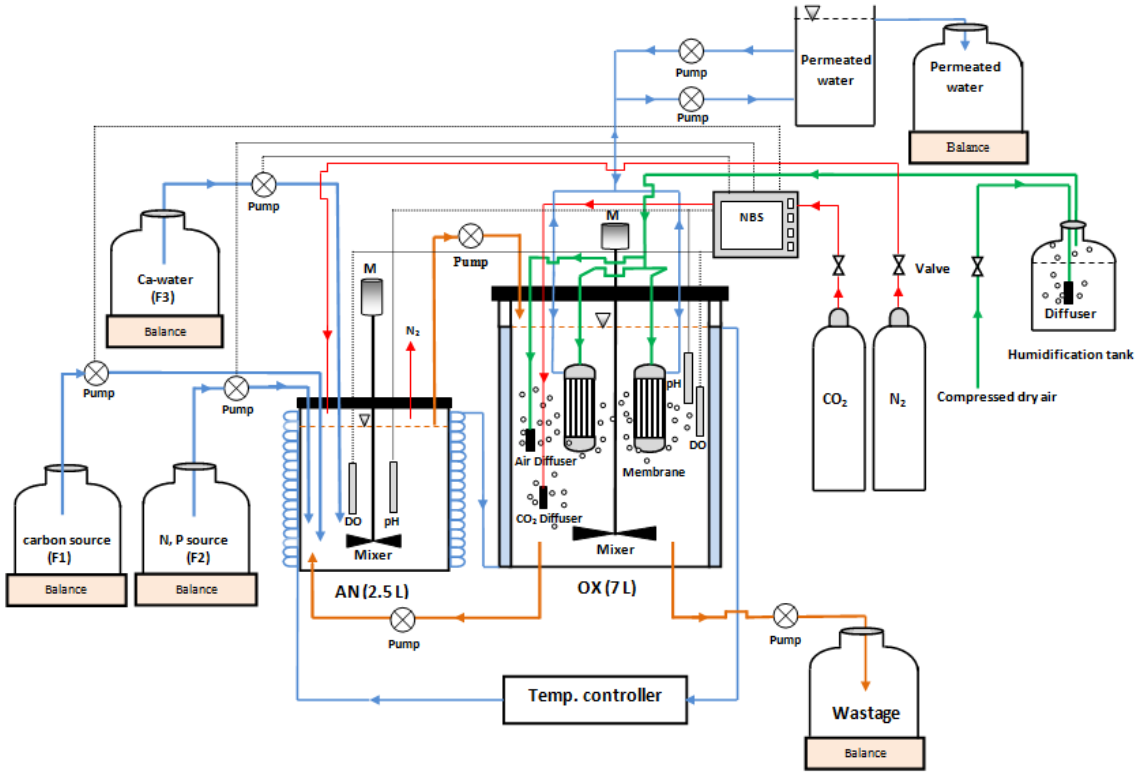

Figure 4-3: Schematic diagram of phase # 3 (AN-OX system).

Note: NBS: New Brunswick Scientific controller software (Model BioFlo 110)

4.5 Tubing lines

Silicon tubing (1/4 in ID × 3/8 in OD) was used for all three feeding peristaltic pumps. Norprene tubing (Masterflex ® 06402-25) was used for the head of other pumps in the system. The tubing extended from feed carboys to the reactor R1, and the connections between reactors were provided by Nalgene tubing (180 PVC, ¼ in ID × 3/8 in OD). The tubes were frequently cleaned using a thin flexible wire covered by a soft brush. Whenever needed, the tubes were replaced with new ones. It should be noted that the silicone tubing on the head of peristaltic pumps were changed every two week to keep a constant influent flow rate.

4.6 Operating conditions

4.6.1 Phase # 1 (OX-OX)

The system was continuously fed using peristaltic pumps (NBS Co., Inc., Model BioFlo110). Three pumps units were used to deliver the solutions F1, F2 and F3 through rigid rods to the reactor R1, near the bottom where the mixer impeller was positioned. The combined F1, F2 and F3 solutions entering the system contained the approximate COD: N: P ratio of 100: 5: 2 which corresponds to an average COD concentration of 980 mg COD/L. A pre-test to check the constancy of flow rate (as low as 2 ml/min) by the peristaltic pump showed that they could not offer a constant flow rate all the time and that the assumption of a constant nominal flow rate resulted in an experimental error. This problem was remedied by quantifying the mass of solutions entering the system instead of the flow rates. That is why the carboys contained the solutions were separately placed on the digital scales (Ohaus EC-series; AESL Instrumentation Inc., AND FP-12K) to determine the mass of solutions entering the system.

Initially, reactors R1 and R2 were positioned at different elevations to allow gravity flow from reactor R1 to R2. To prevent problem that may arise from clogging the connection tube between the two reactors, a Masterflex® pump (L/S series, Model No. 7523-80) was programmed to transfer the mixed liquor from reactor R1 to R2. A stainless steel rod connected to the pump inlet was positioned at the level in reactor R1 to maintain constant the volume needed. The flow rate of the pump was always higher than the summation of the feed and recycle flow rates.

A recycle flow was set up with a Masterflex® pump (L/S series, Model No. 7523-80) from reactor R2 and dispensed close to the bottom of reactor R1. The recycle-to-influent flow ratio (a) was 4.5 L/L. The influent flow rate and hydraulic retention time (HRT) is shown in Table 4.5.

The SRT was kept at about 10 days for all three phase. Regarding the volume of reactors, continuous wasting needed a flow rate of about 0.7 ml/min which could not be properly programmed. Thus, the SRT was controlled by wasting 1 L mixed liquor (once a day) directly from reactor R2 with a Masterflex® pump (console drive, model No. 7520-40, Cole-Parmer). The temperature of both reactors (R1 and R2) was regulated at 20 °C with a digital temperature controller (PolyScience, Model 9702). The reactors were equipped with pH and DO probes. The pH values were controlled by introducing CO_2 into the reactor R2 through a fine bubble diffuser stone. A CO_2 gas cylinder was equipped with a regulator (Model 25-50, Harris Calorific co., Ohio, USA). The cylinder and pH probe (NBS Co. Inc., ELEC, 405-DPAS-SC-K8S/225) were connected to a Gas/pH controller (NBS Co., Inc., Model BioFlo110) to adjust the pH at 7.8. A compressed air supply was applied to provide oxygen requirement in the reactors. The compressed air was initially passed through air filter to filter out the possible dust and then blown through a fine bubble diffuser stone into the reactors. It should be noted that the air was humidified in a carboy with minimum liquid depth of 0.5 meter before introducing into the reactors to minimize the evaporation from the liquid surface. The DO was adjusted between 6 and 7 mg O_2/L.

The membrane module was intermittently operated to minimize membrane fouling. The permeation and backwash pumps (Masterflex®, L/S® Series, Model NO. 7523-80) were programmed to operate in a cycle of 10 minutes of permeation which followed by 10 seconds relaxation and 1 minute of backwashing with permeated water. The chemical washing of membrane module was carried out once a month with a 0.02 % sodium hypochlorite (NaOCl) solution to recover its permeability.

4.6.2 Phase # 2 (AX-OX)

To move from phase # 1 to # 2, the in-line air shut off valve was switched off to stop blowing air to the reactor R1. A movable cover was designed but it was not properly sealed because the rod of mixer should have passed through a hole positioned in the center of the cover. Therefore,

oxygen transferring from liquid surface was inevitable. This term is considered in the COD mass balance calculation.

Initially, any changes were made in the feed composition and the system operated with a COD, TN and TP of about 1000 mg COD/L, 50 mg N/L and 20 mg P/L, respectively. The flow rates, temperature, pH and working volume of reactors were remained constant as phase # 1.

The initial goal was to be sure the reactor R1 was properly operating under AX conditions. To achieve this goal, enough amount of NO_3^- should be present in the reactor R1 but the summation of NO_3^- and NO_2^- was less than 1 mg N/L all the time. Therefore, ammonia in the feed was increased 5 mg NH_4-N/L every two days and alkalinity required was provided with sodium bicarbonate but, NO_3^- and NO_2^- were not appeared (less than 1 mg N/L) even ammonia concentration in the feed reached to 230 mg NH_4-N/L. It should be noted that starting from about 150 mg NH_4-N/L, the color of sludge changed from brown to yellowish brown and becoming viscous and more severe at concentration of 230 mg NH_4-N/L. It was observed that sludge attached and surrounded the impellers of mixer led to system failure. Thus, the entire sludge was replaced with fresh sludge taken from Sainte-Hyacinthe WRRF and some changes were made in the feed compositions. The feed contained a COD: TN: TP of about 500: 130: 20 compared to phase # 1 which was 1000: 50: 20. The concentration of cations such (Mg^{2+}) and (K^+) was increased about 2 times. Mg^{2+} concentration increased from 9 to 25 mg Mg/L and K^+ concentration from 25 to 75 mg K/L. Following these changes, that problem attributed to yellowish viscous sludge was not anymore encountered and the system worked properly. Enough amount of nitrate (about 35 mg NO_3^--N/l) was observed in AX reactor (reactor R1).

4.6.3 Phase # 3 (AN-OX)

To move from phase # 2 to # 3, initially, the reactor R1 was replaced with a New Brunswick Bioflo 110 reactor made up of glass with total and active volume of 3 and 2.5 L, respectively, which was properly sealed (shown in Figure 4.4). In addition, the liquid head space was continuously flushed with N_2 to be ensuring of the precise control of preventing oxygen transfer from surface. N_2 cylinder was equipped with Alphagaz high pressure regulator (Model No. 2500, Liquid Air Corp.).

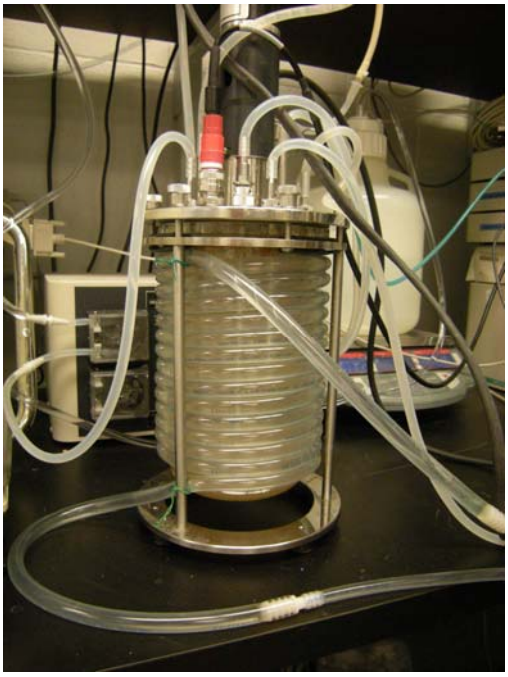

Figure 4-4: Photo of AN reactor used in phase # 3

(vol. = 2.5 L, liquid depth = 20.4 cm)

The parameters such as influent and wastage flow rates, volume of reactor R2, temperature and the mixers speed remained constant as phases # 1 and # 2. Based on the changes made in the feed composition, phase # 3 was divided into 2 main phases of # 3A and 3B described below.

4.6.3.1 Phase # 3A (AN-OX with citrate)

The carbon source remained as citrate and the system operated with the same influent COD concentration (about 500 mg COD/L) while the influent ammonia concentration and recycle-to-influent flow ratio (a) decreased from about 130 to about 30 mg N/L and 4.5 to an average value of about 2.6 L/L, respectively. The reason of this change was to minimize NO_3^- in the recycle stream entering AN reactor and to be sure that the reactor R1 did not become AX. Because the objective was to evaluate COD loss in an EBPR system, phosphorus concentration in the influent increased from 20 to about 50 mg P/L to prevent phosphorus limitation that could result from the growth of phosphate accumulating organisms (PAOs). The data derived from this phase categorized as sub-phases # 3A.1, 3A.2, 3A.3 and 3A.4 depending on PAOs activities.

4.6.3.2 Phase # 3B (AN-OX with acetate)

Citrate was replaced by acetate, termed phase # 3B. Because citrate is fermentable and acetate is non-fermentable, it could be a good indicator to focus on the effect PAOs and fermentation on COD mass balance in the systems incorporating an AN reactor. The feed flow rate and the HRT in reactors R1 and R2 with considering the recycle flow for all phases are described in Table 4.5.

Table 4-5: Design parameters of reactors R1 and R2 in this study

Phase	Q_{inf} (L/d)	Q_r (L/d)	Reactor R1				Reactor R2			
			volume	units	HRT	units	volume	units	HRT	units
1	12.2	55.0	3.0	L	1.1	h	7	L	2.5	h
2	11.9	52.4	3.0	L	1.1	h	7	L	2.6	h
3A.1	11.0	28.6	2.5	L	1.5	h	7	L	4.2	h
3A.2	11.8	30.7	2.5	L	1.4	h	7	L	4.0	h
3A.3	10.6	31.8	2.5	L	1.4	h	7	L	4.0	h
3A.4	10.9	21.8	2.5	L	1.8	h	7	L	5.1	h
3B	10.7	32.1	2.5	L	1.4	h	7	L	4.0	h

Note: Q_{inf}: influent flow rate; Q_r: recycle flow from the reactor R2 to R1

4.7 Oxygen mass transfer coefficient (k_La) determination

The COD mass balance for the systems are open to the atmosphere at the top is therefore influenced by oxygen transferred into the system. An experiment was performed to determine k_La in the reactors R1 and R2 using tap water. The reactors R1 and R2 contained the same liquid volume as operated (3 and 7 L, respectively). Temperature regulated at 20 °C and the mixers speed adjusted as mentioned in section 3.4.

4.7.1 Experiment procedure

The reactor R2 was partially filled up with 7 L tap water and then the recorder of DO and digital temperature controller were simultaneously started. When the temperature was stable at 20 ^oC, de-oxygenation of the reactor content performed. Amount of 50 mL of a solution containing 0.158 M Na_2SO_3 and 0.001 M $CoCl_2.6H_2O$ was added to the reactor. The mechanical mixer was

turned on and regulated at the appropriate speed (175 rpm). Then after, the reactor content was allowed to reach the saturation DO concentration by absorbing oxygen from liquid surface.

4.7.2 Equations

In non-steady state experiment, the expression describing the absorption rate of oxygen to the water can be defined as Equation (4.1).

$$\frac{dDO}{dt} = k_L a \times (DO_{sat.} - DO) \quad (4.1)$$

where,

$k_L a$: oxygen mass transfer coefficient (h^{-1})

$DO_{sat.}$: saturation DO concentration in water (mg O_2/L)

DO: oxygen concentration in water at time t (mg O_2/L).

Integrating of the Equation (4.1) results in Equation (4.2).

$$\ln(DO_{sat.} - DO) = -k_L a \times t + const \quad (4.2)$$

The same approach was followed for reactor R1.

4.8 OUR measurement technique

OUR is an indicator to evaluate the activity of microorganism in an aerobic activated sludge process. It can be calculated by determination the amount of oxygen which is consumed by bacteria during a short period. In general, OUR can be estimated by two different methods: in-situ and biochemical oxygen demand (BOD) bottle method. In this study, the former method was performed as described below.

The in-line air shut off valve was switched off to stop introducing air into the reactor and the decline in DO concentration recorded. The slope of the straight line obtained from plotting of DO concentration over time represents the negative value of OUR, termed measured OUR (OUR_{meas}). It should be noted that during the period of non-aeration, the mixer and the feeding pump were on.

The OUR_{meas} was corrected (termed biomass OUR (OUR_B)) due to oxygen mass transfer through liquid surface and oxygen entering the system via liquid streams (discussed in Chapter 2).

4.9 Measurement of dissolved H_2 in AN reactor

A technique of in-situ used for dissolved H_2 measurement in AN reactor (Figure 4.5). The mixed liquor from AN reactor was continuously pumped using a Masterflex® pump (L/S series, Model No. 7523-80) through a Norprene tubing (Masterfelex ® 06402-25) to a glass bottle with a volume of approximately 40 mL. Another Masterflex® pump was installed to return back the mixed liquor to the AN reactor. The pumps were operated at the flow rates to give an HRT of about 10 seconds. The bottle was capped with rubber stopper and all the time full of mixed liquor with no headspace. In the centre of the rubber stopper, a hole was made through which a H_2 probe (MS08-multi sensor, AquaMS) with detection limit of 0.02 µg/L extended to monitor dissolved H_2 over a period of 3 hours.

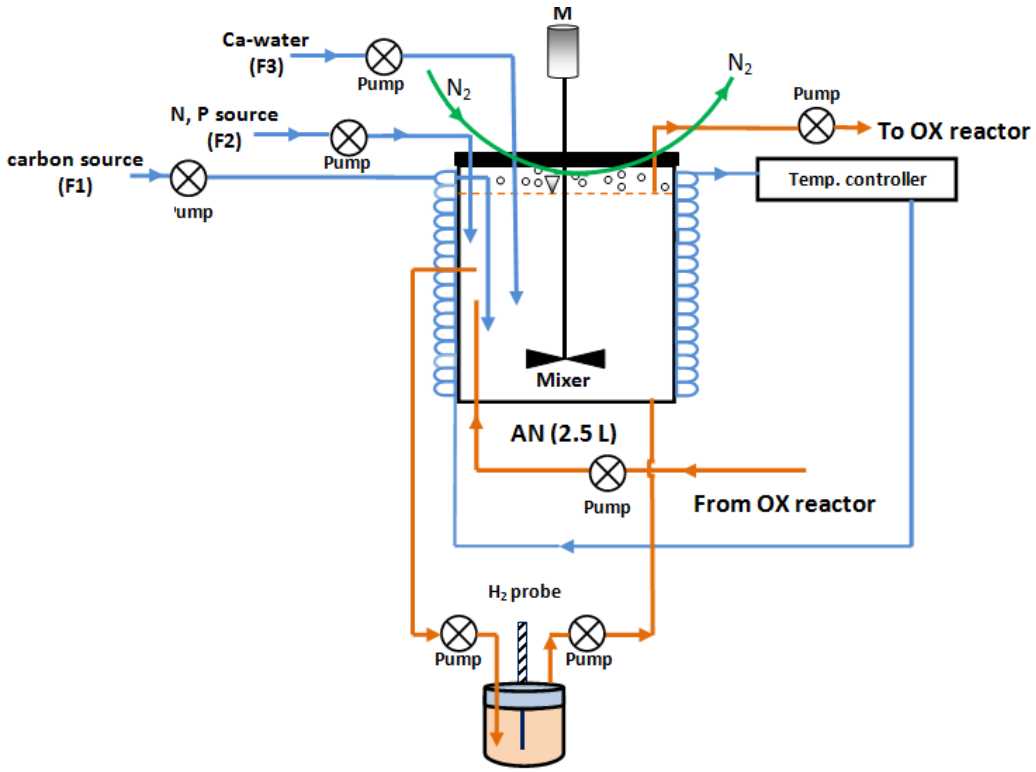

Figure 4-5: Schematic of lab-scale AN reactor (measurement of dissolved H_2)

4.10 Determination of dissolved CH_4 in AN reactor

Two methods were used for determination of dissolved CH_4 based on GC technique as follows:

Method 1: Serum bottles (40 mL EPA vials) were used to collect the AN mixed liquor samples. The mixed liquor was slowly transferred into the vials to push out the air. The vials were

completely filled up with no head space. After collection, they were capped and sealed. The vials with ice packs were shipped to RPC (Research and Production Council) laboratory in Fredericton (New Brunswick, Canada) where the headspace was generated from the samples and analyzed for CH_4 using GC technique with a flame ionization detector (FID).

Method 2: Glass tubes with a total volume of 11 mL were partially filled with AN mixed liquor. The headspace of the tubes was gently flushed with N_2, immediately capped and severely agitated for 10 min to establish equilibrium between gas and liquid phases. The headspace of the tubes was sampled for CH_4 analysis using SCION 456 GC-FID.

4.11 Batch tests:

4.11.1 Aerating and mixing induced stripping of acetate

A batch test was performed to evaluate whether or not acetate would strip under aerating and mixing. The test was conducted in a glass cylindrical reactor which had an active volume and liquid depth of 8.4 L and 25 cm, respectively. The reactor was equipped with a fine bubble diffuser stone, a Rushton turbine mixer and a pH probe. Sodium acetate solution was prepared using distilled water with initial COD concentration of about 45 mg COD/L and poured in the reactor. The in-line air vale and mixer were simultaneously switched on. The aeration rate and mixer speed were adjusted at 5 l/min and 175 rpm, respectively. The pH was controlled at 6.0 using HCl 1M throughout the test. The samples were taken within the interval of 0-30 (0, 3, 5, 10 and 30 minutes) for COD analysis. The test was repeated at pH of 4, 5, 7 and 8.

4.11.2 H_2 stripping test

A 1000 mL graduated cylinder (KIMAX®, KIMBLE, No. 20023) was equipped with a fine bubble diffuser (2 cm diameter × 2.5 cm high) positioned at the bottom. The cylinder was filled with 750 mL distilled water. Hydrogen gas (purity grade of 99.99 %) with a flow rate of 2.5 l/min was bubbled into the contents of cylinder through the diffuser for a period of 120 minutes. The distilled water samples were analyzed for COD at several intervals (0, 3, 5, 30, 60 and 120 minutes).

The test conducted at room temperature in a hood. A photograph of the experimental set-up used is shown in Figure 4.6.

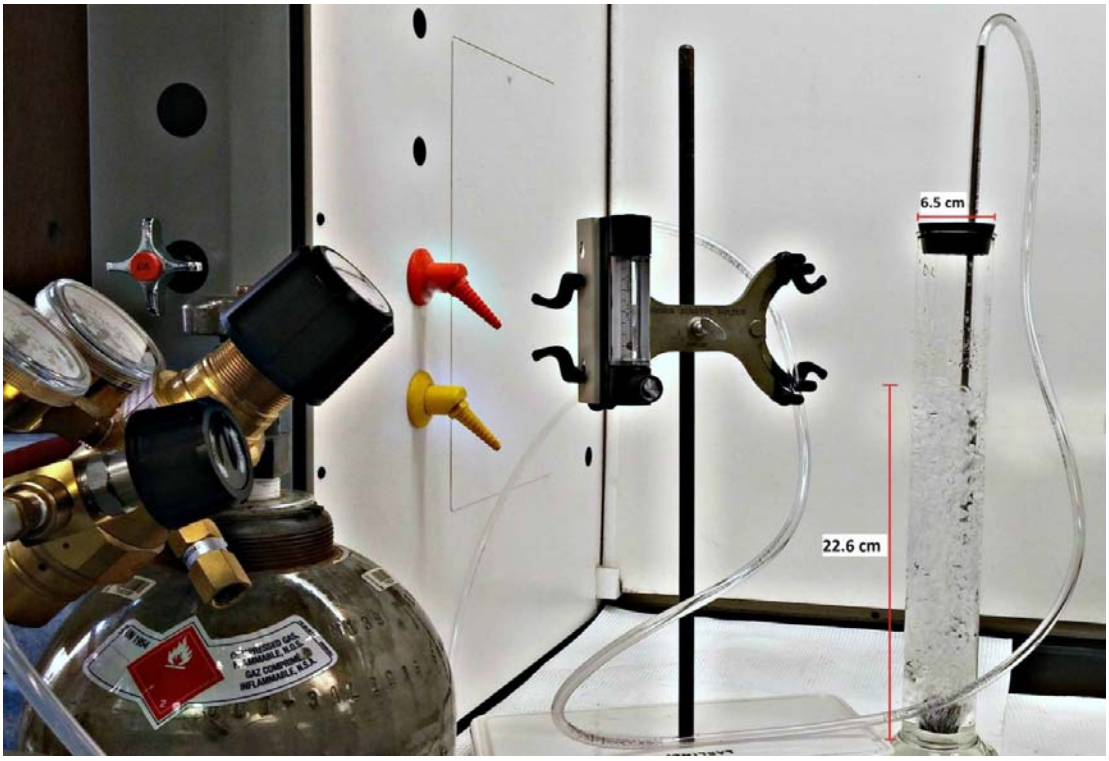

Figure 4-6: Photograph of the set-up used in the H_2 stripping batch test

4.12 COD test limitation

A test performed to investigate the hypothesis that the COD test limitation may underestimate the COD leading to a COD loss in EBPR systems.

Poly (3-hydroxybutyrate-co-3-hydroxyvalerate), known as PHBV, was chosen as a metabolic product in EBPR systems that may be subject to the COD test limitation. A PHBV sample was provided from a polymer laboratory in chemical engineering department (Ecole polytechnique de Montreal), and its theoretical COD value compared with the measured value.

4.13 Sampling procedure

This section briefly describes the sampling procedure locations where the samples collected (Figure 4.7 and Table 4.6).

4.13.1 Influent

- A sample was taken from the carbon source solution (F1) line at the point of entering reactor R1 (point 'a' in Figure 4.7) and analyzed for COD, total Kejeldahl nitrogen (TKN) and TP.
- The N and P source solution (F2) was sampled at the point 'b' (Figure 4.7). The COD, TKN, TP and SO_4^{2-} measurements were performed.
- Since some measurements on different days showed that calcium-distilled water line (F3) was free of COD, TKN and TP, no more attempts made throughout this study. It should be mentioned that the tube line was cleaned every two days.

4.13.2 Effluent

A volume of 100 mL of effluent was collected at the outlet of reactor R2 (point 'e' in Figure 4.7) and initially divided into fractions (A) and (B).

- Fraction (A): It was filtered through a 0.45 μm sterilized membrane filter (Pall membrane, 47 mm GN-6 Grid) for NO_2^-, NO_3^-, NH_4, o-PO_4^{3-} and SO_4^{2-} analysis.
- Fraction (B): This fraction (termed unfiltered) was analysed for COD, TKN and TP.

4.13.3 Mixed liquor (reactor R2)

A volume of 200 mL of mixed liquor was collected from reactor R2 (point 'd' in Figure 4.7) and stirred by agitator plate using a magnetic stirrer bar to be homogenized. Amount of 40 mL placed in a 50 mL-plastic tube and kept at 4 ^oC for TKN and TP analysis. The 160 mL remained was initially analysed for total suspended solids (TSS), volatile suspended solids (VSS) and COD, and the rest, filtered through a 0.45 μm sterilized membrane filter for further analysis (such as NO_2^-, NO_3^-, NH_4, o-PO_4^{3-} and SO_4^{2-}).

4.13.4 Mixed liquor (reactor R1 effluent)

The same procedure as mentioned in section 4.13.3 (except TKN and TP analysis) was followed for the sample taken from reactor R1 effluent (point 'c' in Figure 4.7). TKN and TP were not measured because the objective was to evaluate N and P mass balances for the whole system R1-R2.

It should be pointed that the volume of mixed liquor for analysis was accounted for within normal daily wasting.

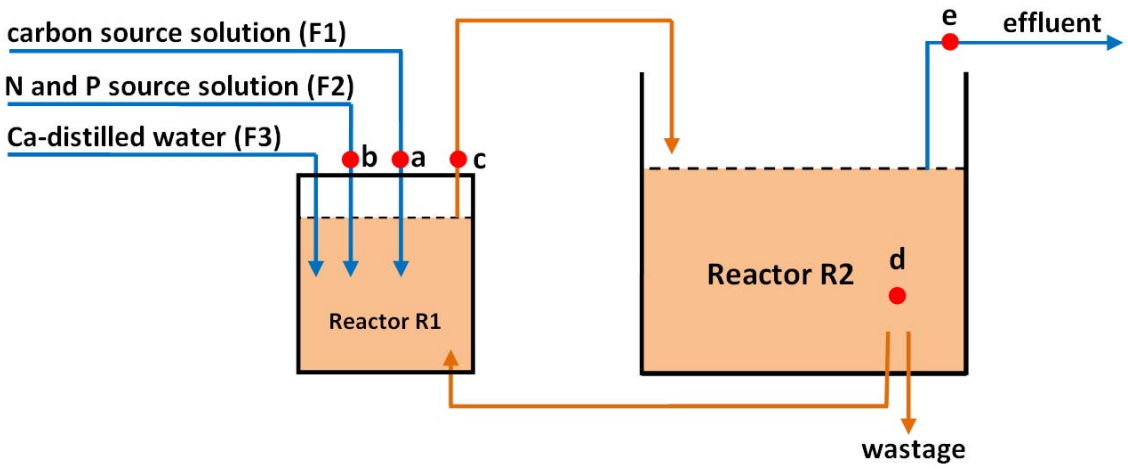

Figure 4-7: Sampling locations for this study

Table 4-6: Type of analysis and sampling locations

Sampling points	Total COD	Soluble COD	TKN	NH_4	NO_2^-	NO_3^-	TP	PO_4^{3-}	SO_4^{2-}	TSS	VSS
a	×		×				×				
b	×		×				×		×		
c	×	×		×	×	×		×	×	×	×
d	×	×	×	×	×	×	×	×	×	×	×
e	×		×	×	×	×	×	×	×		

Note: oxygen uptake rate in reactor R1 for phase # 1, and in reactor R2 for all phases were also determined.

4.14 Analytical methods

4.14.1 COD

The COD analysis was performed according to the Standard Method for the Examination of Water and Wastewater (APHA et al., 2012) using Hach COD vial and DR 2800

Spectrophotometer. Depending on the COD strength of the samples, high range (20-1500 mg COD/L), low range (3-150 mg COD/L) or ultra low range (0.7-40 mg COD/L) COD vials was used.

- *Accuracy and precision*

The accuracy and precision of Hach's COD vials examined using a standard solution of potassium hydrogen phthalate (KHP) described in Table 4.7.

Table 4-7: Hach COD tubes precision and accuracy

Standard solution	COD concentration				CV		number of replicate	Ref.
	avg	units	std	units	value	units		
KHP	193	mg COD/L	± 17	mg COD/L	8.7	%	48[1]	[2]
	22	mg COD/L	± 0.4	mg COD/L	1.7	%	10	this study
	100	mg COD/L	± 1	mg COD/L	1.4	%	10	
	797	mg COD/L	± 5	mg COD/L	0.6	%	10	

Note**:** CV: coefficient of variation; [1]for 48 samples analyzed by 5 laboratories; [2]APHA et al. (2012).

4.14.2 Solids

- TSS

The TSS was measured according to the Standard Methods for the Examination of Water and Wastewater (APHA et al. 2012). The glass microfiber filter 1.2 µm (Whatman, 934-AH^{TM}, circle 47 mm ∅, Cat. No. 1827 047) was used for filtration.

- VSS

The VSS was measured according to the Standard Methods for the Examination of Water and Wastewater (APHA et al. 2012).

4.14.3 pH

The pH was measured with a pH meter (NBS Co. Inc., ELEC, 405-DPAS-SC-K8S/225). Over this study, the pH value was controlled by introducing CO_2 into the OX reactor. Both CO_2

cylinder and pH probe were connected to a Gas/pH controller (NBS Co., Inc., Model BioFlo110) to regulate the pH on 7.8. The probe was calibrated once a week.

4.14.4 DO

The DO was determined with a DO meter (NBS Co. Inc., Model InPro6110/220). DO probe was calibrated once a week.

4.14.5 Temperature

The temperature of both reactors was regulated at 20 °C with a digital temperature controller (PolyScience, Model 9702). Reactor R1 was equipped with external coil (Nalgene tubing, 180 PVC, 1/4 in ID × 3/8 in OD) and R2 was a double jacket reactor.

4.14.6 TP and TKN

TP and TKN analysis performed with a Flow Injection Analyzer Lachat. The model of Quick Chem AE (10-115-01-1C) and (10-107-06-2D) were used for TP and TKN, respectively.

4.14.7 Ammonia, NO_2^- and NO_3^-

Ammonia, NO_2^- and NO_3^- measurements were performed according to Hach methods as described in Table 4.8.

Table 4-8: Hach methods for NO_2^- and NO_3^- and ammonia analysis

Parameter	Method		conc. range	Units
NO_2^-	No. 8153	Ferrous sulfate	0.6 – 76.1	mg NO_2^--N/L
	No. 10207	Diazotization	0.015 – 0.600	mg NO_2^--N/L
NO_3^-	No. 10020	Chromotropic acid	0.2 – 30.0	mg NO_3^--N/L
	No. 8192	Cadmium reduction	0.01 – 0.50	mg NO_3^--N/L
ammonia	No. 10031	Salicylate	0.4 – 50.0	mg NH_3-N/L
	No. 8155	Salicylate	0.01 – 0.50	mg NH_3-N/L

4.14.8 SO_4^{2-} and o-PO_4^{3-}

SO_4^{2-} and o-PO_4^{3-} analysis performed according to Hach method (SulfaVer 4 Method, Method 8051, range: 0.7 – 23.3 mg SO_4^{2-}-S/L) and (No. 8114, Molybdovanadate method, range: 0.3 – 32.6 mg PO_4^{3-}-P/L), respectively.

4.14.9 Dissolved hydrogen

Dissolved H_2 was measured using a H_2 probe (MS08-multi sensor, AquaMS) with a detection limit of 0.02 µg/L.

4.14.10 Dissolved methane

The head space generated from the liquid sample was analyzed using GC-FID for CH_4 and then the dissolved CH_4 determined according to Henry's law.

CHAPTER 5 RESULTS AND DISCUSSION

This chapter provides an overview of phases studied and discusses phosphorus removal and sulfate reduction results obtained during this research.

The result of a typical experiment for k_La and biomass OUR determination which are the important factors affecting the COD mass balance followed by the COD and N mass balances results.

The most probable causes contributing to the observed COD loss are interpreted.

In addition, the chapter provides:

- Sensitivity analysis on COD loss for aeration correction factors α and β,
- Interpretation of the COD mass balance results around separate reactors AN and OX,
- Statistical analysis of the COD mass balance results and
- Comparison of the oxygen consumption and the observed yield obtained for phases studied.

5.1 Overview of phases studied

The operational parameters and influent characteristics for each phase (# 1, 2, 3A and 3B) are briefly summarized in Table 5.1.

Phase # 1 (OX-OX):

The influent synthetic wastewater contained citrate as a sole carbon source. The concentrations of COD, N, P and SO_4 in the influent were about 980 mg COD/L, 50 mg N/L, 20 mg P/L and 6 mg SO_4-S/L, respectively. The working volume of reactors R1 and R2 was 3 and 7 L giving an HRT of about 1.1 and 2.5 hours, respectively. The pH value was adjusted at 7.8 and recycle ratio with respect to the influent flow rate was about 4.5 L/L. The system operated at an SRT and temperature of 10 days and 20 °C, respectively.

Phase # 2 (AX-OX):

The influent COD and N concentrations were about 500 mg COD/L and 130 mg N/L, respectively. No more significant changes made compared to phase # 1 except aeration in the reactor R1 stopped.

Phase # 3A (AN-OX):

Phase # 2 moved to phase # 3A with respect to the following changes:

- Influent N concentration decreased from 130 to about 30 mg N/L to minimize nitrate concentration in the AN reactor,
- Phosphorus concentration in the influent increased from 20 to about 50 mg P/L to prevent phosphorus limitation for PAOs growth,
- Recycle ratio decreased from 4.5 to a value ranging between 2 and 3 L/L,
- This phase divided into sub-phases # 3A.1, 3A.2, 3A.3 and 3A.4 because it was observed that PAOs were active or non active throughout phase # 3A,
- Influent Iron concentration increased from 0.1 to about 0.5 Fe/L in phases 3A.3 through 3B.

Phase # 3B (AN-OX):

The significant difference between phases # 3A and 3B was that the carbon source changed from citrate in phase # 3A to acetate in phase # 3B.

Table 5-1: Summary of operational data and concentration of various compounds over phases studied

# Phase	Flow rate				DO		SRT		HRT			a[1]	
	Inf	Eff	Sludge wastage	Units	Value	Units	Value	Units	# R1	# R2	Units	Value	Units
1 (OX-OX)	12.2	11.2	1.0	L/d	6.5	mg O_2/L	10.0	day	1.1	2.5	h	4.5	L/L
2 (AX-OX)	11.9	10.8	1.0	L/d	6.5	mg O_2/L	10.0	day	1.1	2.6	h	4.4	L/L
3A.1 (AN-OX)	11.0	9.9	1.0	L/d	6.5	mg O_2/L	9.5	day	1.5	4.2	h	2.6	L/L
3A.2 (AN-OX)	11.8	10.6	1.0	L/d	6.5	mg O_2/L	9.5	day	1.4	4.0	h	2.6	L/L
3A.3 (AN-OX)	10.6	9.3	1.0	L/d	6.5	mg O_2/L	9.5	day	1.4	4.0	h	3.0	L/L
3A.4 (AN-OX)	10.9	9.7	1.0	L/d	4.0	mg O_2/L	9.5	day	1.8	5.1	h	2.0	L/L
3B (AN-OX)	10.7	9.5	1.0	L/d	3.5	mg O_2/L	9.5	day	1.4	4.0	h	3.0	L/L

Note: [1]a: recycle ratio with respect to the influent flow rate;
The volume of reactors R1 and R2 was 3.0 and 7.0 L, respectively, except for phase # 3 with a volume of 2.5 L for reactor R1;
All phases were conducted using citrate as sole carbon source except for phase # 3B with acetate;
Inf: influent, Eff: Effluent.

Table 5-1: Summary of operational data and concentration of various compounds over phases studied (continued)

Phase	Influent				Reactor R1				Effluent						WAS				
	COD	TP	TKN	SO_4	NO_2	NO_3	o-PO_4	SO_4	COD	TP	TKN	SO_4	NO_3	NO_2	TSS (mg/L)	VSS (mg/L)	f_{VT} (g VSS/g TSS)	% f_P (g P/g VSS)	COD
1	979	19.0	46.8	6.0	nd	nd	nd	nd	13	16.3	1.3	nd	25	0.8	2402	2231	0.93	1.4	3398
2	538	19.6	128	6.0	< 0.1	33.0	nd	nd	25	17.6	0.4	nd	54	0.5	1116	1031	0.92	1.5	1561
3A.1	528	47.5	29.2	6.0	< 0.1	0.4	46.7	nd	7	46.1	0.4	nd	5.6	0.2	941	869	0.92	1.7	1410
3A.2	486	50.9	30.5	6.0	< 0.1	0.3	54.3	0.8	6	45.7	1.3	5.7	5.0	< 0.1	1146	963	0.84	5.0	1445
3A.3	521	51.4	30.8	6.1	< 0.1	0.7	51.3	3.5	10	50.1	0.5	4.0	5.2	0.1	1067	976	0.91	2.0	1446
3A.4	548	44.6	30.0	5.7	< 0.1	0.1	66.0	0.7	8	33.3	1.0	0.7	6.2	< 0.1	1348	855	0.63	13.0	1321
3B	516	43.2	29.1	5.8	< 0.1	0.4	61.1	0.7	11	31.6	0.5	0.7	5.3	< 0.1	1401	887	0.63	12.1	1352

nd: not determined; N and P compounds in mg N/L and mg P/L, respectively; COD and SO4 in mg COD/L and mg S/L, respectively.

5.2 Phosphorus removal

Values obtained for amount of phosphorus captured in the biomass (f_P) during phases studied are presented in Figure 5.1. For phases # 1 and 2, f_P value was about 1.5 % mg P/mg VSS which is in good agreement with typical f_P values ranging between 1.35 and 2.0 % (Hoover and Porges, 1952; Henze et al., 2008; Cretu and Tobolcea, 2005).

- For phases # 3A.1 and 3A.3, the f_P value ranged between 1.7 to 2.0 % mg P/mg VSS indicating these two phases operated as a non-EBPR system,
- For phase # 3A.2, the f_P value increased from 3.5 to 7.5 % mg P/mg VSS, indicating that the biomass was capable of removing increasingly more phosphorus,
- For phases # 3A.4 and 3B, f_P was about 13 % mg P/mg VSS indicating efficient EBPR.

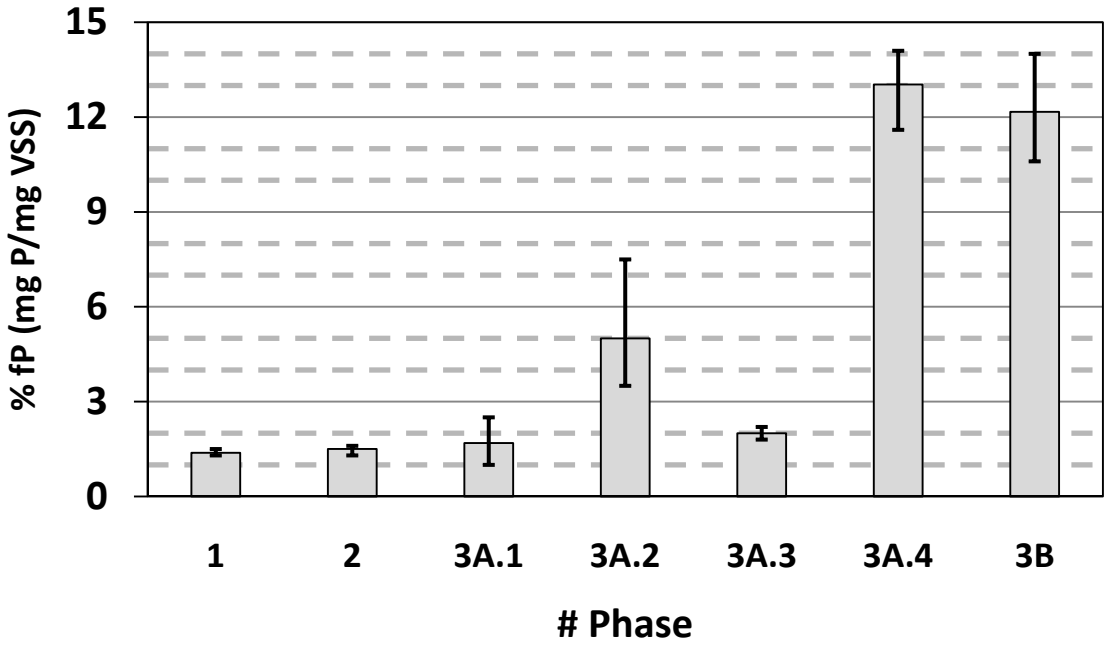

Figure 5-1: Observed changes in f_P values during phases # 1 through 3B

The amount of phosphate release and uptake on the basis of mg phosphorus per liter of influent on days 40-42 for phase # 3A.4, and days 43-45 for phase # 3B is presented in Figure 5.2

(phosphorus release being positive; phosphorus uptake being negative). Phosphate concentration in the influent, AN reactor and effluent are also presented.

The amount of phosphate release and uptake in phase # 3A.4 averaged 91 and 108 mg phosphorus per liter influent. The figure illustrates an average value of 112 and 128 mg phosphorus per liter influent for phosphate release and uptake, respectively, in phase # 3B. These findings suggest that PAOs were capable of growing either using citrate or acetate as carbon source.

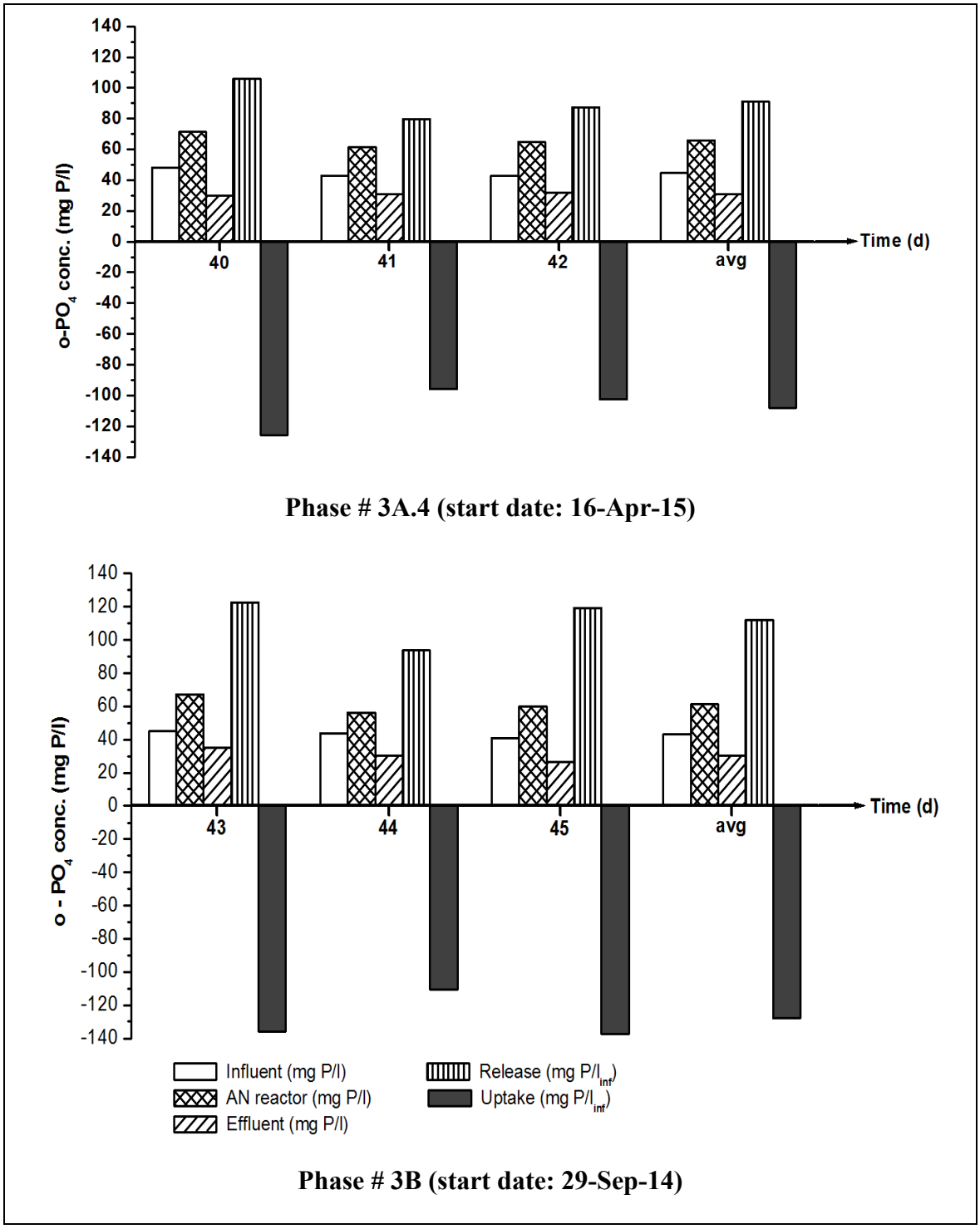

Figure 5-2: Phosphate release and uptake as well as comparison of phosphate in the influent, AN reactor and effluent (Phases # 3A.4 and 3B)

The good phosphorus removal observed in phases # 3A.4 and 3B compared to phases # 3A.1-3A.3 was associated with lower recycle ratio in phase # 3A.4 and DO concentration in the OX reactor of both 3A.4 and 3B phases:

- *Recycle ratio:*

The recycle ratio in phase # 3A.4 was 2 L/L while it ranged between 2.6 and 3 L/L during phases # 3A.1 and 3A3,

- *DO concentration in the OX reactor*:

DO concentration in the OX reactor in phases # 3A.4 and 3B was 4 and 3.5 mg O_2/L, respectively, compared to 6.5 mg O_2/L in phases # 3A.1-3A.3.

The main point is that the AN reactor in phases # 3A.4 and 3B received a lower nitrate and oxygen loads resulted in good phosphorus removal (Table 5.2). Although nitrate loading to the AN reactor in phase # 3A.2 was lower than that in phases # 3B, it received a higher oxygen load. It can be concluded that the presence of oxygen in AN reactor of EBPR systems can negatively affect phosphorus removal efficiency.

Table 5-2: Nitrate and oxygen loading to AN reactor in phases # 3A.1 through 3B

# Phase	Nitrate load		Oxygen load	
	Quantity	Units	Quantity	Units
3A.1	175	mg NO_3-N/d	283	mg O_2/d
3A.2	165	mg NO_3-N/d	308	mg O_2/d
3A.3	191	mg NO_3-N/d	311	mg O_2/d
3A.4	136	mg NO_3-N/d	185	mg O_2/d
3B	172	mg NO_3-N/d	212	mg O_2/d

5.2.1 Phosphorus mass balance

Phosphorus mass balances during phases studied (# 1 to 3B) ranged between about 96 and 100%. These findings highlight that phosphorus mass balance in activated sludge system either under OX or unaerated (AX/AN) conditions should be close to 100%.

5.3 Sulfate reduction

This section discusses the results of sulfate reduction/sulfide oxidation for phases # 3A.2, 3A.3, 3A.4 and 3B.

The comparison of sulfate concentration in the influent with that in the AN reactor and the effluent in phases # 3A.2 through 3B are illustrated in Figure 5.3. Influent sulfate concentration throughout all phases was about 6 mg SO_4-S/L. It was reduced under AN conditions and maintained constant at a value of 0.7 mg SO_4-S/L (approximately 90 % reduction) in phase # 3A.2. The Figure shows that the effluent sulfate concentration did not significantly change compared to that in the influent. It can be concluded that the sulfate reduced under anaerobic conditions was reoxidized under aerobic conditions.

The influent sulfate concentration was reduced by about 45 % during phase # 3A.3 while it was reduced by about 90 % during all other phases. This major difference was connected with the amount of nitrate entering the AN reactor. The mass rate of nitrate introduced in the AN reactor via recycle flow was about 191 mg NO_3-N/d in phase # 3A.3 whereas it ranged from about 136 to 172 during phases # 3A.2, 3A.4 and 3B. Anaerobic sulfate reduction appears to have been negatively affected by the higher nitrate load.

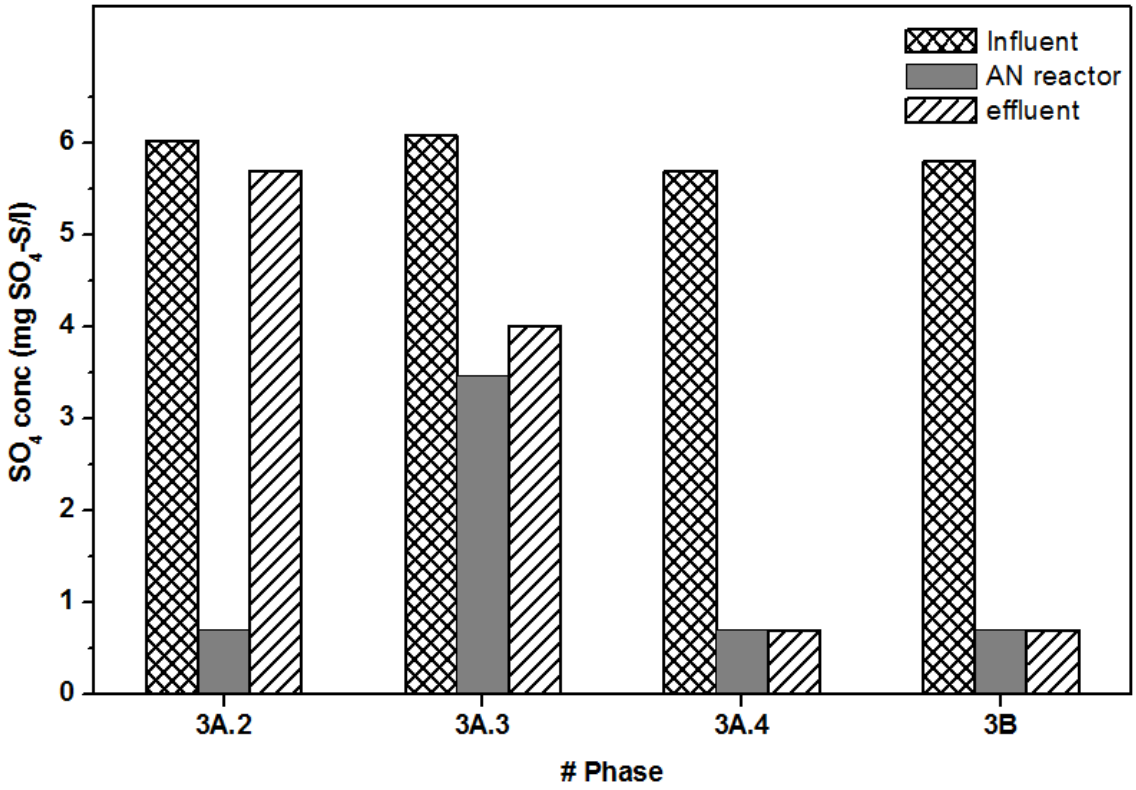

Figure 5-3: Comparison of sulfate concentration in the influent, AN reactor and effluent (Phases # 3A/B)

Note: sulfate concentration was not determined during phase # 3A.1.

The influent sulfate reduced in the AN reactor was not much reoxidized during phases # 3A.3, 3A.4 and 3B in comparison to phase # 3A.2. A black precipitate observed on the inside wall of the tube transferring mixed liquor from the AN reactor to the OX reactor (Figure 5.4). It is seems that the influent sulfate was anaerobically reduced to sulfide which then reacted with heavy metals (particularly iron) present in the influent resulting in the removal of some soluble sulfide in the form of a black precipitate.

Influent iron concentration in phase # 3A.2 was about 0.1 mg Fe/l and it was increased to about 0.5 mg Fe/l for phases # 3A.3, 3A.4 and 3B. This change may have resulted in a black precipitate of iron sulfide (the sulfur contribution in COD mass balance calculation is discussed in section 5.7.1).

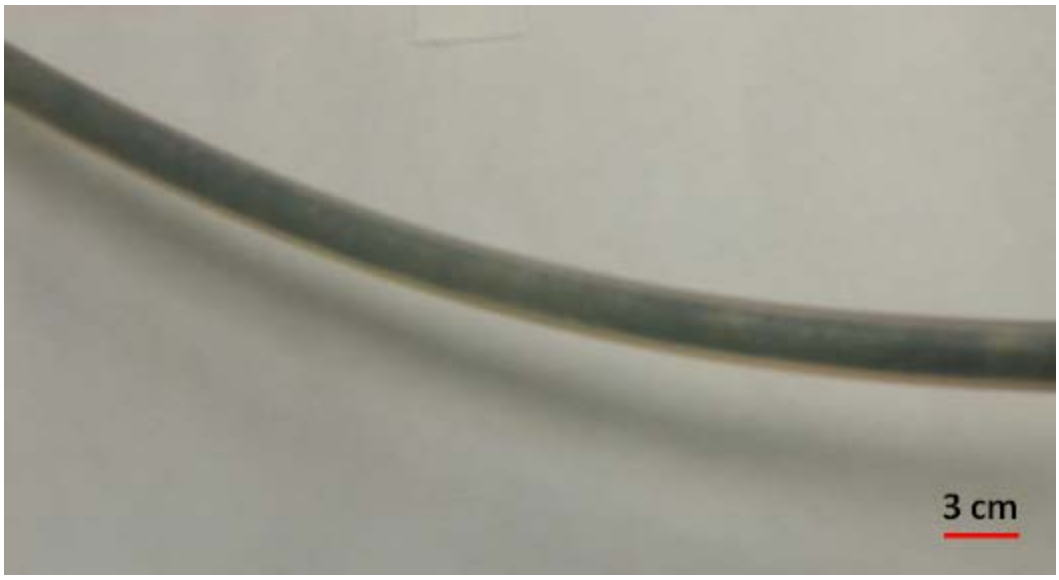

Figure 5-4: Black precipitate observed on the inside wall of the tube (1/4 in ID × 3/8 in OD) transferring mixed liquor from AN reactor to the OX reactor (Phase # 3B)

5.4 k_La evaluation

A typical profile of the DO concentration against time during an experiment (for reactor R2) and k_La obtained are shown in Figure 5.5 and 5.6. Since the amount of sodium sulphite (Na_2SO_3) added for de-oxygenation of tap water was twice the theoretical value, the DO concentration at the beginning of the experiment remained at zero until all of the added Na_2SO_3 was completely oxidized.

k_La value using clean water and process water is not the same. Therefore, Equation (2.25) was applied for correcting the k_La value. The k_La measured and used values for reactors R1 and R2 to perform COD mass balances are summarized in Table 5.3.

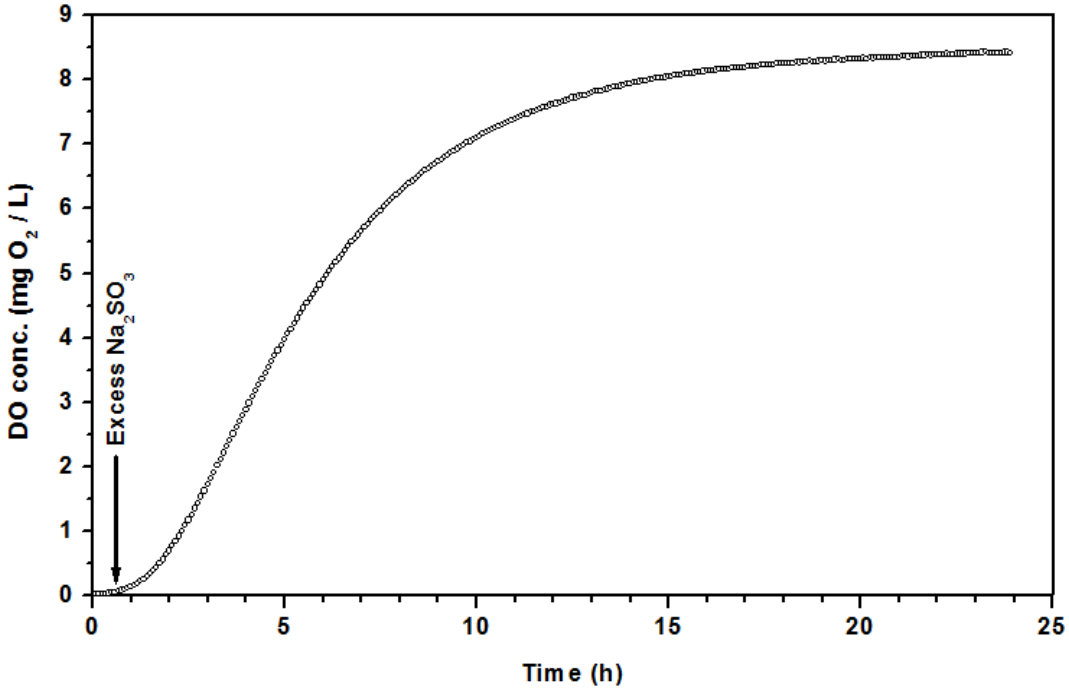

Figure 5-5: Time course of DO concentration (a typical experiment performed on reactor R2)

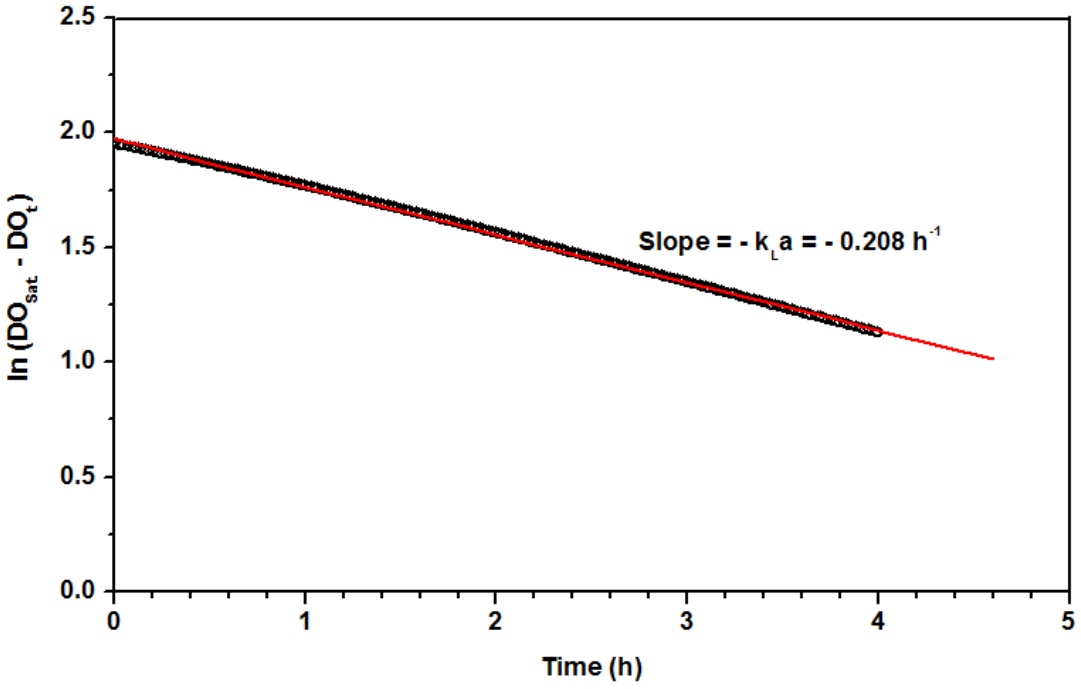

Figure 5-6: k_La obtained during a typical experiment in reactor R2

Table 5-3: The kLa values used for reactors R1 and R2 (Phase # 1)

# Reactor	# Experiment	k_La measured	k_La used*	Units
1	1	0.247	0.173	h^{-1}
	2	0.261	0.185	h^{-1}
2	1	0.208	0.146	h^{-1}

* The major difference between k_La measured and used is due to applying an α value of 0.7 as aeration correction factor according to Equation (2.25).

5.5 Biomass oxygen uptake rate (OUR_B)

OUR is one of the most important parameters affecting the COD mass balance calculation in the activated sludge systems and good care should be taken for its measurement. The in-situ method instead of the BOD method (described in Chapter 4) was used for OUR measurements to be sure that it was properly quantified. The results of a typical OUR determination run in reactors R1 and R2 is shown in Figure 5.7. The OUR value of 63.8 mg O_2 l^{-1} h^{-1} for reactor R1 was greater than the value of 28.3 mg O_2 l^{-1} h^{-1} in reactor R2. This is because the reactors R1 and R2 were connected in series and the feed was delivered to reactor R1 resulting in a biomass that was more active in reactor R1.

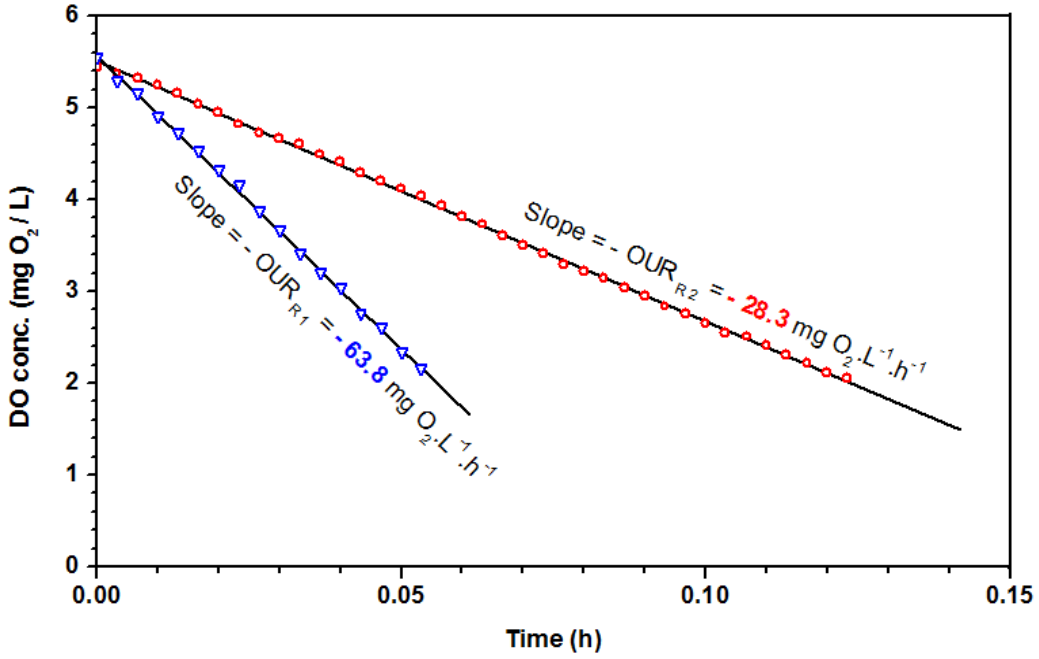

Figure 5-7: A typical graph of OUR determination for reactors R1 and R2 (Phase # 1)

Considering the k_La in reactors R1 and R2, and the DO concentration in the streams entering/leaving the reactors, the OUR_{meas} was corrected (termed OUR_B) according to Equation (2.23). As an example, the OUR_{meas} and OUR_B values for reactors R1 and R2 (Phase # 1) are shown in Figure 5.8. This results suggest that neglecting the k_La and DO concentration in the input and output streams results in an underestimation of the OUR value, affecting the COD mass balance results. This correction has not been clearly stated in the COD mass balance calculations of some previous studies.

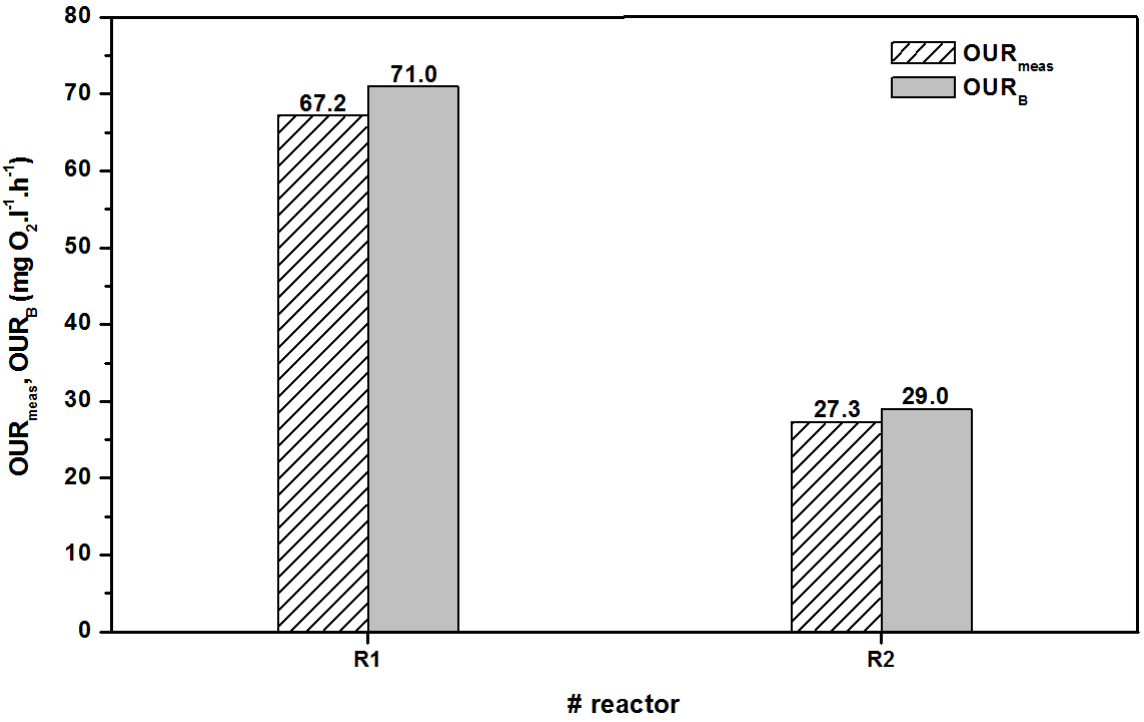

Figure 5-8: A comparison of OUR_{meas} and OUR_B in reactors R1 and R2 (phase # 1)

5.6 COD and N mass balances

5.6.1 Phase # 1

The COD and N mass balances results of 5 runs performed are listed in Table 5.4. The COD mass balance ranged between 100 and 103% with an average value of about 101%. N mass balance resulted in an average value of about 101%. These observations confirm that the COD and N mass balances on a strictly OX system should be close to 100%.

Table 5-4: COD and N mass balance results for phase # 1

Date	# Day	% COD mass balance	% N mass balance
16-Apr-11	48	100.2	102.5
17-Apr-11	49	101.6	103.8
12-May-11	*		
02-Jul-11	52	103.1	99.3
03-Jul-11	53	101.0	100.3
04-Jul-11	54	101.2	100.4
avg		101.4	101.3
std		1.1	1.8

* The system re-started on 12-May-11 (system failure occurred on 21-Apr-11 and 11-May-11)

5.6.2 Phase # 2

The k_La values determined for phase # 1 were used for the COD mass balances of phase # 2 because no changes were made in the system configuration (such as reactor shape and depth of liquid) and the speed of mixers compared to phase # 1. Regarding the OUR determination, it was only needed to measure the OUR in reactor R2 because the environmental conditions of the reactor R1 was switched from OX to AX. It should be noted that k_La and DO concentration in the influent/recycle streams remain to be considered.

The COD and N mass balance results for 9 runs are presented in Table 5.5. The COD mass balance ranged between 94 and 100% with an average value of 97% which is statistically significant (as discussed later). Therefore, it seems that the systems incorporating AX zones show COD balances a little lower than 100%.

Generally, a possible reason for AX systems showing a COD mass balance lower than 100% may be associated with the nitrate to oxygen conversion factor (Barker and Dold, 1995). If gases intermediates (NO and N_2O) are generated through denitrification process, the typical assumption of 2.86 mg COD/mg NO_3-N will result in an error in the COD mass balance calculation.

Since performing the N mass balance (Table 5.5) resulted in an average value of approximately 100%, NO and N_2O production and release could not be the cause of COD loss observed in this phase.

Fermentation in the presence of nitrate in pure culture experiments has been reported (Stouthamer and Bettenhausen, 1972) although fermentation occurs under AN conditions, possibly deep enough inside a floc for nitrate to have all been consumed.

Table 5-5: COD and N mass balances results for phase # 2

Date	# Day	% COD mass balance	% N mass balance
16-Jan-12	31	98.0	101.8
18-Jan-12	33	95.8	95.4
20-Jan-12	35	99.2	nd
02-Feb-12	48	96.2	97.2
04-Feb-12	50	93.9	97.8
06-Feb-12	52	100.0	101.6
13-Feb-12	59	97.3	105.0
15-Feb-12	61	96.6	97.9
17-Feb-12	63	95.2	98.4
avg		96.9	99.4
std		1.9	3.1

nd: not determined

5.6.3 Phase # 3A.1

The COD and N mass balances results over a period of 15 consecutive days are described in Table 5.6. The results suggest that N mass balance was good with an average value of close to 100% while the COD mass balance averaged approximately 78% which was much lower than that the values obtained during phases # 1 and # 2. This means that a portion of the influent COD mass disappeared in the system incorporating an AN zone.

A likely explanation for this significant amount of COD loss (approximately 22%) could be associated with fermentation reactions. It is hypothesized that fermentation reactions taking place in the AN reactor led to the production of volatile compounds which were stripped either in the

AN reactor to the nitrogen gas flushing or in the OX reactor due to the vigorous aeration in a shallow reactor.

The fermentable carbon sources could be the influent citrate which is a fermentable substrate, and the biomass itself which was fermented by the death-regeneration processes.

Table 5-6: COD and N mass balances results for phase # 3A.1

Date	# Day	% COD mass balance	% N mass balance
27-Nov-12	58	78.4	96.1
28-Nov-12	59	76.5	99.1
29-Nov-12	60	80.9	104.2
30-Nov-12	61	82.1	95.6
01-Dec-12	62	82.5	97.9
02-Dec-12	63	83.8	103.1
03-Dec-12	64	81.8	99.0
04-Dec-12	65	76.2	97.2
05-Dec-12	66	73.4	104.3
06-Dec-12	67	72.4	98.0
07-Dec-12	68	73.2	95.8
08-Dec-12	69	69.1	102.4
09-Dec-12	70	76.6	97.7
10-Dec-12	71	78.7	99.5
11-Dec-12	72	79.4	100.8
avg		77.7	99.4
std		4.3	2.9

5.6.4 Phases # 3A.2-3A.4

The COD and N mass balances results for phases # 3A.2, 3A.3 and 3A.4 are presented in Tables 5.7 to 5.9.

The average COD mass balance in phases # 3A.2 to 3A.4 ranged between from about 83 to 90%. A good N mass balance with an average value of about 99% was obtained for phases 3A.2 and

3A.3. The N mass balance was not experimentally determined for phase # 3A.4. It was calculated on the assumption that nitrogen compounds concentrations were more similar to the previous phases # 3A.1, 3A.2 and 3A.3.

Table 5-7: COD and N mass balances results for phase # 3A.2

Date	# day	% COD mass balance	% N mass balance
05-Aug-13	144	81.9	102.6
06-Aug-13	145	81.0	94.8
08-Aug-13	147	89.3	93.2
09-Aug-13	148	86.4	96.4
10-Aug-13	149	82.7	98.2
12-Aug-13	151	88.6	109.1
15-Aug-13	154	82.7	94.6
18-Aug-13	157	76.2	97.5
21-Aug-13	160	80.3	104.0
22-Aug-13	161	80.8	98.6
23-Aug-13	162	80.4	99.9
avg		82.7	99.0
std		3.9	4.7

Table 5-8: COD and N mass balances results for phase # 3A.3

Date	# Day	% COD mass balance	% N mass balance
24-Feb-14	40	85.4	95.6
26-Feb-14	42	92.3	102.7
27-Feb-14	43	95.7	99.0
01-Mar-14	45	86.7	95.2
04-Mar-14	48	87.0	99.6
avg		89.4	98.4
std		4.4	3.1

Table 5-9: COD and N mass balances results for phase # 3A.4

Date	# Day	% COD mass balance	% N mass balance
25-May-15	40	87.6	100.4
26-May-15	41	84.2	98.6
27-May-15	42	86.0	101.2
avg		86.0	100.0
std		1.7	1.3

5.6.5 Phase # 3B

The carbon source for fermentation was citrate and biomass for phase # 3A but for phase # 3B it was acetate and biomass. Acetate may be transformed into methane by acetoclastic methanogens but it is not a fermentable substrate. The sequential exposure of the biomass to AN and OX conditions would greatly reduce the activity of the strictly anaerobic acetoclastic methanogens. Thus, it is believed that methane production should have been negligible during this phase # 3B.

The COD and N mass balance results over a-5 day period (day 43-47 of the system operation) are presented in Table 5.10. Average values of about 90 and 100% for COD and N mass balances, respectively, are reported.

Table 5-10: COD and N mass balance results for phase # 3B

Date	# Day	% COD mass balance	% N mass balance
10-Nov-14	43	85.7	105.5
11-Nov-14	44	95.4	98.8
12-Nov-14	45	91.5	99.2
13-Nov-14	46	89.2	106.6
14-Nov-14	47	89.9	91.2
avg		90.3	100.2
std		3.5	6.2

5.7 Possible mechanisms contributing in the COD loss observed

5.7.1 Sulfate reduction

It is hypothesized that sulfate reduced in the AN reactor provides an insight into the fermentation propensity. The amount of sulfate reduced in reactor R1 versus COD mass balance is presented in Table 5.11 and illustrated in Figure 5.9.

Table 5-11: COD mass balance and sulfate reduced in reactor R1 results for phases # 1, 2 and 3

# Phase	COD balance		Sulfate reduced		
	Value	Units	Value	Units	Remarks
1	101.4	%	0	mg SO_4-S/d	assumed
2	96.9	%	0	mg SO_4-S/d	assumed
3A.1	77.7	%	211	mg SO_4-S/d	assumed
3A.2	82.7	%	213	mg SO_4-S/d	
3A.3	89.4	%	45	mg SO_4-S/d	
3A.4	86.0	%	54	mg SO_4-S/d	
3B	90.3	%	54	mg SO_4-S/d	

Note: sulfate concentration was not monitored during phases # 1 to # 3A.1.

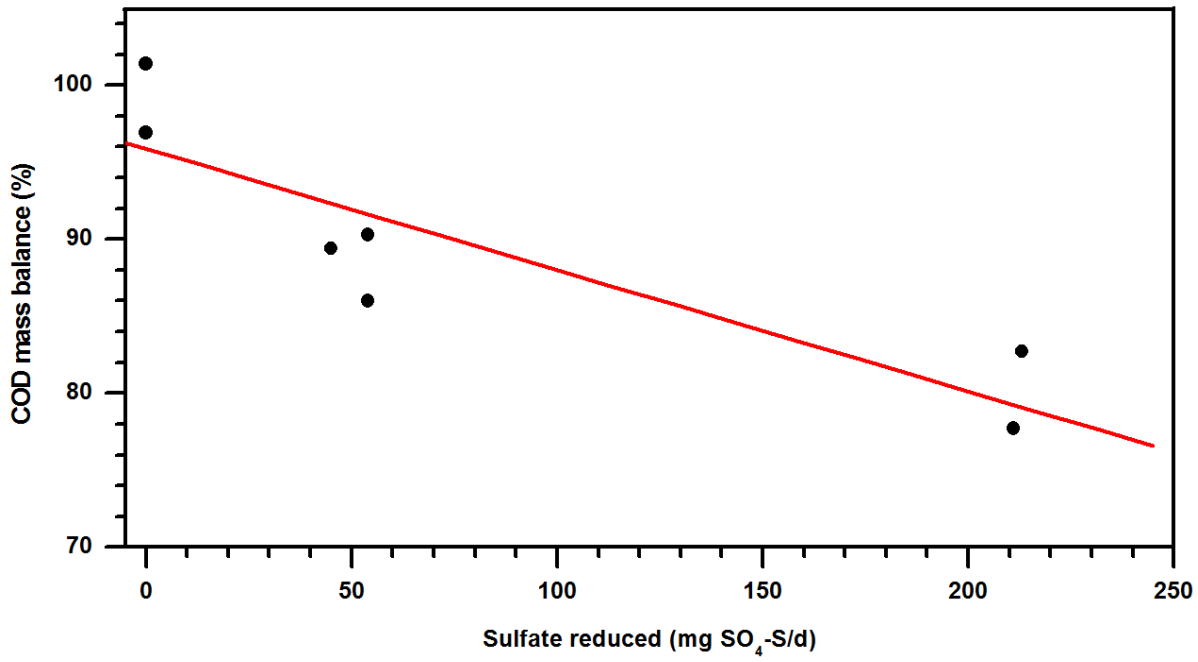

Figure 5-9: COD mass balance versus mass rate of sulfate reduced in reactor R1 in phases # 1, # 2 and # 3A/B

Sulfate reduced in reactor R1 during phases # 1 and 2 was negligible and the corresponding COD mass balances were near 100%. Sulfate reduced in reactor R1 during phases # 3A.3, # 3A.4 and # 3B was approximately 50 mg SO_4-S/d, with corresponding COD mass balances averaging

between 86 and 90% (Figure 5.9 and Table 5.11). Sulfate reduced in reactor R1 during phases # 3A.1 and # 3A.2 was about 210 mg SO_4-S/d and the COD mass balances ranged between 78 and 83%. It can be concluded that the intensity of sulfate reduction in reactor R1 confirms the propensity for fermentation reactions to occur. Such conditions would favor the production of reduced and potentially volatile compounds that could be stripped either in the AN reactor or the downstream OX reactor.

- *Stripping of hydrogen sulfide or sulfide precipitation*

The percent of COD mass balance that can be explained by sulfur in phases # 3A.2, # 3A.3, # 3A.4 and # 3B are presented in Table 5.12.

Table 5-12: Estimated contribution of sulfur in the COD mass balance for phases # 3A and 3B

# Phase	avg SO_4 concentration			Units	% COD mass balance contributed by sulfur
	inf	AN reactor	eff		
3A.2	6.0	0.8	5.7	mg SO_4-S/L	0.13
3A.3	6.1	3.5	4.0	mg SO_4-S/L	0.80
3A.4	5.7	0.7	0.7	mg SO_4-S/L	1.80
3B	5.8	0.7	0.7	mg SO_4-S/L	1.96

It appears that the contribution of sulfur in the COD mass balance in phase # 3A.2 was negligible (0.13%) mainly because the anaerobic sulfate reduced was reoxidized in the OX reactor.

The results presented in the bottom part of the Table 5.12 (Phases # 3A.4 and # 3B) show that the anaerobic sulfate reduced was not anymore reoxidized, as described earlier. It resulted in a contribution of sulfur in the COD mass balance calculation of about 2% which could be associated with either stripping of hydrogen sulfide or with the formation of a sulfide precipitate. This phenomenon could be an original explanation for a portion of the COD loss.

5.7.2 Methane production

Attempts to measure the dissolved methane in the AN reactor of phases # 3A.3 and # 3A.4 resulted in a maximum concentration of 0.02 mg CH_4/L in the AN mixed liquor (Table 5.13). This amount could contribute to only 0.05% of the observed COD loss.

Theoretical methane concentration needed to explain about 10 to 14% COD loss observed in phases # 3A.3 and 3A.4 is also presented in Table 5.13. The large difference between the measured and theoretical methane concentration may be explained by the fact that methanogenic bacteria are obligate anaerobes and that they were probably not active in the AN-OX system studied. If there were any CH_4 produced in the AN zone or under anaerobic conditions inside flocs, methane stripping should have resulted in a negligible amount of dissolved CH_4.

Table 5-13: Measured and theoretical dissolved methane concentration in the AN mixed liquor to explain the observed COD loss in phases # 3A.3 (10.6 %) and 3A.4 (14.0 %)

Phase	Date	# Day	CH_4 concentration		Units	% COD loss explained by CH_4
			Measured*	Theoretical		
3A.3	24-May-14	129	0.01	3.3	mg CH_4/L	0.03
	25-May-14	130	0.01	3.6	mg CH_4/L	0.03
	26-May-14	131	0.02	3.4	mg CH_4/L	0.06
	27-May-14	132	0.02	3.5	mg CH_4/L	0.06
	avg		0.02	3.5	mg CH_4/L	0.05
3A.4	27-Aug-15	134	0.01	6.4	mg CH_4/L	0.02
	28-Aug-15	135	0.01	6.4	mg CH_4/L	0.01
	avg		0.01	6.4	mg CH_4/L	0.02

*detection limit = 0.01 mg CH_4/L

5.7.3 Hydrogen production/stripping

Hydrogen production through citrate fermentation could be one of the mechanisms contributing to the COD loss observed in phase # 3A. The equivalent of hydrogen production in the AN

reactor, if it is supposed that all of the observed COD loss is due to hydrogen production, is described in Table 5.14. The actual dissolved hydrogen concentration in the AN mixed liquor is also presented (analyses made from phase # 3A.3).

Table 5-14: Measured and theoretical H_2 concentration in the AN mixed liquor to explain the observed 9.7 to 14.0 % COD loss in phases # 3A.3, # 3B and # 3A.4

# Phase	Date	# Day	H_2 concentration			
			Theoretical	Units	Measured	Units
3A.3	24-Feb-14	40	2300	µg/L	< 0.02	µg/L
	26-Feb-14	42	1200	µg/L	< 0.02	µg/L
	27-Feb-14	43	700	µg/L	< 0.02	µg/L
	01-Mar-14	45	2200	µg/L	< 0.02	µg/L
	04-Mar-14	48	2100	µg/L	< 0.02	µg/L
3A.4	25-May-15	40	2800	µg/L	< 0.02	µg/L
	26-May-15	41	3700	µg/L	< 0.02	µg/L
	27-May-15	42	3300	µg/L	< 0.02	µg/L
3B	10-Nov-14	43	2300	µg/L	< 0.02	µg/L
	11-Nov-14	44	700	µg/L	< 0.02	µg/L
	12-Nov-14	45	1400	µg/L	< 0.02	µg/L
	13-Nov-14	46	1700	µg/L	< 0.02	µg/L
	14-Nov-14	47	1600	µg/L	< 0.02	µg/L

Note: The detection limit for the dissolved H_2 probe was 0.02 µg H_2/L.

Although no dissolved hydrogen could be detected in the AN reactor with the methodology used, this possibility should not be ignored. One of the possible processes that makes difficult the detection of hydrogen in the AN reactor is hydrogen stripping.

- *H_2 stripping batch test*

The result of attempts made to quantify the dissolved hydrogen in distilled water which was subjected to hydrogen gas bubbling is shown in Figure 5.10. A maximum COD increase of only 4 mg COD/L recorded over a period of 120 minutes which is approximately 32% of the expected saturation value of 12.8 mg H_2-COD/L at 20 °C.

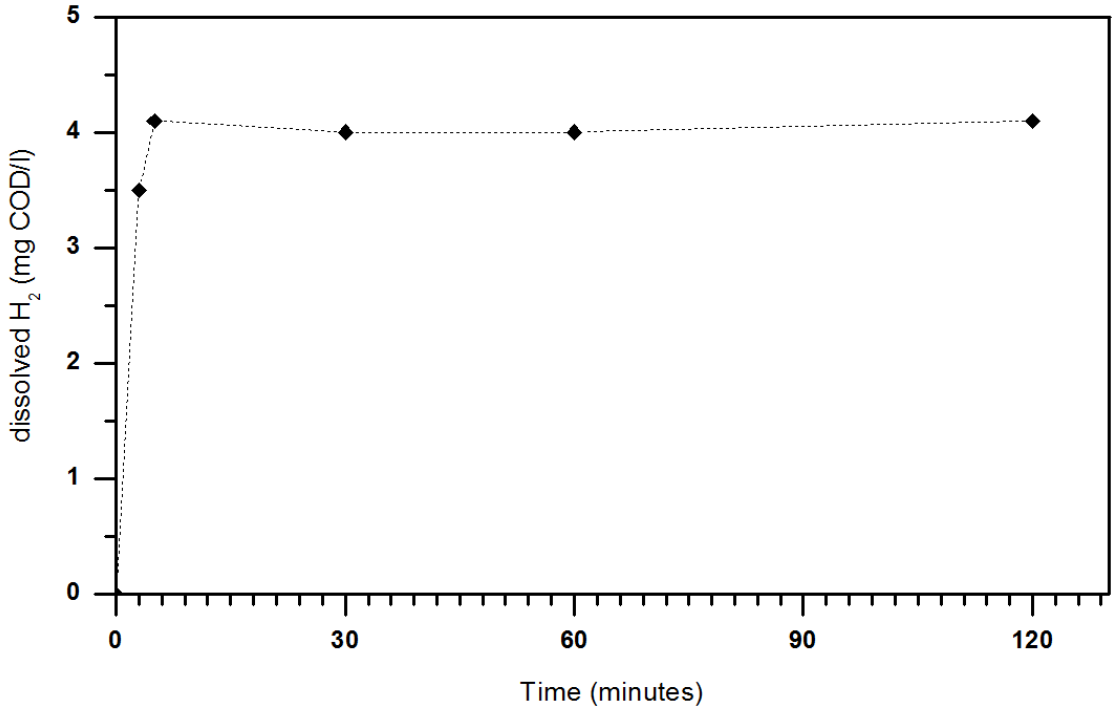

Figure 5-10: Dissolution of hydrogen gas in distilled water over time as measured by the COD test

These results suggest that the shallow lab scale reactors are inefficient in transferring gas. Therefore, the observed COD loss in phase # 3 is likely to be related to H_2 stripping in the AN reactor. The AN reactor had a liquid depth of only about 20 cm equipped with a mechanical mixer and had its head space continuously vented at 0.3 vvm with N_2, hydrogen could have been stripped due to its low solubility (1.6 mg H_2/l at 20 °C).

Another possibility is that the anaerobic hydrogen produced would be transferred via the liquid to the downstream shallow OX reactor where it would be release due to the vigorous aeration. The aeration flow rate for the OX reactor used was about 5 l/min resulting in oxygen transfer efficiency (OTE) of only 0.2% in the shallow reactor (Table B.17). Thus, any solubilised gas entering the OX reactor could be easily stripped.

5.7.4 Aeration and mixing induced stripping of acetate

Acetate stripping tests with aeration and mixing were conducted on the synthetic wastewater prepared with acetate (initial COD concentration of about 45 mg COD/L; Table 5.15).

No significant change in COD concentration was observed over a period of 30 minutes in the presence of aeration and mixing at pH values of 4, 5, 6, 7 and 8. It can be concluded that the stripping of acetate did not contributed significantly to the observed COD loss.

Table 5-15: COD changes in a synthetic wastewater (prepared with acetate) depending on aerating and mixing time

COD analysis						
Time (min)	pH & COD values					units
	4	5	6	7	8	-
0	43	47	44	42	42	(mg COD/L)
3	42	49	46	41	41	(mg COD/L)
5	43	48	44	41	42	(mg COD/L)
10	41	48	43	41	42	(mg COD/L)
30	43	47	44	43	43	(mg COD/L)

Note: The experiment was performed at room temperature (23 ^{o}C)

5.7.5 COD test limitation

The COD mass balance calculations were done with the assumption that all metabolic products in the biological systems are completely oxidized in the Hach test tube COD test conditions (with dichromate at 150°C for 2 hours). If there is only a partial oxidation of intracellular carbon storage products such as polyhydroxyalkanoates (PHA) in EBPR systems, a portion of the observed COD loss could be explained by COD test limitation.

Theoretical oxygen demand (ThOD) and observed COD values on a sample containing a PHA mixture of PHB and PHV were nearly identical at 1.86 and 1.81 mg COD/mg PHBV (Table

5.16). Thus, the hypothesis that the COD test limitation may underestimate the COD value was rejected.

Table 5-16: Comparison of ThOD and observed COD values of PHBV sample

Comp	ThOD determination						Observed COD	
	Molecular weight		Chemical formula			ThOD		
	value	units	general form	X	estimated form	value	#	value
PHBV	4.5E5	g/mol	$(C_4H_6O_2)_X(C_5H_8O_2)_Y$	1	$C_{22500}H_{35999}O_{9000}$	1.92	1	1.82
				10	$C_{22497}H_{35991}O_{9003}$	1.92	2	1.80
				100	$C_{22470}H_{35912}O_{9028}$	1.92	3	1.80
				1000	$C_{22200}H_{35120}O_{9280}$	1.87	4	1.79
				5000	$C_{21000}H_{31600}O_{10400}$	1.69	5	1.82
						avg = 1.86	6	1.81
							7	1.81
							avg	1.81

Note: ThOD and observed COD values in mg COD/mg PHBV units

5.7.6 Death-regeneration

Based on the death-regeneration phenomenon (Dold et al. 1980), the decay of biomass results in two fractions of unbiodegradable and slowly biodegradable substances. The last one can then be hydrolyzed to readily biodegradable matter. The following example shows the amount of substrate generated through decaying biomass in phase # 3B.

The average VSS during phase # 3B was about 890 mg VSS/L where the total working volume of the system and influent flow rate were 9.5 L and 10.7 L/d, respectively. Since the system was operated at an SRT of about 10 days, the active fraction of biomass can be estimated to be about 65%.

Considering a decay rate of about 0.2 d^{-1} and an f_{CV} value of 1.48 mg COD/mg VSS gives an amount of 122 mg COD per liter of influent. This shows that the amount of substrate cycled through decaying of biomass is significant compared to the average influent COD of 516 mg COD/L, representing about 20 % of the combined available COD (122 / (516 + 122)).

It can be concluded that fermentation reactions may occur in the AN-OX systems even with acetate as the sole influent carbon source which is non fermentable. This could be a likely explanation for the COD loss observed in phase # 3.

5.8 Sensitivity analysis on COD loss for aeration parameters α and β

As α and β aeration parameters depend on the characteristics of the wastewater, they can be variable. A sensitivity analysis on the COD loss for parameters α and β was conducted by applying α values ranging from 0.4 to 0.8 and β values of 0.7 to 0.9 (Table 5.17).

Table 5-17: Sensitivity analysis on the COD loss for aeration parameters α and β

Parameter		Phase # / COD loss (%)				
α	β	3A.1	3A.2	3A.3	3A.4	3B
0.4	0.7	23.5	18.5	11.8	15.2	10.9
	0.8	23.3	18.2	11.6	15.0	10.7
	0.9	23.1	18.0	11.4	14.8	10.5
0.5	0.7	23.4	18.3	11.7	15.1	10.8
	0.8	23.1	18.0	11.4	14.8	10.5
	0.9	22.8	17.8	11.1	14.6	10.2
0.7	0.7	23.1	18.0	11.4	14.8	10.4
	0.8	22.7	17.6	11.0	14.4	10.0
	0.9	**22.3**	**17.3**	**10.6**	**14.0**	**9.7**
0.8	0.7	22.9	17.9	11.2	14.6	10.3
	0.8	22.5	17.4	10.8	14.2	9.8
	0.9	22.1	17.0	10.3	13.8	9.4
Range of deviation from the α and β used[1]		(-0.2,1.2)	(-0.3,1.2)	(-0.3,1.2)	(-0.2,1.2)	(-0.3,1.2)

[1]The α value of 0.7 and β of 0.9 used for the various phases of this study as they are the typical values for a variety of industrial and municipal wastewaters (U.S.EPA., 1979).

The following description explains that the COD loss sensitivity for α and β (selected ranges) would not be greater than 1.2%.

The mass fraction of oxygen entering an AN-OX system (from the liquid surface) with respect to the mass of influent COD is given by Equation (5.1) (c.f. Chapter 2 for the notations).

$$\frac{f(\alpha,\beta)}{FCOD_{INPUT}} = \frac{24 \times V_{R1} \times \alpha \times k_L a_{R1} \times (\beta \times DO_{sat} - DO_{mid,R1}) + 24 \times V_{R2} \times \alpha \times k_L a_{R2} \times (\beta \times DO_{sat} - DO_{mid,R2})}{FCOD_{INPUT}} \quad (5.1)$$

Considering phase # 3A.1 as an example (V_{R2} = 7 L, k_La_{R1} = 0.0 h^{-1}; k_La_{R2} = 0.21 h^{-1}; DO_{sat} = 8.8 mg O_2/L and $DO_{mid,R2}$ = 3.8 mg O_2/L; $FCOD_{INPUT}$ = 5807 mg COD/L), Equation (5.1) is simplified into Equation (5.2)

$$\frac{f(\alpha,\beta)}{FCOD_{INPUT}} = 0.006\alpha \times (8.8\beta - 3.8) \quad (5.2)$$

The α and β values of 0.7 and 0.9, respectively, were used in this research project.

Thus,

$$\frac{f(\alpha,\beta)}{FCOD_{INPUT}} = 1.75\%$$

If α value ranges from 0.4 to 0.8 and β between 0.7 and 0.9:

$$0.57\ \% < \frac{f(\alpha,\beta)}{FCOD_{INPUT}} < 1.98\ \%$$

It seems that the COD loss observed was not very sensitive to α and β, being less than 1.2%, because the k_La value for the system determined had a low value of 0.21 h^{-1}.

As an example, applying a k_La value of 2 h^{-1} results in:

$$5.7\ \% < \frac{f(\alpha,\beta)}{FCOD_{INPUT}} < 19.8\ \%$$

These findings suggest that the COD mass balance sensitivity for parameters α and β strongly depends on the k_La value.

5.9 COD mass balance around separate AN and OX reactors

Performing COD mass balances around each reactor (AN and OX) was done to see if some information could be gained about the COD loss observed for the whole AN-OX system.

The flow rate and influent COD concentration averaged about 11 L/d and 520 mg COD/L, respectively, during phase # 3 (AN-OX) (Table 5.1). The COD mass balance conducted for the whole AN-OX system resulted in a significant COD loss (about 10 to 22 % of the daily mass of influent COD) which means about 600-1300 mg COD/d disappeared across the system.

The COD mass rates entering and leaving reactors AN and OX were of the order of 50 000 mg COD/d (Tables B.18 and B.19). It was not easy to identify differences of 600 to 1300 mg COD/d. Therefore, doing COD mass balances around separate reactors did not provide much insight in explaining the observed COD loss due to the large recirculation of COD overwhelming relatively small changes in COD loss.

5.10 Statistical analysis of the COD mass balance results

The results of this research revealed that the COD mass balance for phases # 2 (AX-OX) and # 3A/B (AN-OX) were less than 100%. It averaged about 97% for phase # 2 and ranged between about 78 and 90% for phases # 3A and 3B. This section provides statistical test results demonstrating whether the COD mass balances performed on these phases were significantly different from 100%.

The p-value can be used as an index demonstrating the strength of evidence for the alternative hypothesis against the null one. In this research, the alternative and null hypotheses are defined as follows:

- null hypothesis: COD mass balance is 100%

- tested hypothesis: COD mass balance is less than100%

The p-value can take any value between 0.00 and 1.00 where a value less than 0.05 is used as the typical one for concluding that there is evidence against the null hypothesis.

Statistical analysis on the COD mass balance results were performed using the MegaStat software. The t-test with respect to a confidence level of 95% was used to estimate the p-value.

The results from the t-test ran on the COD mass balances results showed a very small p-value between 1.8E-03 and 4.7E-12 for phases # 2, 3A/B, meaning that there is strong evidence that the null hypothesis can be rejected (Table 5.18). Thus, this analysis suggests that the COD mass balances for phases # 2 (AX-OX) and 3A/B (AN-OX) were significantly less than 100%.

A p-value of 0.98 was obtained for phase # 1 (OX-OX) suggesting that the COD mass balance for the OX systems should be close to 100%.

Table 5-18: Statistical t-test results ran on the COD mass balances for phases # 1, 2, 3A and 3B

# Phase	1	2	3A.1	3A.2	3A.3	3A.4	3B	Units
null hypothesis	100	100	100	100	100	100	100	%
alternative hypothesis	< 100	< 100	< 100	< 100	< 100	< 100	< 100	%
avg value	101.4	96.9	77.7	82.8	89.4	86.0	90.3	%
std value	1.07	1.93	4.28	3.90	4.39	1.70	3.53	%
std. error	0.48	0.65	1.11	1.18	1.96	0.98	1.58	%
n*	5	9	15	11	5	3	5	
p-value	0.98	7E-4	4.7E-12	2.2E-8	2.9E-3	2.4E-3	1.8E-3	%
Evidence against the null hypothesis	NO	YES	YES	YES	YES	YES	YES	

Note: Input data to quantify p-value comes from the Tables 5.4 through 5.10.

* Number of replicates

5.11 Comparison of oxygen consumption and observed yield (Y_{OBS})

Oxygen consumption and sludge production significantly influence the operational and capital costs in activated sludge process. This section discusses the relationships between COD mass balances, oxygen consumption and sludge production for phases studied.

- **Oxygen consumption**

Oxygen consumption is defined the mass rate of total electron acceptors utilized across the system to the mass rate of COD removed in units of (%g COD/g COD). It is calculated according to Equation (B.1). For an AN-OX system, oxygen consumption is the summation of the following terms with respect to +/- signs:

(1) oxygen utilized via OUR_B (+)

The terms involved in the determination of OUR_B are as follows:

- measured OUR in the OX reactor
- oxygen transferred to the OX reactor from the liquid surface

- oxygen transferred to the AN reactor through influent/recycle streams

(2) oxygen needed for nitrification and sulfide oxidation under OX conditions (-)

(3) oxygen equivalent for the following terms:

- anaerobic sulfate reduction (+)
- denitrification (+).

Oxygen consumed for phases # 3A and # 3B was lower than that for phases # 1 and # 2. This is because COD mass balances in phases # 1 and # 2 were close to 100% while it ranged between 78 and 90 % for phases # 3A and # 3B. These findings suggest that the amount of oxygen consumption is related to the COD loss observed. It can be concluded that when comparing two systems, the mass portion of the influent COD which is oxidized across the system would be less for the one showing a COD loss (Figure 5.11a).

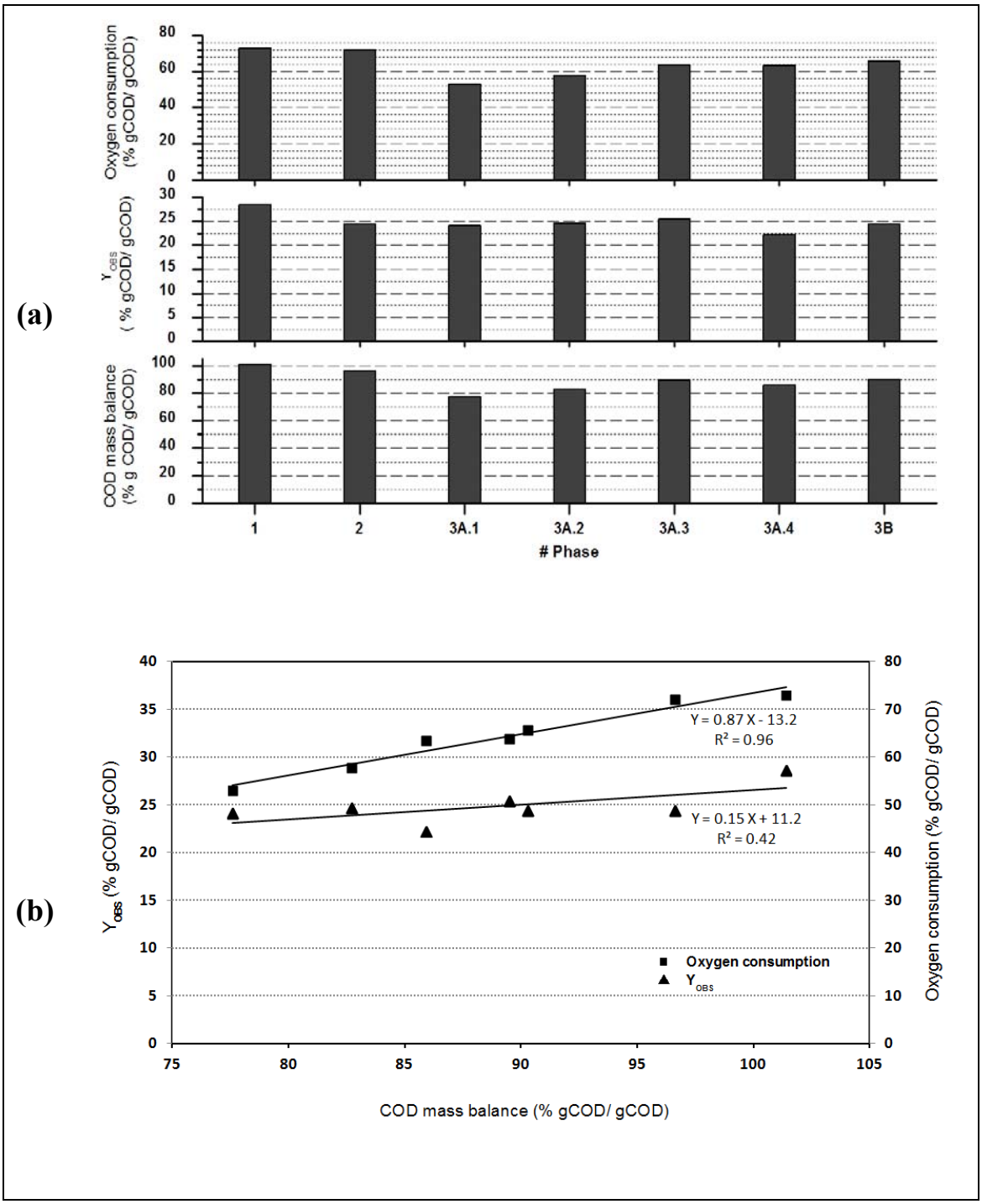

Figure 5-11: **(a).** Changes in the COD mass balance,Y_{OBS} and oxygen consumption during phases # 1, 2 and 3; **(b).** Relationships between COD mass balance,Y_{OBS} and oxygen consumption

- **Y_{OBS}**

The Y_{OBS} is defined as the ratio of biomass produced to the substrate consumed and is expressed in g VSS/g COD or g COD/g COD. It can be calculated according to the Equation (B. 2).
The average value of Y_{OBS} in phases # 1 and # 2 were 28.6% and 24.4% g COD/g COD, respectively (Figure 5.11a). Thus, for phase # 2 the Y_{OBS} was 85.3% that of phase # 1. These results confirm that less sludge is produced under AX-OX (phase # 2) than OX-OX conditions (phase # 1).
Y_{OBS} averaged 24.2% g COD/g COD throughout whole phase # 3 (AN-OX) which is about 86% the value determined for phase # 1, confirming that system incorporating AN zones result in less sludge production (Figures 5.11a).
Figures 5.11b shows relationships between COD mass balance, Y_{OBS} and oxygen consumption throughout phases studied. It can be concluded that a consequence of COD loss occurring in EBPR system is a reduction in both oxygen consumption and sludge production.

5.12 Integration of results

- **Phosphorus removal**

Phases # 3A.4 and # 3B showed good phosphorus removal (approximately 13% mg P/mg VSS) compared to phases # 3A.1 to # 3A.3. The reason was due to a lower recycle ratio in phase # 3A.4 and a lower DO concentration in the OX reactor during both phases # 3A.4 and # 3B which reduced oxygen loading to the AN reactor.

- **COD mass balances**

- A summary of COD mass balance results obtained during this research is presented in Table 5.19. The COD mass balance varied significantly between about 78 and 101 %.

- The results indicated that COD mass balance during phase # 1 (OX-OX) was close to 100% while during phase # 2 (AX-OX), it averaged approximately 97%.

- The COD mass balance results for phase # 3 (AN-OX) with either citrate (phase # 3A) or acetate (phase # 3B) are summarized below.

- The COD mass balances during phase # 3A with citrate as carbon source ranged between about 78 and 90%.

- The COD mass balances for phase # 3B with acetate as carbon source averaged about 90 % which is in good agreement with the results presented by Barker and Dold (1995) who reported an average value of about 91% on Wentzel et al. (1989) systems operated with acetate.

- PAO activity did not seem to be correlated with COD imbalance. During phase # 3, the COD loss was observed either in the presence or absence of PAO activity.

- Acetate stripping was not found to be the cause of the COD loss.

- CH_4 production explained only 0.05% of that COD loss.

- COD test limitation was not shown to contribute to the COD loss.

Therefore, it is hypothesized that the possible explanation for the observed COD loss (approximately 10-22%) could be attributed to fermentation reaction taking place under AN conditions leading to volatile substances production which are then stripped either in the AN or OX reactor. A useful indicator of fermentation activity was provided by the reduction of sulfate under AN conditions. It was hypothesized that fermentation did produce hydrogen but this compound could not be detected in the AN mixed liquor. This may have been due to hydrogen stripping because the system used consisted of a very shallow lab scale reactors (liquid depth of about 20 cm) equipped with a mechanical mixer and where the head space of the AN was continuously vented at 0.3 vvm with N_2.

Decaying biomass was shown to contribute to a significant amount of readily biodegradable matter (122 mg COD per liter of influent versus about 520 mg acetate-COD per liter of influent) as shown by a calculation for phase # 3B for which acetate was the sole carbon source and a non fermentable substrate.

- **N mass balances**

The N mass balance obtained for all phases was approximately 100%, indicating no significant loss.

- **P mass balances**

The P mass balances during this research ranged between about 96 and 100%, indicating little loss of this compound.

- **Y_{OBS}**

The Y_{OBS} averaged 24.2% g COD/g COD for phase # 3 (AN-OX) which was about 14% less than that in phase # 1 (OX-OX), as expected from using some nitrate instead of oxygen as an electron acceptor for biomass growth.

Table 5-19: Integration of operational and COD, N and P mass balances results

Phase	Q_{inf} (L/d)	Reactor R1		Reactor R2			a (L/L)	Y_{OBS}	f_P	f_{VT}	Mass balance (%)		
		NO_3 (mg N/L)	NO_2 (mg N/L)	O_2 (mg O_2/L)	NO_3 (mg N/L)	NO_2 (mg N/L)					COD	N	P
1	12	-	-	6.5	25	0.8	4.5	0.286	1.4	0.93	101.4	101.3	99.2
2	12	33	< 0.1	6.5	55	0.5	4.4	0.245	1.5	0.92	96.9	99.4	96.2
3A.1	11	0.4	< 0.1	6.5	5.9	0.2	2.6	0.242	1.7	0.92	77.7	99.4	98.7
3A.2	12	0.3	< 0.1	6.5	5.3	0.0	2.6	0.248	5.0	0.84	82.7	99.0	96.1
3A.3	11	0.7	< 0.1	6.5	5.7	0.1	3.0	0.255	2.0	0.91	89.4	98.4	98.0
3A.4	11	0.1	< 0.1	4.0	6.2	0.0	2.0	0.222	13.0	0.63	86.0	100.0	96.0
3B	11	0.4	< 0.1	3.5	5.2	0.0	3.0	0.245	12.1	0.63	90.3	100.2	96.0

Note:

- The volume of reactors R1 and R2 was 3 and 7 L, respectively, except for phase # 3 with a volume of 2.5 L for reactor R1;

- All phases were conducted using citrate as sole carbon source except for phase # 3B with acetate. The influent COD, TKN and TP concentrations were about 500 mg/L, 30 mg N/L and 50 mg P/L except for phase # 1 with 980 mg COD/L, phases # 1 and 2 with 50 and 130 mg N/L respectively, and phases # 1 and 2 with 20 mg P/L;

-The COD, N and P mass balances were close to 100% except for COD mass balances under AN-OX conditions where it varied between 78 and 90%;

-Y_{OBS}, f_P and f_{VT} in mg COD/ mg COD, % mg P/ mg VSS and mg VSS/ mg TSS, respectively.

CHAPTER 6 CONCLUSIONS AND RECOMMENDATIONS

6.1 Conclusions

This research on the COD loss in lab scale EBPR system allowed to draw the following conclusions:

1. The COD and N mass balances on strictly aerobic (OX-OX) system were close to 100%

2. The COD and N mass balances on anoxic-aerobic (AX-OX) system were close to 100%

3. The anaerobic-aerobic (AN-OX) system exhibited poor COD mass balance ranging between approximately 78 and 90%.

Regarding AN-OX system, the following points are summarized:

a) A COD loss was observed using either acetate or citrate as sole influent carbon source.

b) EBPR and non-EBPR systems exhibited a significant COD loss (10-22%).

- PAO activity was negatively affected by nitrate and oxygen load in the AN reactor.

c) Methane production and loss appeared to only account for 0.05% of the COD loss.

d) Acetate stripping under mixing/aerating conditions was shown to be non significant.

e) Sulfur was shown to contribute to the COD loss (0.1-2.0%) when the anaerobic sulfate reduced was not reoxidized under aerobic conditions.

f) Death-regeneration phenomenon contributing to the production of biodegradable substrate that can be fermented can explain some COD loss even in the absence of a fermentable influent carbon source.

g) Hydrogen could not be detected in the anaerobic mixed liquor but remains as a likely hypothesis to explain some COD loss as this very volatile gas was easily stripped in a hydrogen bubble lab scale column in which no more than 32% of the saturation concentration could be achieved.

4. The AN-OX system showed about 14% reduction in sludge production compared to that in the OX-OX system as expected from the use of nitrate instead of oxygen as an electron acceptor for biomass growth.

5. The COD loss was not very sensitive (0.6-2.0%) for α and β values at the low k_La value reported for this project (0.2 h^{-1}).

6. COD mass balance calculations around separate reactors AN and OX in the AN-OX system did not provide much insight into the observed COD loss.

7. COD test limitations that could result in the partial oxidation of PHBV were not found to be significant.

6.2 Recommendations

The main topics recommended to obtain a deeper insight into the COD loss in EBPR systems are as follows:

- This study proposes that the reason for the absence of hydrogen gas detection in the AN mixed liquor was related to the fact that it can be easily stripped in the laboratory scale shallow reactors. Therefore, performing a COD mass balance around a lab scale AN-OX system using taller reactors may provide a better insight into the contribution of hydrogen to the COD loss because hydrogen could be consumed by other H_2-consuming bacteria such as sulfate reducing organisms in deep enough AN reactors.

- Hydrogen production activity test using fermentable substrates such as citrate and using biomass taken from full scale AN-OX such as EBPR systems is recommended.

- Analysis of the AN mixed liquor resulted in a negligible concentration of about 0.02 mg CH_4/L for methane. This low value may be associated with either stripping or the presence of a minimal concentration of methanogenic bacteria in the lab scale AN-OX system. Thus, metagenomic analyses of microbial population of the lab scale AN-OX system could provide information concerning the presence and activity of methanogenic bacteria.

- Off-gas analysis of a lab scale shallow AN-OX system for H_2, CH_4, H_2S, and other volatile compounds such VFAs is recommended. Extending this investigation to the off-gas and to AN mixed liquor of an AN-OX full scale system may reveal that the COD loss only is a laboratory artefact related to very inefficient gas transfer in shallow lab scale reactors and that this phenomenon may not occur in the full scale AN-OX systems.

REFERENCES

Appeldoorn, K. J., Kortstee, G. J. J. and Zehnder, A. B. 1992. Biological phosphate removal by activated sludge under defined conditions. *Water Research,* 26 (4): 453-460.

APHA, AWWA and WEF. 2012. Standard methods for the examination of water and wastewater, 22nd edition, American Public Health Association, Washington, D.C., USA.

Arkley, M. J. and Marais, G. V. R. 1981. The effect of anoxic zone on sludge production and settleability in the activated sludge process, Research report No. 38, Department of Civil Engineering, University of Cape Town, South Africa.

Barker, P. S. and Dold, P. L. 1995. COD and nitrogen mass balances in activated sludge systems, *Water Research*, 29 (2): 633-643.

Barker, P. S. and Dold, P. L. 1996. Sludge production and oxygen demand in nutrient removal activated sludge systems, *Water Science and Technology*, 34 (5-6): 43-50.

Barnard, J. L. 1975. Biological nutrient removal without the addition of chemicals, *Water Research*, 9: 485-490.

Barnard, J. L. 1974. Cut P and N without chemicals, *Water Wastes Engineering*, 11: 33-36.

Batstone, D. J., Keller, J., Angelidaki, I., Kalyuzhnyi, S.V., Pavlostathis, S.G., Rozzi, A., Sanders, W. T. M., Siegrist, H. and Vavilin, V. A. 2002. Anaerobic Digestion Model No.1, London, UK: IWA Publishing.

Beckers, L., Masset, J., Hamilton, C., Delvigne, F., Toye, D., Crine, M., Thonart, P., Hiligsmann, S. 2015. Investigation of the links between mass transfer conditions, dissolved hydrogen concentration and biohydrogen production by the pure strain *Clostridium butyricum* CWBI1009, *Biochemical Engineering Journal*, 98: 18–28.

Bielefeldt, A. R. and Stensel, H. D. 1999. Treating VOC-contaminated gases in activated sludge: Mechanistic model to evaluate design and performance, *Environmental Science and Technology*, 33 (18): 3234-3240.

Bordacs, K. and Tracy, K. 1988. Retention of organic storage products in anaerobic-aerobic activated sludge, 61th annual conference of the Water Pollution Control Federation, Dallas, USA.

Brannan, K. P. 1986. Substrate stabilization in the anaerobic stage of a biological phosphorus removal system, PhD thesis, Virginia Polytechnic Institute and State University, Virginia, USA.

Brett, S. 1997. Phosphorus removal and recovery technologies, London, UK: Selper Publications.

Campos, J. L., Otero, L., Franco, A., Mosquera-Corral, A. and Roca, E. 2009. Ozonation strategies to reduce sludge production of a seafood industry WRRF, *Bioresource Technology*, 100 (3): 1069–1073.

Canales, A., Pareilleux, A., Rols, J. L., Goma, G. and Huyard, A. 1994. Decreased sludge production strategy for domestic wastewater treatment, *Water Science and Technology*, 30 (8): 97-106.

Chen, K. Y. 1970, Oxidation of aqueous sulfide by O2, PhD thesis, Harvard University, Division of Engineering and Applied Physics, USA.

Cheremisinoff, P. N. 1994. Biomanagement of Wastewater and Wastes. Englewood Cliffs, New Jersey, USA: Prentice-Hall.

Coker A. K. 2007. Ludwig's applied process design for chemical and petrochemical plants, vol. 1, 4th edition, Oxford, UK : Gulf professional publishing

Comeau, Y. 1990. La déphosphatation biologique – Procédés et conception, *Sciences et techniques de l'eau*, 23 (2): 199-219.

Comeau, Y., Hall, K. J., Hancock R. E. W. and Oldham, W. K. 1986. Bio-chemical model for enhanced biological phosphorus removal, *Water Research*, 20: 1511-1521.

Copp, J. B. 1998. COD balances in biological nutrient (nitrogen and phosphorus) removal activated sludge systems, Ph.D. Thesis, McMaster University, Canada.

Cretu, V. and Tobolcea, V. 2005. Phosphorus removal by biological processes. Annals series: Civil Engineering, Ovidius University, Romania, 1 (7): 97-102.

Dold, P. L., Ekama, G. A. and Marais, G. V. R. 1980. Ageneral model for the activated sludge, *Progress in Water Technology*, 12 (6): 47-77.

Erdal, Z. K., Erdal, U. G. and Randall, C. W. 2005. Biochemistry of enhanced biological phosphorus removal and anaerobic COD stabilization, *Water Science and Technology*, 52 (10-11): 557–567.

Henze, M., van Loosdrecht, M. C. M., Ekama, G. A. and Brdjanovic, D. 2008. Biological Wastewater Treatment- Principles, Modeling and Design, London, UK: IWA Publishing.

Hoover, S. R. and Porges, N. 1952. Assimilation of dairy wastes by activated sludge II: The equation of synthesis and oxygen utilization, *Sewage and Industrial Wastes*, 24 (3): 306-312.

Johansson, P. 1994. SIPHOR: A kinetic model for simulation of biological phosphate removal. Ph.D. thesis, Lund University, Sweden.

Koren, D. W., Gould, W. D. and Bedard, P. 2000. Biological removal of ammonia and nitrate from simulated mine and mill effluents. *Hydrometallurgy,* 56, 127-144.

Kraemer, J. T. and Bagley, D. M. 2007. Improving the yield from fermentative hydrogen production, *Biotechnology Letters*, 29 (5):685–695.

Kristiansen, R., Nguyen, H. T., Saunders, A. M., Nielsen, J. L., Wimmer, R., Le VQ, McIlroy, S. J., Petrovski, S., Seviour, R. J., Calteau, A., Nielsen, K. L. and Nielsen, P. H. 2013. A metabolic model for members of the genus *Tetrasphaera* involved in enhanced biological phosphorus removal, *The International Society for Ecological Modelling Journal*, 7(3):543-54.

Lan, J. C. Benefield, L. and Randall, C. W. 1983. Phosphorus removal in the activated sludge process, *Water Research*, 17 (9): 1193-1100.

Levin, G. V., Shapiro, J. 1965. Metabolic uptake of phosphorus by wastewater organisms, Journal of the *Water Pollution Control Federation*, 37: 800-821.

Li, Q. and Lancaster, J. R. 2013. Chemical foundations of hydrogen sulfide biology, Nitric Oxide, 35: 21–34.

Lide, D. R. 2003. Hand book of chemistry and physics, 84th edition, Boca Raton, Florida, USA: CRC Press LLC.

Marais, G. V. R. and Ekama, G. A. 1976. The activated sludge process, Part I: Steady state behavior, *Water SA*, 2 (4): 164-200.

McClintock, S. A., Sherrard, J. H., Novak, J. T. and Randall, C. W. 1988. Nitrate versus oxygen respiration in the activated sludge process, *Journal of the Water Pollution Control Federation*, 60: 342-350.

Mino, T., van Loosdrecht, M. C. M., Heijnen, J. J. 1998. Microbiology and biochemistry of the enhanced biological phosphate removal process, *Water Research*, 32 (11): 3193-3207.

Mino, T., Arun, V., Tsuzuki, Y. and Matsuo, T. 1987. Effect of phosphorus accumulation on acetate metabolism in the biological phosphorus removal process. Ramadori, R. (ed), Advances in Water Pollution Control, pp. 27-38, IAWPRC, Oxford, UK: Pergamon Press.

Mitchell, R. and Gu, J. D. 2010. Environmental Microbiology, 2nd edition, New York, USA: Wiley-Blackwell.

Mueller, J. A. and Stensel, H. D. 1987. Biologically enhanced oxygen transfer in the activated sludge process-fact of folly?, 60th annual WPCF conference, Philadelphia, USA.

Muszynski, A., Lebkowska, M., Tabernacka, A. and Milobedzka, A. 2013. From macro to lab-scale: Changes in bacterial community led to deterioration of EBPR in lab reactor, *Central European Journal of Biology*, 8(2): 130-142.

Nicholls, H. A. 1975. Full scale experimentation at the new Johannesburg aeration plants, *Water SA*, 1: 121-132.

Nielsen, A. H., hvitved-Jacobsen, T. and Vollertsen, J. 2008. Effect of pH and iron concentration on sulfide precipitation in wastewater collection systems, *Water Environment Research*, 80 (4): 380-384.

Oehmen, A., Lemos, P. C., Carvalho, G., Yuan, Z., Keller, J., Blac kall, L. and Reis, M. A. M. 2007. Advances in enhanced biological phosphorus removal: From micro to macro scale, *Water Research*, 41 (11): 2271–2300.

Payne, W. J. 1981. Denitrification, New York, USA: Wiley-Interscience.

Perez-Elvira, S. I., Nieto Diez, P. and Fdz-Polanco. F. 2006. Sludge minimisation technologies: Review, *Environmental Science and Biotechnology*, 5: 375–398.

Power, S. P. B., Ekama, G. A., Wentzel, M. C. and Marais, G. V. R. 1992. Chemical phosphorus removal from municipal wastewater by the addition of waste alum sludge to the activated sludge system, Research report No. W66, Department of Civil Engineering, University of Cape Town, South Africa.

Ramadori, R., Tandoi, V. and Misiti, A. 1985. Bench scale and pilot scale experiments on biological phosphorus removal, *Water Science and Technology*, 17 (12-13): 287-288.

Randall, C. W., Brannan, C. P. and Benefield, L. D. 1987. Factors affecting anaerobic stabilization during biological phosphorus removal, in *Biological Phosphate Removal from Wastewaters* (editor: Ramadori), Proceedings of an IAWPRC specialized conferences (Rom, Italy), Pergamon Press.

Randall, C. W., Brannan, K. P., McClintock, S. A. and Pattarkine, V. M. 1992. The case of anaerobic reduction of oxygen requirements in biological phosphorus removal systems, *Water Environment Research*, 64 (6): 824-833.

Rensink, J. H. 1981. Biologische defosfatering en procesbepalende factoren, NVA Symposium Proceedings, Nederland.

Schepers, J. S. and Raun, W. R. 2008. Nitrogen in Agricultural Systems, Madison, Wisconsin, USA: American Society of Agronomy.

Schink, B. 2002. Synergistic interactions in the microbial world, Journal Antonie van Leeuwenhoek, 81: 257–261.

Schroeter, W. D., Dold, P. L. and Marais, G. V. R. 1982. The COD/VSS ratio of the volatile solids in the activated sludge process, Research report No. W45, Department of Civil Engineering, University of Cape Town, South Africa.

Singh, K. S. and Viraraghavan, T. 1998. Start-up and operation of UASB reactors at 20C for municipal wastewater treatment, *Journal of Fermentation and Bioengineering*, 85 (6): 609-614.

Smyth, S. A. M. 1994, Sludge production in aerobic and anoxic activated sludge systems, Master thesis, McMaster University, Hamilton, Canada.

Srinath, E. G., Sastry, C. A. and Pillai, S. C. 1959. Rapid removal of phosphorus from sewage by activated sludge, *Cellular and Molecular Life Sciences,* 15: 339-340.

Stams, A. J. M. 1994. Metabolic interactions between anaerobic bacteria in methanogenic environments, *Journal Antonie van Leeuwenhoek*, 66: 271–294.

Stouthamer, A. H. and Bettenhausen, C. 1972. Influence of hydrogen acceptors on growth and energy production of Proteus mirabilis. Antonie van Leeuwenhoek, 38 (1): 81-90.

Tchobanoglous, G., Burton, F. L. and Stensel, H. D. 2003. Wastewater engineering treatment and reuses, Metcalf and Eddy, New York, USA: McGraw-Hill.

Treybal R. 1980. Mass-transfer operations, NY, USA: McGraw-Hill

U.S. Environmental Protection Agency. 1979. Workshop Toward an Oxygen Transfer Standard (edited by Boyle W. C.), EPA/600-9-78-021, pp. 147, U.S. Environmental Protection Agency: Cincinnati, Ohio.

Van Haandel, A. and van der Lubbe, J. 2007. Handbook biological wastewater treatment: Design and optimization of activated sludge systems, Leidschendam, The Netherlands, UK: Quist Publishing.

Von Sperling, M. 2007. Biological wastewater treatment series: Basic principles of wastewater treatment, vol. 2, London, UK: IWA publishing.

Wable, M. V. and Randall, C. W. 1994. Investigation of hypothesized anaerobic stabilization mechanisms in biological nutrient removal systems, *Water Environment Research*, 66 (2): 101-167.

Wable, M. W. and Randall, C. W. 1992. Investigation of reduction in oxygen requirements of biological phosphorus removal systems, *Water Science and Technology*, 26 (9-11): 2221-2223.

Wang, J. C., Park, J. K. and Whang, L.M. 2002. Comparison of fatty acid composition and kinetics of PAO and GAO, *Water Environment Research,* 73 (6): 704–710.

Wentzel, M. C., Ekama, G. A.., Dold, P. L. and Marais, G. V. R. 1990. Biological excess phosphorus removal-steady state process design, *Water SA*, 16: 29-48.

Wentzel, M. C., Ekama, G. A., Loewenthal, R. E., Dold, P. L., and Marais, G. V. R. 1989. Enhanced polyphosphate organism cultures in activated sludge systems. Part II: Experimental behaviour. *Water SA*, 15 (2): 71–88.

Wentzel, M. C., Lotter, L. H., Loewenthal, R. E. and Marais, G. V. R. 1986. Metabolic behaviour of *Acinetobacter sp.* in enhanced biological phosphorus removal: A biochemical model, *Water SA*, 12: 209-224.

Yang, X., Peng, Y., Ren. N., Guo, J., Tang, X. and Song, J. 2013. Nutrient removal performance and microbial community structure in an EBPR system under the limited filamentous bulking state, *Bioresource Technology*, 144: 86-93.

Yuan, Z., Pratt, S. and Batstone, D. J. 2012. Phosphorus recovery from wastewater through microbial processes, *Journal of Current Opinion in Biotechnology*, 23 (6):878-883.

Zhang, L., De Schryver, P., De Gusseme, B., De Muynck, W. and Boon, N. 2008. Chemical and biological technologies for hydrogen sulfide emission control in sewer systems: A review, Water Research, 42 (1-2): 1-12.

APPENDIX A – TIME SCHEDULE FOR PHASES STUDIED

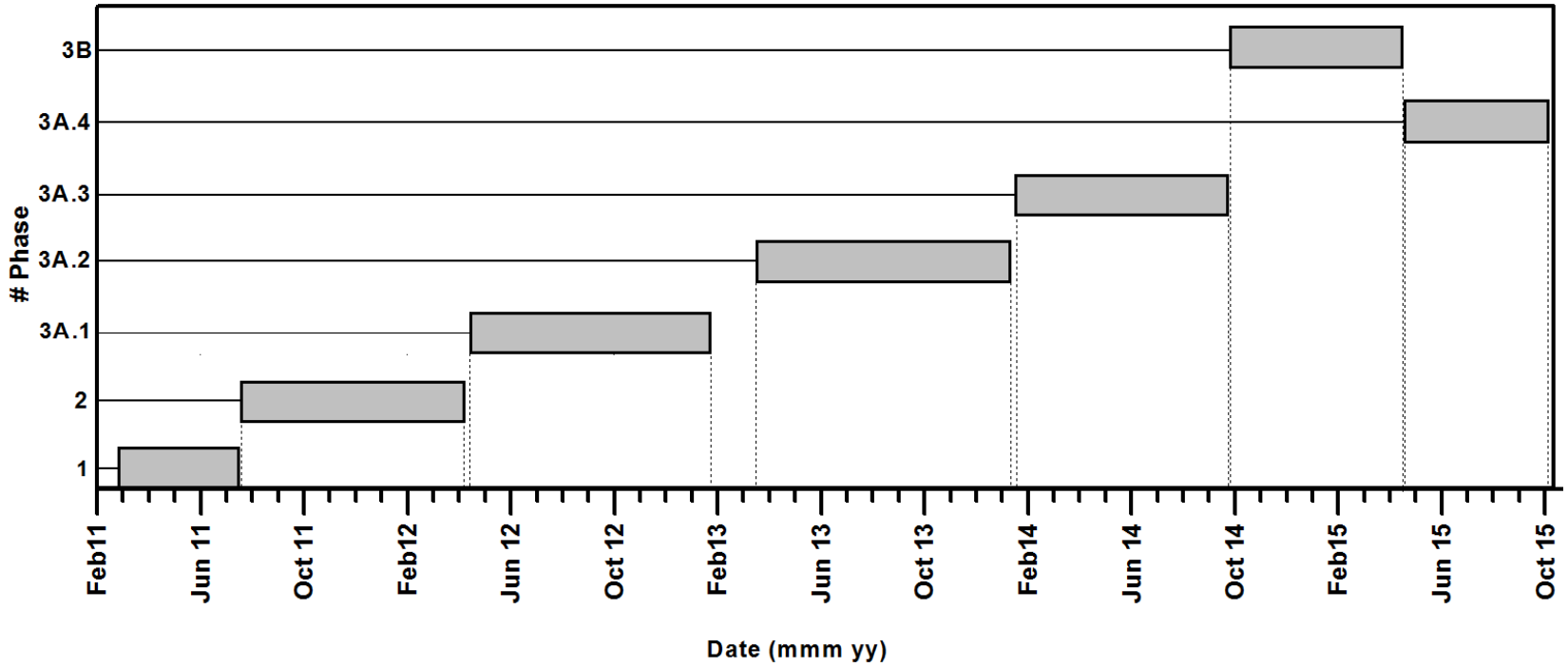

Figure A. 1: Schematic illustrating the timeline for phases studied

Table A. 1: Time schedule for phases studied

Phase	Date	Experimental activity/remarks
1	28-Feb-11	Start-up[1]
	16-Apr-11	Performing COD, N and P mass balances
	17-Apr-11	
	21-Apr-11 & 11-May-11	A pump failure occurred because of a power interruption. The pump transferring the biomass from reactor R1 to R2 stopped running resulted in losing the whole biomass.
	12-May-11	Restart[1]
	02-Jul-11	Performing COD, N and P mass balances
	03-Jul-11	
	04-Jul-11	
	15-Jul-11	End of operation
2	16-Jul-11	- Begin phase # 2 operation • The only change made compared to phase # 1 was that the in-line air shut off valve was switched off to stop blowing air to the reactor R1.
	16-Jul-11 to 16-Dec-11	The biomass did not properly behave (see section 4.6.2).
	17-Dec-11	- Restart[1] • The concentration of the influent composition was modified (see section 4.6.2).
	16-Jan-12	Performing COD, N and P mass balances
	18-Jan-12	
	20-Jan-12	
	02-Feb-12	
	04-Feb-12	
	06-Feb-12	
	13-Feb-12	
	15-Feb-12	
	17-Feb-12	
	04-Apr-12	End of operation

Table A. 1: Time line for phases studied (continued)

Phase	Date	Experimental activity/remarks
3A.1	13-Apr-12	Begin phase # 3A operation
	13-Apr-12 to 26-Sep-12	The influent COD, TKN and TP concentrations were about 500 mg COD/L, 18 mg N/L and 50 mg P/L, respectively. An excessive growth of filamentous bacteria with a high f_{CV} value of about 1.9 mg COD/mg VSS was observed (data not shown)
	01-Oct-12	- Restart[1] • COD = 500 mg/L, TKN = 30 mg N/L, TP = 50 mg P/L
	27-Nov-12	Performing COD, N and P mass balances
	28-Nov-12	
	29-Nov-12	
	30-Nov-12	
	01-Dec-12	
	02-Dec-12	
	03-Dec-12	
	04-Dec-12	
	05-Dec-12	
	06-Dec-12	
	07-Dec-12	
	08-Dec-12	
	09-Dec-12	
	10-Dec-12	
	11-Dec-12	
	28-Jan-13	End of operation
	31-Jan-13 to 14-Mar-13	The system was out of action
3A.2	15-Mar-13	Restart[1]
	05-Aug-13	Performing COD, N and P mass balances
	06-Aug-13	
	08-Aug-13	
	09-Aug-13	
	10-Aug-13	
	12-Aug-13	
	15-Aug-13	
	18-Aug-13	
	21-Aug-13	
	22-Aug-13	
	23-Aug-13	
	10-Jan-14	End of operation because of a system failure

Table A. 1: Time line for phases studied (continued)

Phase	Date	Experimental activity/remarks
3A.3	16-Jan-14	Restart[1]
	24-Feb-14 26-Feb-14 27-Feb-14 01-Mar-14 04-Mar-14	- Performing COD, N and P mass balances - Testing dissolved H_2
	24-May-14 25-May-14 26-May-14 27-May-14	Testing dissolved CH_4
	28-Sep-14	End of operation
3B	29-Sep-14	The substrate changed from citrate to acetate
	10-Nov-14 11-Nov-14 12-Nov-14 13-Nov-14 14-Nov-14	- Performing COD, N and P mass balances - Testing dissolved H_2
	15-Apr-15	End of operation
3A.4	16-Apr-15	The substrate was switched back to citrate
	25-May-15 26-May-15 27-May-15	- Performing COD and P mass balances - Testing dissolved H_2
	27-Aug-15 28-Aug-15	Testing dissolved CH_4
	03-Oct-15	End of operation

[1] Activated sludge was taken from Saint-Hyacinthe WRRF, Quebec.

APPENDIX B – EXPERIMENTAL DATA FOR PHASES # 1, 2, 3A AND 3B

Table B. 1: Flow rates data for phases # 1, 2, 3A and 3B

Phase	Date	# Day	Flow rate (L/d)			Recycle ratio (L/L_{inf})
			Influent	Effluent	WAS	
1	16-Apr-11	48	11.8	10.8	1.0	4.5
	17-Apr-11	49	11.6	10.7	1.0	4.5
	12-May-11*					
	02-Jul-11	52	12.5	11.5	1.0	4.5
	03-Jul-11	53	12.7	11.4	1.0	4.5
	04-Jul-11	54	12.8	11.5	1.0	4.5
	avg		12.0	11.0	1.0	4.5
2	16-Jan-12	31	12.1	10.7	1.0	4.4
	18-Jan-12	33	12.1	10.9	1.0	4.4
	20-Jan-12	35	12.1	10.9	1.0	4.4
	02-Feb-12	48	11.8	10.6	1.0	4.5
	04-Feb-12	50	11.8	10.7	1.0	4.5
	06-Feb-12	52	11.6	10.9	1.0	4.5
	13-Feb-12	59	11.7	11.0	1.0	4.5
	15-Feb-12	61	12.1	11.0	1.0	4.5
	17-Feb-12	63	12.1	11.0	1.0	4.4
	avg		11.9	10.8	1.0	4.4
3A.1	27-Nov-12	58	11.2	10.0	1.0	2.6
	28-Nov-12	59	11.3	10.4	1.0	2.6
	29-Nov-12	60	10.9	10.0	1.0	2.7
	30-Nov-12	61	10.9	9.8	1.0	2.7
	01-Dec-12	62	10.7	9.7	1.0	2.7
	02-Dec-12	63	10.9	9.6	1.0	2.7
	03-Dec-12	64	10.9	9.8	1.0	2.6
	04-Dec-12	65	11.1	9.8	1.0	2.6
	05-Dec-12	66	11.0	9.6	1.0	2.6
	06-Dec-12	67	11.3	9.9	1.0	2.5
	07-Dec-12	68	11.2	10.3	1.0	2.6
	08-Dec-12	69	11.3	10.0	1.0	2.6
	09-Dec-12	70	11.0	9.6	1.0	2.6
	10-Dec-12	71	10.9	9.8	1.0	2.6
	11-Dec-12	72	10.7	9.8	1.0	2.7
	avg		11.0	9.9	1.0	2.6

* A system failure occurred 11-May-11 because of a power interruption. The system was restarted on 12-May-11.

Table B. 1: Flow rates data for phases # 1, 2, 3A and 3B (continued)

Phase	Date	# Day	Flow rate			Recycle ratio (L/L_{inf})
			Influent	Effluent	WAS	
3A.2	05-Aug-13	144	11.7	10.8	1.0	2.6
	06-Aug-13	145	12.2	11.1	1.0	2.6
	08-Aug-13	147	11.8	10.8	1.0	2.7
	09-Aug-13	148	12.1	10.8	1.0	2.6
	10-Aug-13	149	11.9	10.3	1.0	2.7
	12-Aug-13	151	10.5	9.6	1.0	2.9
	15-Aug-13	154	12.0	10.8	1.0	2.5
	18-Aug-13	157	12.1	10.5	1.0	2.5
	21-Aug-13	160	11.8	10.8	1.0	2.5
	22-Aug-13	161	11.8	10.6	1.0	2.5
	23-Aug-13	162	11.6	10.4	1.0	2.6
	avg		11.8	10.6	1.0	2.6
3A.3	24-Feb-14	40	10.9	9.6	1.0	3.0
	26-Feb-14	42	10.8	9.6	1.0	3.0
	27-Feb-14	43	10.5	9.5	1.0	3.1
	01-Mar-14	45	10.5	8.9	1.0	3.0
	04-Mar-14	48	10.3	8.9	1.0	3.1
	avg		10.6	9.3	1.0	3.0
3A.4	25-May-15	40	11.0	10.5	1.0	2.0
	26-May-15	41	10.9	9.4	1.0	2.0
	27-May-15	42	10.7	9.2	1.0	2.0
	avg		10.9	9.7	1.0	2.0
3B	10-Nov-14	43	10.7	9.8	1.0	3.1
	11-Nov-14	44	10.7	9.5	1.0	3.1
	12-Nov-14	45	10.7	9.4	1.0	3.0
	13-Nov-14	46	10.7	9.6	1.0	3.0
	14-Nov-14	47	10.7	9.3	1.0	3.0
	avg		10.7	9.5	1.0	3.0

Note: The values are rounded off to one decimal place.

Table B. 2: COD data for phases # 1, 2, 3A and 3B

Phase	Date	# Day	Total COD (mg COD/L)			Soluble COD (mg COD/L)
			Influent	Effluent	WAS	WAS
1	16-Apr-11	48	1038	12	3357	52
	17-Apr-11	49	1027	8	3440	59
	12-May-11*					
	02-Jul-11	52	931	17	3379	56
	03-Jul-11	53	944	16	3442	31
	04-Jul-11	54	956	13	3370	34
	avg		979	13	3398	46
2	16-Jan-12	31	544	29	1451	62
	18-Jan-12	33	548	22	1493	69
	20-Jan-12	35	521	23	1439	78
	02-Feb-12	48	527	27	1519	65
	04-Feb-12	50	551	27	1588	78
	06-Feb-12	52	513	23	1728	85
	13-Feb-12	59	561	29	1592	81
	15-Feb-12	61	545	25	1604	60
	17-Feb-12	63	536	20	1636	70
	avg		538	25	1561	72
3A.1	27-Nov-12	58	509	8	1423	35
	28-Nov-12	59	512	5	1426	32
	29-Nov-12	60	517	4	1366	31
	30-Nov-12	61	517	12	1401	37
	01-Dec-12	62	525	8	1391	27
	02-Dec-12	63	506	8	1389	28
	03-Dec-12	64	495	7	1463	25
	04-Dec-12	65	525	4	1437	24
	05-Dec-12	66	521	6	1456	26
	06-Dec-12	67	541	9	1373	28
	07-Dec-12	68	535	6	1449	32
	08-Dec-12	69	566	6	1474	39
	09-Dec-12	70	548	5	1383	40
	10-Dec-12	71	546	12	1342	46
	11-Dec-12	72	551	7	1371	43
	avg		528	7	1410	33

Note:

* A system failure occurred 11-May-11 because of a power interruption. The system was restarted on 12-May-11.

- The HF membrane module was replaced with a new one starting from phase # 3A.1

Table B. 2: COD data for phases # 1, 2, 3A and 3B (continued)

Phase	Date	# Day	Total COD (mg COD/L)			Soluble COD (mg COD/L)
			Influent	Effluent	WAS	WAS
3A.2	05-Aug-13	144	493	6	1390	76
	06-Aug-13	145	482	3	1383	92
	08-Aug-13	147	509	6	1490	109
	09-Aug-13	148	490	7	1431	102
	10-Aug-13	149	502	6	1409	99
	12-Aug-13	151	486	8	1429	72
	15-Aug-13	154	501	6	1474	41
	18-Aug-13	157	500	6	1502	38
	21-Aug-13	160	457	6	1433	39
	22-Aug-13	161	460	4	1472	35
	23-Aug-13	162	461	5	1479	43
	avg		486	6	1445	68
3A.3	24-Feb-14	40	502	9	1504	64
	26-Feb-14	42	518	10	1353	68
	27-Feb-14	43	510	10	1500	96
	01-Mar-14	45	537	10	1444	91
	04-Mar-14	48	539	10	1428	104
	avg		521	10	1446	85
3A.4	25-May-15	40	532	7	1361	14
	26-May-15	41	554	8	1286	17
	27-May-15	42	559	10	1315	25
	avg		548	8	1321	19
3B	10-Nov-14	43	513	13	1345	30
	11-Nov-14	44	500	13	1380	43
	12-Nov-14	45	533	10	1352	36
	13-Nov-14	46	511	6	1335	29
	14-Nov-14	47	524	11	1346	56
	avg		516	11	1352	39

Table B. 3: TKN data for phases # 1, 2, 3A and 3B

Phase	Date	# Day	TKN (mg N/L)		
			Influent	Effluent	WAS
1	16-Apr-11	48	45.6	0.9	278
	17-Apr-11	49	46.4	0.8	264
	12-May-11*				
	02-Jul-11	52	48.7	1.9	239
	03-Jul-11	53	47.1	2.1	238
	04-Jul-11	54	46.2	0.9	237
	avg		47.0	1.3	251
2	16-Jan-12	31	123	0.1	123
	18-Jan-12	33	124	0.8	111
	20-Jan-12	35	nd	nd	nd
	02-Feb-12	48	131	0.1	114
	04-Feb-12	50	133	0.7	120
	06-Feb-12	52	131	1.0	117
	13-Feb-12	59	128	0.1	131
	15-Feb-12	61	128	0.1	120
	17-Feb-12	63	123	0.1	129
	avg		128	0.4	121
3A.1	27-Nov-12	58	29.2	0.7	102
	28-Nov-12	59	28.7	0.6	94
	29-Nov-12	60	28.0	0.4	105
	30-Nov-12	61	27.6	0.1	105
	01-Dec-12	62	28.1	0.3	87
	02-Dec-12	63	29.0	0.2	97
	03-Dec-12	64	30.5	0.3	104
	04-Dec-12	65	30.2	0.1	100
	05-Dec-12	66	30.1	0.1	103
	06-Dec-12	67	29.1	0.3	101
	07-Dec-12	68	29.0	0.7	106
	08-Dec-12	69	28.3	0.4	112
	09-Dec-12	70	27.4	0.3	92
	10-Dec-12	71	31.1	0.6	104
	11-Dec-12	72	31.6	0.3	86
	avg		29.2	0.4	100

* A system failure occurred 11-May-11 because of a power interruption. The system was restarted on 12-May-11; nd: not determined.

Table B. 3: TKN data for phases # 1, 2, 3A and 3B (continued)

Phase	Date	# Day	TKN (mg N/L)		
			Influent	Effluent	WAS
3A.2	05-Aug-13	144	32.3	1.1	120
	06-Aug-13	145	30.9	1.3	117
	08-Aug-13	147	28.2	1.3	124
	09-Aug-13	148	30.3	1.2	126
	10-Aug-13	149	29.4	1.1	126
	12-Aug-13	151	31.5	1.4	126
	15-Aug-13	154	30.3	1.1	142
	18-Aug-13	157	31.0	1.2	158
	21-Aug-13	160	31.5	1.4	157
	22-Aug-13	161	30.3	1.2	143
	23-Aug-13	162	29.9	1.9	152
	avg		30.5	1.3	136
3A.3	24-Feb-14	40	33.4	0.5	112
	26-Feb-14	42	31.9	0.5	114
	27-Feb-14	43	31.3	0.5	117
	01-Mar-14	45	29.1	0.5	103
	04-Mar-14	48	28.5	0.5	98
	avg		30.8	0.5	109
3A.4	25-May-15	40	30	1.0	120
	26-May-15	41	30	1.0	119
	27-May-15	42	30	1.0	122
	avg		30	1.0	120
3B	10-Nov-14	43	29.5	0.5	115
	11-Nov-14	44	29.3	0.5	98
	12-Nov-14	45	29.1	0.5	98
	13-Nov-14	46	28.8	0.5	92
	14-Nov-14	47	29.0	0.5	88
	avg		29.1	0.5	98

Table B. 4: TP data for phases # 1, 2, 3A and 3B

Phase	Date	# Day	TP (mg P/L)		
			Influent	Effluent	WAS
1	16-Apr-11	48	19.2	16.2	50.1
	17-Apr-11	49	19.6	16.8	49.0
	12-May-11*				
	02-Jul-11	52	18.6	16.7	45.7
	03-Jul-11	53	18.7	15.9	46.7
	04-Jul-11	54	18.6	15.8	46.0
	avg		19.0	16.0	48.0
2	16-Jan-12	31	19.5	18.5	31.5
	18-Jan-12	33	19.7	18.4	30.5
	20-Jan-12	35	nd	nd	nd
	02-Feb-12	48	20.1	18.1	32.3
	04-Feb-12	50	20.0	17.2	33.7
	06-Feb-12	52	20.4	17.4	33.6
	13-Feb-12	59	19.6	17.0	34.1
	15-Feb-12	61	18.9	16.8	34.1
	17-Feb-12	63	18.7	17.6	34.6
	avg		20.0	18.0	33.0
3A.1	27-Nov-12	58	45.7	43.9	64.0
	28-Nov-12	59	46.6	45.3	59.9
	29-Nov-12	60	45.6	45.5	60.6
	30-Nov-12	61	44.9	44.8	63.1
	01-Dec-12	62	45.6	44.6	60.6
	02-Dec-12	63	47.3	45.5	61.4
	03-Dec-12	64	49.8	47.7	61.9
	04-Dec-12	65	49.1	46.8	59.1
	05-Dec-12	66	49.0	47.6	61.7
	06-Dec-12	67	47.3	46.7	60.2
	07-Dec-12	68	47.1	47.3	60.6
	08-Dec-12	69	45.9	45.2	59.9
	09-Dec-12	70	44.4	43.5	55.7
	10-Dec-12	71	50.6	47.5	61.4
	11-Dec-12	72	51.4	49.5	57.4
	avg		47.5	46.1	60.5

* A system failure occurred 11-May-11 because of a power interruption. The system was restarted on 12-May-11.

Table B. 4: TP data for phases # 1, 2, 3A and 3B (continued)

# Phase	Date	# Day	TP(mg P/L)		
			Influent	Effluent	WAS
3A.2	05-Aug-13	144	53.9	46.8	76.4
	06-Aug-13	145	51.6	48.0	83.8
	08-Aug-13	147	46.9	45.5	81.8
	09-Aug-13	148	50.5	45.4	81.4
	10-Aug-13	149	48.9	45.7	80.8
	12-Aug-13	151	52.5	46.2	83.2
	15-Aug-13	154	50.4	47.1	100
	18-Aug-13	157	51.6	44.6	116
	21-Aug-13	160	52.7	45.5	96.6
	22-Aug-13	161	50.6	43.7	95.8
	23-Aug-13	162	49.9	43.7	100
	avg		50.9	45.7	90.5
3A.3	24-Feb-14	40	55.9	55.0	72.2
	26-Feb-14	42	53.2	51.0	71.5
	27-Feb-14	43	52.2	50.3	69.5
	01-Mar-14	45	48.3	48.8	67.6
	04-Mar-14	48	47.4	45.2	64.4
	avg		51.4	50.1	69.0
3A.4	25-May-15	40	48.2	32.4	150
	26-May-15	41	42.9	33.8	145
	27-May-15	42	42.8	33.6	132
	avg		44.6	33.3	142
3B	10-Nov-14	43	45.0	35.8	130
	11-Nov-14	44	43.5	31.5	141
	12-Nov-14	45	41.0	27.3	153
	13-Nov-14	46	nd	nd	nd
	14-Nov-14	47	nd	nd	nd
	avg		43.2	31.6	141

nd: not determined

Table B. 5: Nitrate and nitrite data for phases # 1, 2, 3A and 3B

Phase	Date	# Day	Nitrate (mg N/L)			Nitrite (mg N/L)	
			Reactor # R1	Reactor # R2	Effluent	Reactor # R1	Effluent
1	16-Apr-11	48	nd	21.3	21.0	nd	0.6
	17-Apr-11	49	nd	22.9	23.1	nd	0.9
	12-May-11*						
	02-Jul-11	52	nd	27.4	26.8	nd	0.7
	03-Jul-11	53	nd	27.5	26.4	nd	1.0
	04-Jul-11	54	nd	27.5	26.8	nd	0.7
	avg			25	25		0.8
2	16-Jan-12	31	39.0	60.6	59.4	0.6	0.9
	18-Jan-12	33	36.8	56.8	57.9	0.6	1.3
	20-Jan-12	35	36.9	57.5	57.9	0.6	nd
	02-Feb-12	48	31.9	53.7	52.0	1.6	< 0.02
	04-Feb-12	50	29.2	50.9	50.5	1.0	1.6
	06-Feb-12	52	30.2	52.2	51.6	2.2	< 0.02
	13-Feb-12	59	29.8	52.3	50.2	0.6	< 0.02
	15-Feb-12	61	35.2	56.4	57.3	1.3	0.3
	17-Feb-12	63	31.6	52.1	53.0	1.0	0.3
	avg		33	55	54	1.1	0.5
3A.1	27-Nov-12	58	0.3	5.4	5.3	< 0.02	0.21
	28-Nov-12	59	0.9	6.3	6.4	< 0.02	0.14
	29-Nov-12	60	0.4	5.7	5.4	< 0.02	0.10
	30-Nov-12	61	0.3	4.8	4.8	< 0.02	0.20
	01-Dec-12	62	0.6	5.9	5.2	< 0.02	0.20
	02-Dec-12	63	0.3	6.1	5.7	< 0.02	0.19
	03-Dec-12	64	0.5	6.1	6.1	< 0.02	0.10
	04-Dec-12	65	0.4	6.3	5.3	< 0.02	0.17
	05-Dec-12	66	0.7	6.9	6.6	< 0.02	0.11
	06-Dec-12	67	0.3	5.8	5.7	< 0.02	0.11
	07-Dec-12	68	0.4	5.4	5.0	< 0.02	0.13
	08-Dec-12	69	0.3	5.5	5.6	< 0.02	0.20
	09-Dec-12	70	0.3	5.4	4.8	< 0.02	0.35
	10-Dec-12	71	0.4	6.2	5.9	< 0.02	0.18
	11-Dec-12	72	0.5	6.8	6.7	< 0.02	0.24
	avg		0.4	5.9	5.6	< 0.02	0.18

* A system failure occurred 11-May-11 because of a power interruption. The system was restarted on 12-May-11.

Table B. 5: Nitrate and nitrite data for phases # 1, 2, 3A and 3B (continued)

# Phase	Date	# Day	Nitrate (mg N/L)			Nitrite (mg N/L)	
			Reactor # R1	Reactor # R2	Effluent	Reactor # R1	Effluent
3A.2	05-Aug-13	144	0.1	6.3	6.1	< 0.02	0.04
	06-Aug-13	145	0.4	5.5	5.5	< 0.02	0.03
	08-Aug-13	147	0.6	4.6	4.4	< 0.02	0.03
	09-Aug-13	148	0.4	5.5	5.1	< 0.02	0.04
	10-Aug-13	149	< 0.01	4.8	4.7	< 0.02	0.04
	12-Aug-13	151	0.3	5.8	5.6	< 0.02	0.05
	15-Aug-13	154	0.1	4.8	4.2	< 0.02	0.04
	18-Aug-13	157	0.1	4.9	4.5	< 0.02	0.04
	21-Aug-13	160	0.3	5.5	5.4	< 0.02	0.05
	22-Aug-13	161	0.4	5.1	5.1	< 0.02	0.03
	23-Aug-13	162	0.9	5.3	4.7	< 0.02	0.04
	avg		0.3	5.3	5.0	< 0.02	0.04
3A.3	24-Feb-14	40	1.3	7.0	5.7	< 0.02	0.20
	26-Feb-14	42	0.2	5.7	5.6	< 0.02	0.13
	27-Feb-14	43	0.9	5.8	5.2	< 0.02	0.11
	01-Mar-14	45	0.6	4.9	5.1	< 0.02	0.05
	04-Mar-14	48	0.4	5.0	4.6	< 0.02	0.05
	avg		0.7	5.7	5.2	< 0.02	0.1
3A.4	25-May-15	40	0.1	6.2	6.2	0	0
	26-May-15	41	0.1	6.2	6.2	0	0
	27-May-15	42	0.1	6.2	6.2	0	0
	avg		0.1	6.2	6.2	0	0
3B	10-Nov-14	43	< 0.01	4.8	5.3	< 0.02	0.03
	11-Nov-14	44	0.9	5.7	5.6	< 0.02	0.03
	12-Nov-14	45	0.6	5.4	5.4	< 0.02	< 0.02
	13-Nov-14	46	< 0.01	5.4	5.3	< 0.02	0.04
	14-Nov-14	47	0.5	4.9	5.1	< 0.02	0.03
	avg		0.4	5.2	5.3	< 0.02	0.0

Table B. 6: Measured oxygen uptake rate (OURmeas) data for phases # 1, 2, 3A and 3B

Phase	Date	# Day	OUR_{meas} (reactor # R1)	OUR_{meas} (reactor # R2)	Units
1	16-Apr-11	48	65.0	27.5	mg $O_2.L^{-1}.h^{-1}$
	17-Apr-11	49	66.9	26.4	mg $O_2.L^{-1}.h^{-1}$
	12-May-11*				
	02-Jul-11	52	66.0	27.5	mg $O_2.L^{-1}.h^{-1}$
	03-Jul-11	53	69.0	26.6	mg $O_2.L^{-1}.h^{-1}$
	04-Jul-11	54	69.3	28.6	mg $O_2.L^{-1}.h^{-1}$
	avg		67.0	27.0	mg $O_2.L^{-1}.h^{-1}$
2	16-Jan-12	31	0.0	50.9	mg $O_2.L^{-1}.h^{-1}$
	18-Jan-12	33	0.0	49.8	mg $O_2.L^{-1}.h^{-1}$
	20-Jan-12	35	0.0	50.0	mg $O_2.L^{-1}.h^{-1}$
	02-Feb-12	48	0.0	46.7	mg $O_2.L^{-1}.h^{-1}$
	04-Feb-12	50	0.0	47.0	mg $O_2.L^{-1}.h^{-1}$
	06-Feb-12	52	0.0	46.0	mg $O_2.L^{-1}.h^{-1}$
	13-Feb-12	59	0.0	49.0	mg $O_2.L^{-1}.h^{-1}$
	15-Feb-12	61	0.0	49.8	mg $O_2.L^{-1}.h^{-1}$
	17-Feb-12	63	0.0	47.6	mg $O_2.L^{-1}.h^{-1}$
	avg		0.0	48.5	mg $O_2.L^{-1}.h^{-1}$
3A.1	27-Nov-12	58	0.0	19.2	mg $O_2.L^{-1}.h^{-1}$
	28-Nov-12	59	0.0	19.5	mg $O_2.L^{-1}.h^{-1}$
	29-Nov-12	60	0.0	20.4	mg $O_2.L^{-1}.h^{-1}$
	30-Nov-12	61	0.0	19.7	mg $O_2.L^{-1}.h^{-1}$
	01-Dec-12	62	0.0	20.4	mg $O_2.L^{-1}.h^{-1}$
	02-Dec-12	63	0.0	20.6	mg $O_2.L^{-1}.h^{-1}$
	03-Dec-12	64	0.0	19.2	mg $O_2.L^{-1}.h^{-1}$
	04-Dec-12	65	0.0	19.5	mg $O_2.L^{-1}.h^{-1}$
	05-Dec-12	66	0.0	18.3	mg $O_2.L^{-1}.h^{-1}$
	06-Dec-12	67	0.0	19.5	mg $O_2.L^{-1}.h^{-1}$
	07-Dec-12	68	0.0	18.6	mg $O_2.L^{-1}.h^{-1}$
	08-Dec-12	69	0.0	18.8	mg $O_2.L^{-1}.h^{-1}$
	09-Dec-12	70	0.0	20.3	mg $O_2.L^{-1}.h^{-1}$
	10-Dec-12	71	0.0	21.2	mg $O_2.L^{-1}.h^{-1}$
	11-Dec-12	72	0.0	21.7	mg $O_2.L^{-1}.h^{-1}$
	avg		0.0	19.8	mg $O_2.L^{-1}.h^{-1}$

* A system failure occurred 11-May-11 because of a power interruption. The system was restarted on 12-May-11.

Table B. 6: Measured oxygen uptake rate (OUR_{meas}) data for phases # 1, 2, 3A and 3B (continued)

Phase	Date	# Day	OUR_{meas} (reactor # R1)	OUR_{meas} (reactor # R2)	Units
3A.2	05-Aug-13	144	0.0	21.9	mg $O_2.L^{-1}.h^{-1}$
	06-Aug-13	145	0.0	21.8	mg $O_2.L^{-1}.h^{-1}$
	08-Aug-13	147	0.0	23.9	mg $O_2.L^{-1}.h^{-1}$
	09-Aug-13	148	0.0	23.3	mg $O_2.L^{-1}.h^{-1}$
	10-Aug-13	149	0.0	21.9	mg $O_2.L^{-1}.h^{-1}$
	12-Aug-13	151	0.0	19.8	mg $O_2.L^{-1}.h^{-1}$
	15-Aug-13	154	0.0	21.7	mg $O_2.L^{-1}.h^{-1}$
	18-Aug-13	157	0.0	19.3	mg $O_2.L^{-1}.h^{-1}$
	21-Aug-13	160	0.0	18.7	mg $O_2.L^{-1}.h^{-1}$
	22-Aug-13	161	0.0	18.5	mg $O_2.L^{-1}.h^{-1}$
	23-Aug-13	162	0.0	17.5	mg $O_2.L^{-1}.h^{-1}$
	avg		0.0	20.8	mg $O_2.L^{-1}.h^{-1}$
3A.3	24-Feb-14	40	0.0	20.2	mg $O_2.L^{-1}.h^{-1}$
	26-Feb-14	42	0.0	23.7	mg $O_2.L^{-1}.h^{-1}$
	27-Feb-14	43	0.0	22.4	mg $O_2.L^{-1}.h^{-1}$
	01-Mar-14	45	0.0	21.0	mg $O_2.L^{-1}.h^{-1}$
	04-Mar-14	48	0.0	20.8	mg $O_2.L^{-1}.h^{-1}$
	avg		0.0	21.6	mg $O_2.L^{-1}.h^{-1}$
3A.4	25-May-15	40	0.0	23.6	mg $O_2.L^{-1}.h^{-1}$
	26-May-15	41	0.0	23.6	mg $O_2.L^{-1}.h^{-1}$
	27-May-15	42	0.0	23.7	mg $O_2.L^{-1}.h^{-1}$
	avg		0.0	23.6	mg $O_2.L^{-1}.h^{-1}$
3B	10-Nov-14	43	0.0	20.9	mg $O_2.L^{-1}.h^{-1}$
	11-Nov-14	44	0.0	22.9	mg $O_2.L^{-1}.h^{-1}$
	12-Nov-14	45	0.0	24.0	mg $O_2.L^{-1}.h^{-1}$
	13-Nov-14	46	0.0	22.4	mg $O_2.L^{-1}.h^{-1}$
	14-Nov-14	47	0.0	22.6	mg $O_2.L^{-1}.h^{-1}$
	avg		0.0	22.6	mg $O_2.L^{-1}.h^{-1}$

Table B. 7: Biomass oxygen uptake rate (OURB) data for phases # 1, 2, 3A and 3B

Phase	Date	# Day	OUR_B (reactor # R1)	OUR_B (reactor # R2)	Units
1	16-Apr-11	48	68.5	28.9	mg $O_2.L^{-1}.h^{-1}$
	17-Apr-11	49	70.4	27.8	mg $O_2.L^{-1}.h^{-1}$
	12-May-11*				
	02-Jul-11	52	70.0	29.2	mg $O_2.L^{-1}.h^{-1}$
	03-Jul-11	53	73.1	28.3	mg $O_2.L^{-1}.h^{-1}$
	04-Jul-11	54	73.4	30.3	mg $O_2.L^{-1}.h^{-1}$
	avg		71.0	29.0	mg $O_2.L^{-1}.h^{-1}$
2	16-Jan-12	31	7.62	50.2	mg $O_2.L^{-1}.h^{-1}$
	18-Jan-12	33	7.63	49.1	mg $O_2.L^{-1}.h^{-1}$
	20-Jan-12	35	7.63	49.3	mg $O_2.L^{-1}.h^{-1}$
	02-Feb-12	48	7.60	46.0	mg $O_2.L^{-1}.h^{-1}$
	04-Feb-12	50	7.60	46.3	mg $O_2.L^{-1}.h^{-1}$
	06-Feb-12	52	7.57	45.3	mg $O_2.L^{-1}.h^{-1}$
	13-Feb-12	59	7.57	48.3	mg $O_2.L^{-1}.h^{-1}$
	15-Feb-12	61	7.63	49.1	mg $O_2.L^{-1}.h^{-1}$
	17-Feb-12	63	7.63	46.9	mg $O_2.L^{-1}.h^{-1}$
	avg		7.61	47.8	mg $O_2.L^{-1}.h^{-1}$
3A.1	27-Nov-12	58	4.8	18.9	mg $O_2.L^{-1}.h^{-1}$
	28-Nov-12	59	4.8	19.2	mg $O_2.L^{-1}.h^{-1}$
	29-Nov-12	60	4.7	20.1	mg $O_2.L^{-1}.h^{-1}$
	30-Nov-12	61	4.7	19.4	mg $O_2.L^{-1}.h^{-1}$
	01-Dec-12	62	4.7	20.1	mg $O_2.L^{-1}.h^{-1}$
	02-Dec-12	63	4.7	20.3	mg $O_2.L^{-1}.h^{-1}$
	03-Dec-12	64	4.7	18.9	mg $O_2.L^{-1}.h^{-1}$
	04-Dec-12	65	4.8	19.2	mg $O_2.L^{-1}.h^{-1}$
	05-Dec-12	66	4.7	18.0	mg $O_2.L^{-1}.h^{-1}$
	06-Dec-12	67	4.8	19.2	mg $O_2.L^{-1}.h^{-1}$
	07-Dec-12	68	4.8	18.3	mg $O_2.L^{-1}.h^{-1}$
	08-Dec-12	69	4.8	18.5	mg $O_2.L^{-1}.h^{-1}$
	09-Dec-12	70	4.7	20.0	mg $O_2.L^{-1}.h^{-1}$
	10-Dec-12	71	4.7	20.9	mg $O_2.L^{-1}.h^{-1}$
	11-Dec-12	72	4.7	21.4	mg $O_2.L^{-1}.h^{-1}$
	avg		4.7	19.5	mg $O_2.L^{-1}.h^{-1}$

* A system failure occurred 11-May-11 because of a power interruption. The system was restarted on 12-May-11.

Table B. 7: Biomass oxygen uptake rate (OUR_B) data for phases # 1, 2, 3A and 3B (continued)

Phase	Date	# Day	OUR_B (reactor # R1)	OUR_B (reactor # R2)	Units
3A.2	05-Aug-13	144	5.0	21.6	mg $O_2.L^{-1}.h^{-1}$
	06-Aug-13	145	5.3	21.4	mg $O_2.L^{-1}.h^{-1}$
	08-Aug-13	147	5.2	23.5	mg $O_2.L^{-1}.h^{-1}$
	09-Aug-13	148	5.1	22.9	mg $O_2.L^{-1}.h^{-1}$
	10-Aug-13	149	5.2	21.5	mg $O_2.L^{-1}.h^{-1}$
	12-Aug-13	151	4.8	19.5	mg $O_2.L^{-1}.h^{-1}$
	15-Aug-13	154	5.0	21.4	mg $O_2.L^{-1}.h^{-1}$
	18-Aug-13	157	5.0	19.0	mg $O_2.L^{-1}.h^{-1}$
	21-Aug-13	160	4.9	18.4	mg $O_2.L^{-1}.h^{-1}$
	22-Aug-13	161	5.0	18.2	mg $O_2.L^{-1}.h^{-1}$
	23-Aug-13	162	4.9	17.2	mg $O_2.L^{-1}.h^{-1}$
	avg		5.0	20.4	mg $O_2.L^{-1}.h^{-1}$
3A.3	24-Feb-14	40	5.1	19.9	mg $O_2.L^{-1}.h^{-1}$
	26-Feb-14	42	5.1	23.3	mg $O_2.L^{-1}.h^{-1}$
	27-Feb-14	43	5.1	22.1	mg $O_2.L^{-1}.h^{-1}$
	01-Mar-14	45	5.0	20.6	mg $O_2.L^{-1}.h^{-1}$
	04-Mar-14	48	5.0	20.4	mg $O_2.L^{-1}.h^{-1}$
	avg		5.1	21.3	mg $O_2.L^{-1}.h^{-1}$
3A.4	25-May-15	40	3.0	23.5	mg $O_2.L^{-1}.h^{-1}$
	26-May-15	41	3.0	23.5	mg $O_2.L^{-1}.h^{-1}$
	27-May-15	42	3.0	23.6	mg $O_2.L^{-1}.h^{-1}$
	avg		3.0	23.6	mg $O_2.L^{-1}.h^{-1}$
3B	10-Nov-14	43	3.5	20.6	mg $O_2.L^{-1}.h^{-1}$
	11-Nov-14	44	3.5	22.5	mg $O_2.L^{-1}.h^{-1}$
	12-Nov-14	45	3.5	23.6	mg $O_2.L^{-1}.h^{-1}$
	13-Nov-14	46	3.4	22.1	mg $O_2.L^{-1}.h^{-1}$
	14-Nov-14	47	3.5	22.3	mg $O_2.L^{-1}.h^{-1}$
	avg		3.5	22.2	mg $O_2.L^{-1}.h^{-1}$

Table B. 8: TSS and VSS data for phases # 1, 2, 3A and 3B

Phase	Date	# Day	Sludge wastage			
			TSS	Units	VSS	Units
1	16-Apr-11	48	2373	mg TSS/L	2198	mg VSS/L
	17-Apr-11	49	2480	mg TSS/L	2269	mg VSS/L
	12-May-11*					
	02-Jul-11	52	2356	mg TSS/L	2209	mg VSS/L
	03-Jul-11	53	2478	mg TSS/L	2337	mg VSS/L
	04-Jul-11	54	2323	mg TSS/L	2141	mg VSS/L
	avg		2402	mg TSS/L	2231	mg VSS/L
2	16-Jan-12	31	1047	mg TSS/L	946	mg VSS/L
	18-Jan-12	33	1020	mg TSS/L	943	mg VSS/L
	20-Jan-12	35	1017	mg TSS/L	934	mg VSS/L
	02-Feb-12	48	1133	mg TSS/L	1066	mg VSS/L
	04-Feb-12	50	1115	mg TSS/L	1023	mg VSS/L
	06-Feb-12	52	1185	mg TSS/L	1097	mg VSS/L
	13-Feb-12	59	1143	mg TSS/L	1081	mg VSS/L
	15-Feb-12	61	1197	mg TSS/L	1098	mg VSS/L
	17-Feb-12	63	1190	mg TSS/L	1091	mg VSS/L
	avg		1116	mg TSS/L	1031	mg VSS/L
3A.1	27-Nov-12	58	935	mg TSS/L	860	mg VSS/L
	28-Nov-12	59	924	mg TSS/L	856	mg VSS/L
	29-Nov-12	60	900	mg TSS/L	840	mg VSS/L
	30-Nov-12	61	940	mg TSS/L	856	mg VSS/L
	01-Dec-12	62	952	mg TSS/L	868	mg VSS/L
	02-Dec-12	63	956	mg TSS/L	872	mg VSS/L
	03-Dec-12	64	971	mg TSS/L	911	mg VSS/L
	04-Dec-12	65	944	mg TSS/L	872	mg VSS/L
	05-Dec-12	66	959	mg TSS/L	893	mg VSS/L
	06-Dec-12	67	937	mg TSS/L	849	mg VSS/L
	07-Dec-12	68	979	mg TSS/L	896	mg VSS/L
	08-Dec-12	69	932	mg TSS/L	869	mg VSS/L
	09-Dec-12	70	937	mg TSS/L	879	mg VSS/L
	10-Dec-12	71	944	mg TSS/L	869	mg VSS/L
	11-Dec-12	72	908	mg TSS/L	840	mg VSS/L
	avg		941	mg TSS/L	869	mg VSS/L

* A system failure occurred 11-May-11 because of a power interruption. The system was restarted on 12-May-11.

Table B. 8: TSS and VSS data for phases # 1, 2, 3A and 3B (continued)

Phase	Date	# Day	Sludge wastage			
			TSS	Units	VSS	Units
3A.2	05-Aug-13	144	1029	mg TSS/L	889	mg VSS/L
	06-Aug-13	145	1049	mg TSS/L	897	mg VSS/L
	08-Aug-13	147	1076	mg TSS/L	924	mg VSS/L
	09-Aug-13	148	1131	mg TSS/L	979	mg VSS/L
	10-Aug-13	149	1076	mg TSS/L	927	mg VSS/L
	12-Aug-13	151	1085	mg TSS/L	940	mg VSS/L
	15-Aug-13	154	1201	mg TSS/L	1021	mg VSS/L
	18-Aug-13	157	1191	mg TSS/L	992	mg VSS/L
	21-Aug-13	160	1245	mg TSS/L	1017	mg VSS/L
	22-Aug-13	161	1264	mg TSS/L	1013	mg VSS/L
	23-Aug-13	162	1260	mg TSS/L	997	mg VSS/L
	avg		1146	mg TSS/L	963	mg VSS/L
3A.3	24-Feb-14	40	1099	mg TSS/L	1003	mg VSS/L
	26-Feb-14	42	1123	mg TSS/L	1027	mg VSS/L
	27-Feb-14	43	1077	mg TSS/L	981	mg VSS/L
	01-Mar-14	45	1059	mg TSS/L	963	mg VSS/L
	04-Mar-14	48	979	mg TSS/L	905	mg VSS/L
	avg		1067	mg TSS/L	976	mg VSS/L
3A.4	25-May-15	40	1381	mg TSS/L	851	mg VSS/L
	26-May-15	41	1327	mg TSS/L	848	mg VSS/L
	27-May-15	42	1337	mg TSS/L	865	mg VSS/L
	avg		1348	mg TSS/L	855	mg VSS/L
3B	10-Nov-14	43	1368	mg TSS/L	901	mg VSS/L
	11-Nov-14	44	1420	mg TSS/L	929	mg VSS/L
	12-Nov-14	45	1397	mg TSS/L	908	mg VSS/L
	13-Nov-14	46	1389	mg TSS/L	859	mg VSS/L
	14-Nov-14	47	1431	mg TSS/L	837	mg VSS/L
	avg		1401	mg TSS/L	887	mg VSS/L

Table B. 9: fP, fVT and fCV data for phases # 1, 2, 3A and 3B

Phase	Date	# Day	Sludge wastage					
			f_P	Units	f_{VT}	Units	f_{CV}	Units
1	16-Apr-11	48	1.5	% g P/g VSS	0.93	g VSS/g TSS	1.50	g COD/g VSS
	17-Apr-11	49	1.4	% g P/g VSS	0.91	g VSS/g TSS	1.49	g COD/g VSS
	12-May-11*							
	02-Jul-11	52	1.3	% g P/g VSS	0.94	g VSS/g TSS	1.50	g COD/g VSS
	03-Jul-11	53	1.3	% g P/g VSS	0.94	g VSS/g TSS	1.46	g COD/g VSS
	04-Jul-11	54	1.4	% g P/g VSS	0.92	g VSS/g TSS	1.56	g COD/g VSS
	avg		1.4	% g P/g VSS	0.93	g VSS/g TSS	1.50	g COD/g VSS
2	16-Jan-12	31	1.4	% g P/g VSS	0.90	g VSS/g TSS	1.47	g COD/g VSS
	18-Jan-12	33	1.3	% g P/g VSS	0.92	g VSS/g TSS	1.51	g COD/g VSS
	20-Jan-12	35	nd	% g P/g VSS	0.92	g VSS/g TSS	1.46	g COD/g VSS
	02-Feb-12	48	1.4	% g P/g VSS	0.94	g VSS/g TSS	1.36	g COD/g VSS
	04-Feb-12	50	1.6	% g P/g VSS	0.92	g VSS/g TSS	1.48	g COD/g VSS
	06-Feb-12	52	1.5	% g P/g VSS	0.93	g VSS/g TSS	1.50	g COD/g VSS
	13-Feb-12	59	1.6	% g P/g VSS	0.95	g VSS/g TSS	1.40	g COD/g VSS
	15-Feb-12	61	1.6	% g P/g VSS	0.92	g VSS/g TSS	1.41	g COD/g VSS
	17-Feb-12	63	1.6	% g P/g VSS	0.92	g VSS/g TSS	1.44	g COD/g VSS
	avg		1.5	% g P/g VSS	0.92	g VSS/g TSS	1.45	g COD/g VSS
3A.1	27-Nov-12	58	2.5	% g P/g VSS	0.92	g VSS/g TSS	1.61	g COD/g VSS
	28-Nov-12	59	1.7	% g P/g VSS	0.93	g VSS/g TSS	1.63	g COD/g VSS
	29-Nov-12	60	1.8	% g P/g VSS	0.93	g VSS/g TSS	1.59	g COD/g VSS
	30-Nov-12	61	2.1	% g P/g VSS	0.91	g VSS/g TSS	1.59	g COD/g VSS
	01-Dec-12	62	2.0	% g P/g VSS	0.91	g VSS/g TSS	1.57	g COD/g VSS
	02-Dec-12	63	1.9	% g P/g VSS	0.91	g VSS/g TSS	1.56	g COD/g VSS
	03-Dec-12	64	1.5	% g P/g VSS	0.94	g VSS/g TSS	1.58	g COD/g VSS
	04-Dec-12	65	1.4	% g P/g VSS	0.92	g VSS/g TSS	1.62	g COD/g VSS
	05-Dec-12	66	1.5	% g P/g VSS	0.93	g VSS/g TSS	1.60	g COD/g VSS
	06-Dec-12	67	1.6	% g P/g VSS	0.91	g VSS/g TSS	1.58	g COD/g VSS
	07-Dec-12	68	1.5	% g P/g VSS	0.92	g VSS/g TSS	1.58	g COD/g VSS
	08-Dec-12	69	1.7	% g P/g VSS	0.93	g VSS/g TSS	1.65	g COD/g VSS
	09-Dec-12	70	1.5	% g P/g VSS	0.94	g VSS/g TSS	1.53	g COD/g VSS
	10-Dec-12	71	1.6	% g P/g VSS	0.92	g VSS/g TSS	1.49	g COD/g VSS
	11-Dec-12	72	1.0	% g P/g VSS	0.93	g VSS/g TSS	1.58	g COD/g VSS
	avg		1.7	% g P/g VSS	0.92	g VSS/g TSS	1.58	g COD/g VSS

* A system failure occurred 11-May-11 because of a power interruption. The system was restarted on 12-May-11.

Table B. 9: f_P, f_{VT} and f_{CV} data for phases # 1, 2, 3A and 3B (continued)

Phase	Date	# Day	Sludge wastage					
			f_P	Units	f_{VT}	Units	f_{CV}	Units
3A.2	05-Aug-13	144	3.5	% g P/g VSS	0.86	g VSS/g TSS	1.48	g COD/g VSS
	06-Aug-13	145	4.4	% g P/g VSS	0.86	g VSS/g TSS	1.44	g COD/g VSS
	08-Aug-13	147	4.6	% g P/g VSS	0.86	g VSS/g TSS	1.49	g COD/g VSS
	09-Aug-13	148	4.1	% g P/g VSS	0.87	g VSS/g TSS	1.36	g COD/g VSS
	10-Aug-13	149	4.3	% g P/g VSS	0.86	g VSS/g TSS	1.41	g COD/g VSS
	12-Aug-13	151	4.2	% g P/g VSS	0.87	g VSS/g TSS	1.44	g COD/g VSS
	15-Aug-13	154	5.5	% g P/g VSS	0.85	g VSS/g TSS	1.40	g COD/g VSS
	18-Aug-13	157	7.5	% g P/g VSS	0.83	g VSS/g TSS	1.48	g COD/g VSS
	21-Aug-13	160	5.4	% g P/g VSS	0.82	g VSS/g TSS	1.37	g COD/g VSS
	22-Aug-13	161	5.4	% g P/g VSS	0.80	g VSS/g TSS	1.42	g COD/g VSS
	23-Aug-13	162	6.1	% g P/g VSS	0.79	g VSS/g TSS	1.44	g COD/g VSS
	avg		5.0	% g P/g VSS	0.84	g VSS/g TSS	1.43	g COD/g VSS
3A.3	24-Feb-14	40	1.8	% g P/g VSS	0.91	g VSS/g TSS	1.44	g COD/g VSS
	26-Feb-14	42	2.1	% g P/g VSS	0.91	g VSS/g TSS	1.25	g COD/g VSS
	27-Feb-14	43	1.9	% g P/g VSS	0.91	g VSS/g TSS	1.43	g COD/g VSS
	01-Mar-14	45	2.0	% g P/g VSS	0.91	g VSS/g TSS	1.40	g COD/g VSS
	04-Mar-14	48	2.2	% g P/g VSS	0.92	g VSS/g TSS	1.46	g COD/g VSS
	avg		2.0	% g P/g VSS	0.91	g VSS/g TSS	1.40	g COD/g VSS
3A.4	25-May-15	40	14.1	% g P/g VSS	0.62	g VSS/g TSS	1.58	g COD/g VSS
	26-May-15	41	13.4	% g P/g VSS	0.64	g VSS/g TSS	1.50	g COD/g VSS
	27-May-15	42	11.6	% g P/g VSS	0.65	g VSS/g TSS	1.49	g COD/g VSS
	avg		13.0	% g P/g VSS	0.63	g VSS/g TSS	1.52	g COD/g VSS
3B	10-Nov-14	43	10.6	% g P/g VSS	0.66	g VSS/g TSS	1.46	g COD/g VSS
	11-Nov-14	44	11.9	% g P/g VSS	0.65	g VSS/g TSS	1.44	g COD/g VSS
	12-Nov-14	45	14.0	% g P/g VSS	0.65	g VSS/g TSS	1.45	g COD/g VSS
	13-Nov-14	46	nd	% g P/g VSS	0.62	g VSS/g TSS	1.52	g COD/g VSS
	14-Nov-14	47	nd	% g P/g VSS	0.58	g VSS/g TSS	1.54	g COD/g VSS
	avg		12.1	% g P/g VSS	0.63	g VSS/g TSS	1.48	g COD/g VSS

Table B. 10: Sulfate data for phases # 3A and 3B

Phase	Date	# Day	Sulfate concentration			
			Influent	AN reactor	effluent	Units
3A.1	27-Nov-12	58	6.0	0.7	6.0	mg SO_4-S/L
	28-Nov-12	59	6.0	0.7	6.0	mg SO_4-S/L
	29-Nov-12	60	6.0	0.7	6.0	mg SO_4-S/L
	30-Nov-12	61	6.0	0.7	6.0	mg SO_4-S/L
	01-Dec-12	62	6.0	0.7	6.0	mg SO_4-S/L
	02-Dec-12	63	6.0	0.7	6.0	mg SO_4-S/L
	03-Dec-12	64	6.0	0.7	6.0	mg SO_4-S/L
	04-Dec-12	65	6.0	0.7	6.0	mg SO_4-S/L
	05-Dec-12	66	6.0	0.7	6.0	mg SO_4-S/L
	06-Dec-12	67	6.0	0.7	6.0	mg SO_4-S/L
	07-Dec-12	68	6.0	0.7	6.0	mg SO_4-S/L
	08-Dec-12	69	6.0	0.7	6.0	mg SO_4-S/L
	09-Dec-12	70	6.0	0.7	6.0	mg SO_4-S/L
	10-Dec-12	71	6.0	0.7	6.0	mg SO_4-S/L
	11-Dec-12	72	6.0	0.7	6.0	mg SO_4-S/L
	avg		6.0	0.7	6.0	mg SO_4-S/L

Note: Sulfate measurement was not performed for phase # 3A.1. It was assumed that the sulfate concentration was more similar to that in phase # 3A.2.

Table B. 10: Sulfate data for phases # 3A and 3B (continued)

Phase	Date	# Day	Sulfate concentration			
			Influent	AN reactor	effluent	Units
3A.2	05-Aug-13	144	6.4	0.7	6.3	mg SO_4-S/L
	06-Aug-13	145	6.1	0.7	6.0	mg SO_4-S/L
	08-Aug-13	147	5.6	0.7	5.3	mg SO_4-S/L
	09-Aug-13	148	6.0	0.7	6.3	mg SO_4-S/L
	10-Aug-13	149	5.8	0.7	5.0	mg SO_4-S/L
	12-Aug-13	151	6.2	0.7	6.0	mg SO_4-S/L
	15-Aug-13	154	6.0	0.7	6.0	mg SO_4-S/L
	18-Aug-13	157	6.1	0.7	5.0	mg SO_4-S/L
	21-Aug-13	160	6.2	0.7	6.0	mg SO_4-S/L
	22-Aug-13	161	6.0	0.7	6.0	mg SO_4-S/L
	23-Aug-13	162	5.9	0.7	5.0	mg SO_4-S/L
	avg		6.0	0.7	5.7	mg SO_4-S/L
3A.3	24-Feb-14	40	6.6	5.0	5.3	mg SO_4-S/L
	26-Feb-14	42	6.3	3.7	4.0	mg SO_4-S/L
	27-Feb-14	43	6.2	3.3	4.0	mg SO_4-S/L
	01-Mar-14	45	5.7	3.0	3.7	mg SO_4-S/L
	04-Mar-14	48	5.6	2.3	3.0	mg SO_4-S/L
	avg		6.1	3.5	4.0	mg SO_4-S/L
3A.4	25-May-15	40	5.9	0.7	0.7	mg SO_4-S/L
	26-May-15	41	5.9	0.7	0.7	mg SO_4-S/L
	27-May-15	42	5.3	0.7	0.7	mg SO_4-S/L
	avg		5.7	0.7	0.7	mg SO_4-S/L
3B	10-Nov-14	43	5.8	0.7	0.7	mg SO_4-S/L
	11-Nov-14	44	5.8	0.7	0.7	mg SO_4-S/L
	12-Nov-14	45	5.8	0.7	0.7	mg SO_4-S/L
	13-Nov-14	46	5.7	0.7	0.7	mg SO_4-S/L
	14-Nov-14	47	5.7	0.7	0.7	mg SO_4-S/L
	avg		5.8	0.7	0.7	mg SO_4-S/L

Table B. 11: Orthophosphate (o-PO4) for phases # 1 and 2

Phase	Date	# Day	$o\text{-}PO_4$ conc.		
			Influent	Effluent	Units
1	16-Apr-11	48	19.2	16.1	mg P/L
	17-Apr-11	49	19.6	16.6	mg P/L
	12-May-11*				
	02-Jul-11	52	18.6	16.6	mg P/L
	03-Jul-11	53	18.7	15.4	mg P/L
	04-Jul-11	54	18.6	15.6	mg P/L
	avg		19.0	16	mg P/L
2	16-Jan-12	31	19.5	18.3	mg P/L
	18-Jan-12	33	19.7	18.0	mg P/L
	20-Jan-12	35	nd	nd	mg P/L
	02-Feb-12	48	20.1	17.6	mg P/L
	04-Feb-12	50	20.0	17.3	mg P/L
	06-Feb-12	52	20.4	17.0	mg P/L
	13-Feb-12	59	19.6	16.9	mg P/L
	15-Feb-12	61	18.9	16.8	mg P/L
	17-Feb-12	63	18.7	17.4	mg P/L
	avg		20	17.0	mg P/L

* A system failure occurred 11-May-11 because of a power interruption. The system was restarted on 12-May-11.

Table B. 12: Orthophosphate (o-PO4) for phases # 3A and 3B

Phase	Date	# Day	$o\text{-}PO_4$ conc.			
			Influent	AN reactor	Effluent	Units
3A.1	27-Nov-12	58	47.5	44.0	42.8	mg P/L
	28-Nov-12	59	46.6	46.4	45.0	mg P/L
	29-Nov-12	60	45.6	46.4	45.6	mg P/L
	30-Nov-12	61	44.9	44.7	45.0	mg P/L
	01-Dec-12	62	45.6	44.3	43.6	mg P/L
	02-Dec-12	63	47.3	48.1	45.0	mg P/L
	03-Dec-12	64	49.8	48.5	47.8	mg P/L
	04-Dec-12	65	49.1	47.9	46.9	mg P/L

Table B. 12: orthophosphate (o-PO_4) for phases # 3A and 3B (continued)

Phase	Date	# Day	o-PO_4 conc.			
			Influent	AN reactor	Effluent	Units
3A.1	05-Dec-12	66	49.0	47.5	47.9	mg P/L
	06-Dec-12	67	47.3	46.7	46.7	mg P/L
	07-Dec-12	68	47.1	46.8	46.8	mg P/L
	08-Dec-12	69	45.9	45.0	45.3	mg P/L
	09-Dec-12	70	44.4	44.5	42.4	mg P/L
	10-Dec-12	71	50.6	50.2	47.4	mg P/L
	11-Dec-12	72	51.4	50.0	49.3	mg P/L
	avg		47.5	46.7	45.8	mg P/L
3A.2	05-Aug-13	144	53.9	58.4	45.0	mg P/L
	06-Aug-13	145	51.6	55.7	44.4	mg P/L
	08-Aug-13	147	46.9	51.6	39.7	mg P/L
	09-Aug-13	148	50.5	52.6	40.8	mg P/L
	10-Aug-13	149	48.9	54.3	40.9	mg P/L
	12-Aug-13	151	52.5	55.0	43.3	mg P/L
	15-Aug-13	154	50.4	51.9	43.5	mg P/L
	18-Aug-13	157	51.6	56.5	41.5	mg P/L
	21-Aug-13	160	52.7	56.1	41.7	mg P/L
	22-Aug-13	161	50.6	54.3	41.0	mg P/L
	23-Aug-13	162	49.9	50.7	39.4	mg P/L
	avg		50.9	54.3	41.9	mg P/L
3A.3	24-Feb-14	40	55.9	55.4	53.7	mg P/L
	26-Feb-14	42	53.2	52.7	50.1	mg P/L
	27-Feb-14	43	52.2	51.4	50.7	mg P/L
	01-Mar-14	45	48.3	50.5	48.4	mg P/L
	04-Mar-14	48	47.4	46.7	44.7	mg P/L
	avg		51.4	51.3	49.5	mg P/L
3A.4	25-May-15	40	48.2	71.3	29.9	mg P/L
	26-May-15	41	42.9	61.6	31.1	mg P/L
	27-May-15	42	42.8	64.7	32.0	mg P/L
	avg		44.6	65.9	31.0	mg P/L
3B	10-Nov-14	43	45.0	67.3	34.9	mg P/L
	11-Nov-14	44	43.5	56.3	30.2	mg P/L
	12-Nov-14	45	41.0	59.8	26.3	mg P/L
	13-Nov-14	46				mg P/L
	14-Nov-14	47				mg P/L
	avg		43.2	61.1	30.5	mg P/L

Table B. 13: Recycle ratio (a) and dissolved oxygen (DO) data for phases # 1, 2, 3A and 3B

Phase	a	Units	DO conc. (mg O_2/L)			DO_{mid}[2] conc. (mg O_2/L)	
			Influent[1]	Reactor		Reactor # R1	Reactor # R2
				# R1	# R2		
1	4.5	L/L_{inf}	8.8	6	6.5	3.6	3.6
2	4.4	L/L_{inf}	8.8	0	6.5	0	3.5
3A.1	2.6	L/L_{inf}	8.8	0	6.5	0	3.8
3A.2	2.6	L/L_{inf}	8.8	0	6.5	0	3.8
3A.3	3.0	L/L_{inf}	8.8	0	6.5	0	3.8
3A.4	2.0	L/L_{inf}	8.8	0	4.0	0	3.6
3B	3.0	L/L_{inf}	8.8	0	3.5	0	3.8

Note:

[1] DO_{sat} in clean water at 20 °C and 738 mmHg,

[2] DO concentration at midpoint during OUR test.

B.1. An example of the mass balances calculations on the whole AN-OX system (Phase # 3)

- *<u>COD mass balance calculation</u> (data from the run performed on 23-Aug-13)*

The mass rate of total COD entering the system is given by Equation (2.10):

$FCOD_{INPUT} = 5329$ mg COD/d

The sludge wastage and effluent COD mass rates are calculated from Equations (2.12), (2.13) and (2.14):

$FS_{WAS} = 43$ mg COD/d

$FX_{WAS} = 1436$ mg COD/d

$FS_{eff} = 52$ mg COD/d

COD oxidized calculations:

The k_La and DO_{sat} values are obtained from Equations (2.25) through (2.27):

k_La used in reactor # R2 = 0.15 h^{-1}

DO_{sat} used = 7.9 mg O_2/L

Then, applying Equations (2.30) and (2.31) gives the OUR_B values for reactors R1 and R2.

Reactor # R1: FO_{OURB} = 293 mg COD/d

Reactor # R2: FO_{OURB} = 2887 mg COD/d

The mass of oxygen equivalent of nitrate denitrified is obtained from Equation (2.48):

$FO_{NO3,denit}$ = 341 mg COD/d

The mass rate of oxygen required for nitrification (FO_{nit}) is calculated by Equation (2.55):

FO_{nit} = 793 mg O_2/d

The daily mass of oxygen equivalent of sulfate reduced/sulfide oxidized is obtained from Equations (2.59) through (2.64):

$FO_{sulfate\ reduc}$ = 374 mg O_2/d

$FO_{sulfide\ oxid}$ = 353 mg O_2/d

$$\%\ \text{Sulfur contributing to COD balance} = \frac{FO_{sulfate\ reduc} - FO_{sulfide\ oxid}}{FCOD_{INPUT}} \times 100 = 0.4\ \%$$

Thus, the total mass of COD oxidized across the system is obtained from Equations (2.19) and (2.20):

$FCOD_{oxid}$ = 2749 mg COD/d

The total output COD is given by Equation (2.11):

$FCOD_{OUTPUT}$ = 4280 mg COD/d

Therefore, the COD mass balance (%) is given by Equation (2.9):

$$\text{COD mass balance (\%)} = \frac{\text{FCOD}_{\text{OUTPUT}}}{\text{FCOD}_{\text{INPUT}}} \times 100 = \frac{4280}{5329} \times 100 = 80.3\ \%$$

A summary of the COD mass balance calculations is presented in Table B.14.

Table B. 14: Summary of the COD mass balance calculation results for phase # 3 (AN-OX)

$FCOD_{INPUT}$		$FCOD_{OUTPUT}$			% COD mass balance $= \frac{FCOD_{OUTPUT}}{FCOD_{INPUT}} \times 100$
Value	Units	Parameter	Value	Units	
5329	mg COD/d	FS_{eff}	52	mg COD/d	80.3
		FS_{WAS}	43	mg COD/d	
		FX_{WAS}	1436	mg COD/d	
		$FCOD_{oxid}$	2749	mg COD/d	

Note: data from the run performed on 23-Aug-13.

Oxygen consumption and Y_{OBS} calculation

The oxygen consumption and Y_{OBS} can be calculated according to Equations (B.1) and (B.2), respectively.

$$\text{Oxygen consumption (\% gCOD/gCOD)} = \frac{\text{FCOD}_{\text{oxid}}}{\text{FS}_{\text{T,inf}} - \text{FS}_{\text{eff}} - \text{FS}_{\text{WAS}}} \times 100 \quad \text{(B.1)}$$

$$\text{Y}_{\text{OBS}}\text{(\% gCOD/gCOD)} = \frac{\text{FX}_{\text{WAS}}}{\text{FS}_{\text{T,inf}} - \text{FS}_{\text{eff}} - \text{FS}_{\text{WAS}}} \times 100 \quad \text{(B.2)}$$

Considering the data from the run performed on 23-Aug-13 gives the oxygen consumption and Y_{OBS} values of 52.5% g COD/g COD and 27.4% g COD/g COD, respectively.

- *<u>N mass balance calculation</u> (data from the run performed on 23-Aug-13)*

The daily mass of TN entering the system is given by Equation (2.65):

$FN_{TN,inf}$ = 346 mg N/d

The daily mass of N leaving the system through the sludge wastage and effluent streams is calculated using Equations (2.66) through (2.71):

$FN_{TKN,WAS}$ = 152 mg N/d

$FN_{NO3,WAS}$ = 5.3 mg N/d

$FN_{NO2,WAS}$ = 0.04 mg N/d

$FN_{TKN,eff}$ = 19.8 mg N/d

$FN_{NO3,eff}$ = 49 mg N/d

$FN_{NO2,eff}$ = 0.4 mg N/d

The mass of nitrate denitrified is given by Equation (2.47):

$FN_{NO3,denit}$ = 119 mg N/d

The TN leaving the system in mg N/d units is given by Equation (2.72):

$FN_{TN,OUTPUT}$ = 346 mg N/d

The N mass balance (%) is calculated by Equation (2.73).

$$\text{N mass balance (\%)} = \frac{FN_{TN,OUTPUT}}{FN_{TN,INPUT}} \times 100 = \frac{346}{346} \times 100 = 100\ \%$$

The N mass balance calculation results are presented in Table B.15.

Table B. 15: Summary of N mass balance calculation results for phase # 3 (AN-OX)

$FN_{TN,INPUT}$		$FN_{TN,OUTPUT}$			% N mass balance $= \frac{FN_{TN,OUTPUT}}{FN_{TN,INPUT}} \times 100$
Value	Units	Parameter	Value	Units	
346	mg N/d	$FN_{TKN,WAS}$	152	mg N/d	100
		$FN_{NO3,WAS}$	5.3	mg N/d	
		$FN_{NO2,WAS}$	0.04	mg N/d	
		$FN_{TKN,eff}$	19.8	mg N/d	
		$FN_{NO3,eff}$	49	mg N/d	
		$FN_{NO2,eff}$	0.4	mg N/d	
		$FN_{NO3,denit.}$	119	mg N/d	

Note: data from the run performed on 23-Aug-13

- *P mass balance calculation (data from the run performed on 23-Aug-13)*

The daily mass of TP entering the system is given by Equation (2.77):

$FP_{TP,INPUT} = 577$ mg P/d

The effluent and sludge wastage TP mass rates are obtained from Equations (2.75) and (2.76):

$FP_{TP,eff} = 455$ mg P/d

$FP_{TP,WAS} = 100$ mg P/d

The P mass balance (%) is calculated by Equation (2.74).

$$\text{P mass balance (\%)} = \frac{FP_{TP,OUTPUT}}{FP_{TP,INPUT}} \times 100 = \frac{555}{577} \times 100 = 96.3\%$$

A summary of the P mass balance calculation is listed in Table B.16.

Table B. 16: Summary of P mass balance calculation results for phase # 3 (AN-OX)

$FP_{TP,INPUT}$		$FP_{TP,OUTPUT}$			% P mass balance $= \frac{FP_{TP,OUTPUT}}{FP_{TP,INPUT}} \times 100$
Value	Units	Parameter	Value	Units	
577	mg P/d	$FP_{TP,WAS}$	100	mg P/d	96.2
		$FP_{TP,eff}$	455	mg P/d	

Note: data from the run performed on 23-Aug-13

Table B. 17: Typical example results of the calculated oxygen transfer efficiency (OTE) for the AN-OX system

	Symbol	Description	Value	Units	remarks
measured & assumed	V_{R2}	Reactor R2 volume	7.0	L	
	Q_{inf}	Influent flow rate	11.0	L/d	
	a	recycle ratio	2.6	L/L_{inf}	
	T	Temperature	20	°C	
	Pres	Pressure	738	mmHg	
	DO_{R1}	DO conc. in reactor R1	0	mg O_2/L	
	DO_{R2}	DO conc. in reactor R2	6.5	mg O_2/L	
	$DO_{mid,R2}$	DO conc. at midpoint during OUR test	3.8	mg O_2/L	
	$DO_{sat,\ clean\ water}$	saturation DO conc. in clean water	8.8	mg O_2/L	
	β	DO_{sat} correction factor	0.9		
	$k_La_{\ measured}$	Measured oxygen mass transfer coefficient in clean water	0.21	h^{-1}	
	α	k_La correction factor	0.7		
	Q_{air}	air flow rate entering reactor R2	5.0	L/min	
	ρ_{air}	Air density	1.2	g/L	
	w_{O2}	Oxygen mass fraction in air	23.2	% g/g	
calculated	OUR_{meas}	Measured oxygen uptake rate	19.8	mg O_2 L^{-1} h^{-1}	
	$DO_{sat.used}$	saturation DO conc. in the mixed liquor	7.9	mg O_2/L	Eq. 2.26
	$k_La_{\ used}$	Oxygen mass transfer coefficient in the mixed liquor	0.15	h^{-1}	Eq. 2.25
	OUR_B	Biomass oxygen uptake rate	19.5	mg O_2 L^{-1} h^{-1}	Eq. 2.23
	FO_{air}	Mass rate of oxygen transferred to the reactor R2	2004	g O_2/d	
	FO_{OURB}	Oxygen utilized by biomass	3.28	g O_2/d	
	OTE = FO_{OURB}/ FO_{air}	Mass fraction of O_2 transferred	0.16	%	

Note: data from phase # 3A.1

B.2. An example of the COD mass balance calculations around the separated AN and OX reactors (data from the run performed on 23-Aug-13)

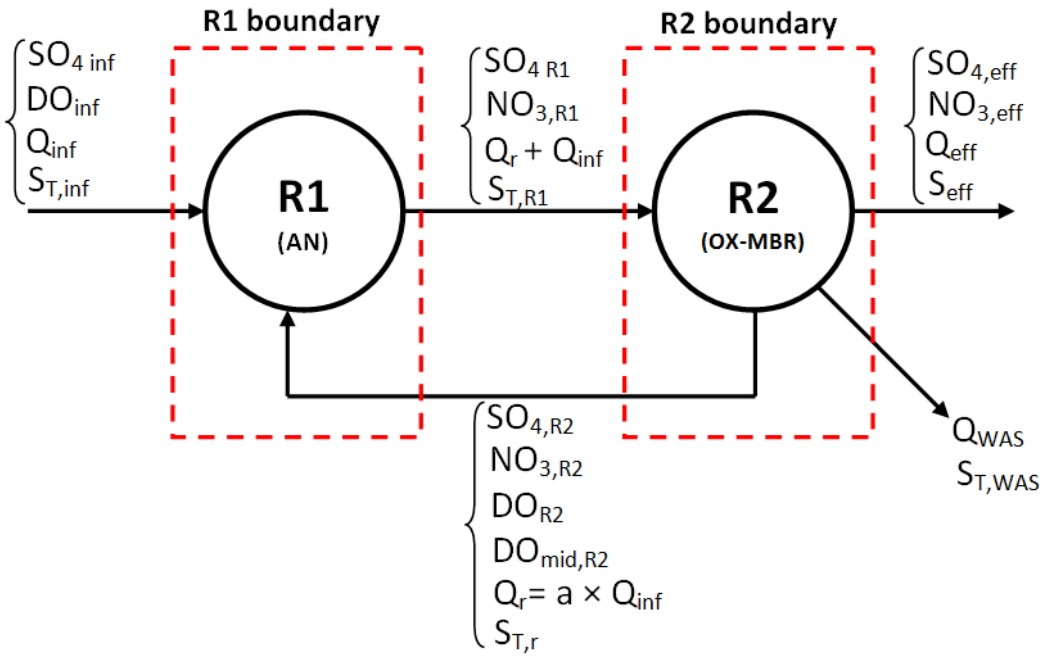

Figure B. 1: Definition sketch for COD mass balance calculation around the separate AN and OX reactors in an AN-OXsystem

- *COD mass balance for reactor R1:*

The daily mass of total input COD ($FCOD_{INPUT}$) and daily mass of total output COD ($FCOD_{OUTPUT}$) are given by Equations (B.3) and (B.4).

$$FCOD_{INPUT,R1} = (Q_{inf} \times S_{T,inf}) + (Q_r \times S_{T,r}) \quad (B.3)$$

$$FCOD_{OUTPUT,R1} = (Q_r + Q_{inf}) \times S_{T,R1} + FCOD_{oxid,R1} \quad (B.4)$$

where,

Q_{inf}: influent flow rate (L/d)

Qr: recycle flow rate (L/d)

$S_{T,inf}$: influent total COD concentration (mg COD/L)

$S_{T,r}$: total COD concentration in the recycle stream (mg COD/L)

$S_{T,R1}$: total COD concentration in the reactor R1 (mg COD/L)

The $FCOD_{oxid,R1}$ can be calculated according to Equation (B.5).

$$FCOD_{oxid,R1} = FO_{OUR_{B,R1}} + FO_{NO3denit,R1} + FO_{SO4reduc,R1} \quad (B.5)$$

A summary of the COD mass balance calculations for reactor R1 considering the data obtained from the run performed on 23-Aug-13 is presented in Table B.18.

Table B. 18: Summary of the COD mass balance calculations for reactor R1

Parameter	Description	Value	Units	Remarks
V_{R1}	Volume of reactor R1	2.5	L	
Q_{inf}	Influent flow rate	11.6	L/d	
Q_r	Recycle flow rate	30.2	L/d	
Q_{eff}	Effluent flow rate	10.4	L/d	
Q_{WAS}	Sludge wastage flow rate	1.0	L/d	
a	Recycle ratio	2.6	L/L	
$S_{T,inf}$	Influent total COD concentration	461	mg COD/L	
$S_{T,r}$	Recycle total COD concentration	1479	mg COD/L	
$S_{T,R1}$	total COD concentration in reactor R1	1277	mg COD/L	
S_{eff}	Effluent COD concentration	5	mg COD/L	
$S_{T,WAS}$	Sludge wastage total COD concentration	1479	mg COD/L	
SO_{4inf}	Influent SO_4 concentration	5.9	mg S/L	
SO_{4R1}	SO_4 concentration in reactor R1	0.7	mg S/L	
SO_{4R2}	SO_4 concentration in reactor R2	5.0	mg S/L	
SO_{4eff}	Effluent SO_4 concentration	5.0	mg S/L	
NO_{3R1}	NO_3 concentration in reactor R1	0.9	mg N/L	
NO_{3R2}	NO_3 concentration in reactor R2	5.3	mg N/L	
NO_{3eff}	Effluent NO_3 concentration	4.7	mg N/L	
DO_{inf}	Influent DO concentration	8.8	mg O_2/L	
DO_{R2}	DO concentration in reactor R2	6.5	mg O_2/L	
$DO_{mid,R2}$	DO_{mid} concentration in reactor R2	3.8	mg O_2/L	
DO_{sat} used	Saturation DO concentration	7.9	mg O_2/L	
$FO_{OURB,R1}$	Mass rate of oxygen consumed by biomass in reactor R1	298	mg COD/d	Eq. (2.30)
$FO_{NO3denit,R1}$	Mass rate of oxygen equivalent of nitrate denitrified in reactor R1	350	mg COD/d	Eq. (2.48)
$FO_{SO4reduc,R1}$	Mass rate of oxygen equivalent of sulfate reduced in reactor R1	380	mg COD/d	Eqs. (2.59)-(2.62)
$FCOD_{INPUT,R1}$	Total input COD mass rate (reactor R1)	50013	mg COD/d	Eq. (B.3)
$FCOD_{oxid,\ R1}$	Mass rate of total COD oxidized in reactor R1	1028	mg COD/d	Eq. (B.5)
$FCOD_{OUTPUT,R1}$	Total output COD mass rate (reactor R1)	54407	mg COD/d	Eq. (B.4)
COD mass balance		108.8	%	Eq. (2.9)

Note: data from the run performed on 23-Aug-13.

- *COD mass balance for reactor R2:*

The daily mass of total input COD ($FCOD_{INPUT}$) and daily mass of total output COD ($FCOD_{OUTPUT}$) are given by Equations (B.6) and (B.7).

$$FCOD_{INPUT,R2} = (Q_r \times Q_{inf}) \times S_{T,R1} \quad \text{(B.6)}$$

$$FCOD_{OUTPUT,R2} = Q_{eff}S_{eff} + Q_{WAS}S_{T,WAS} + Q_rS_{T,r} + FCOD_{oxid,R2} \quad \text{(B.7)}$$

where,

The $FCOD_{oxid,R2}$ can be calculated according to Equation (B.8).

$$FCOD_{oxid,R2} = FO_{OUR_{B,R2}} - FO_{nit,R2} - FO_{sulfide,oxid,R2} \quad \text{(B.8)}$$

A summary of the COD mass balance calculations for reactor R2 considering the data obtained from the run performed on 23-Aug-13 is presented in Table B.19.

Table B. 19: Summary of the COD mass balance calculations for reactor R2

Parameter	Description	Value	Units	Remarks
V_{R2}	Volume of reactor R2	7	L	
$k_La_{use,R2}$	Oxygen transfer coefficient in reactor R2	0.15	h^{-1}	
$OUR_{meas,R2}$	Measured oxygen uptake rate in reactor R2	17.5	mg O_2 $L^{-1}h^{-1}$	
$FO_{OURB,R2}$	Mass rate of oxygen consumed by biomass in reactor R2	2885	mg COD/d	Eq. (2.31)
$FO_{nit,R2}$	Mass rate of oxygen consumed for nitrification in reactor R2	806	mg COD/d	Eq. (2.55)
$FO_{sulfide\ oxid,R2}$	Mass rate of oxygen equivalent of sulphide oxidize in reactor R2	359	mg COD/d	Eq. (2.64)
$FCOD_{INPUT,R2}$	Total input COD mass rate (reactor R2)	53379	mg COD/d	Eq. (B.6)
$FCOD_{oxid,R2}$	Mass rate of total COD oxidized in reactor R1	1720	mg COD/d	Eq. (B.8)
$FCOD_{OUTPUT}$	Total output COD mass rate (reactor R2)	47917	mg COD/d	Eq. (B.7)
COD mass balance		89.8	%	Eq. (2.9)

Note: data from the run performed on 23-Aug-13.

APPENDIX C – LIST OF REACTIONS AND EQUATIONS

Table C. 1: List of reactions and equations

Reaction/equation	No.
$H_2S \leftrightarrow H^+ + HS^-$ pKa1 = 6.97 to 7.06 (at 25°C)	2.1
$HS^- \leftrightarrow H^+ + S^{2-}$ pKa2 = 12.35 to 15.0 (at 25°C)	2.2
$Fe^{2+} + HS^- \rightarrow FeS\downarrow + H^+$	2.3
$J_A = k_L a_A \times (C_{A,liquid} - C_{A,i}) = K_L a_A \times (C_{A,liquid} - C_A^*)$	2.4
$J_A = K_L a_A \times \left(C_{A,liquid} - \frac{p_{A,gas}}{H_A}\right)$	2.5
$K_L a_{H2} = K_L a_{O2} \times (\frac{D_{H2}}{D_{O2}})^{0.5}$	2.6
Fraction of VC stripped $= 1 - [1 + \frac{Q_{air}H}{Q_l} \times \left[1 - \exp\left(-\frac{K_L a_{VC}.h.A}{Q_{air}H}\right)\right]]^{-1}$	2.7
$CH_4 + 2\,O_2 \rightarrow CO_2 + 2\,H_2O$	2.8
COD mass balance (%) $= (FCOD_{OUTPUT}/FCOD_{INPUT}) \times 100$	2.9
$FCOD_{INPUT} = S_{T,inf} \times Q_{inf}$	2.10
$FCOD_{OUTPUT} = FS_{eff} + FX_{eff} + FS_{WAS} + FX_{WAS} + FCOD_{oxid}$	2.11
$FS_{WAS} = S_{WAS} \times Q_{WAS}$	2.12
$FX_{WAS} = X_{WAS} \times Q_{WAS}$	2.13
$FS_{eff} = S_{eff} \times Q_{eff}$	2.14
$FX_{eff} = X_{eff} \times Q_{eff}$	2.15
$FCOD_{oxid} = FO_{OUR_B} - FO_{nit}$	2.16

Table C. 1: List of reactions and equations (continued)

Reaction/equation	**No.**
$FO_{OUR_B} = FO_{OUR_{meas}} + FO_{surface} + FO_{streams\ entering\ R1}$	2.17
$FCOD_{oxid} = FO_{NO3,denit} + FO_{surface} + FO_{streams\ entering\ R1}$	2.18
$FCOD_{oxid,R1} = FO_{NO3,denit} + FO_{stream\ enting\ R1} + FO_{SO4\ reduc}$	2.19
$FCOD_{oxid,R2} = FO_{OUR_{meas}} + FO_{surface} + FO_{streams\ entering\ reactor} - FO_{nit} - FO_{sulfide\ oxid}$	2.20
[Rate of accumulation] = [Rate of input from flow] + [Rate of input through surface] − [Rate of depletion by biomass] − [Rate of output from flow]	2.21
$V_R \times (dDO/dt) = Q \times DO_{inf} + [k_L a_{used} \times (DO_{sat.,used} - DO) \times V_R] - (OUR_B \times V_R) - (Q \times DO)$	2.22
$OUR_B = OUR_{meas} + \frac{Q}{V_R} \times (DO_{inf} - DO) + k_L a_{used} \times (DO_{sat.,used} - DO)$	2.23
$FO_{OUR_B} = 24 \times V_R \times OUR_B$	2.24
$k_L a_{used} = \alpha \times k_L a_{meas}$	2.25
$DO_{sat.used\ at\ T} = \beta \times DO_{sat.clean\ water\ at\ T}$	2.26
$DO_{sat.clean\ water\ at\ T} = DO_{sat.clean\ water\ at\ 20C} \times 51.6/(31.6 + T)$	2.27
OX-OX system: $FO_{OUR_{B,\ R1}} = 24 \times V_{R1} \times [OUR_{meas,R1} + \frac{Q_{inf}}{V_{R1}} \times (DO_{inf} - DO_{mid,R1}) + \frac{Q_{inf} \times a}{V_{R1}} \times (DO_{R2} - DO_{mid,R1}) + k_L a_{used,R1} \times (DO_{sat.,used} - DO_{mid,R1})]$	2.28
AX-OX system: $FO_{OUR_{B,\ R1}} = 24 \times V_{R1} \times [\frac{Q_{inf}}{V_{R1}} \times DO_{inf} + \frac{Q_{inf} \times a}{V_{R1}} \times DO_{R2} + k_L a_{used,R1} \times DO_{sat.,used}]$	2.29
AN-OX system: $FO_{OUR_{B,\ R1}} = 24 \times V_{R1} \times [\frac{Q_{inf}}{V_{R1}} \times DO_{inf} + \frac{Q_{inf} \times a}{V_{R1}} \times DO_{R2}]$	2.30

Table C. 1: List of reactions and equations (continued)

Reaction/equation	**No.**
$FO_{OUR_{B,\ R2}} = 24 \times V_{R2} \times [OUR_{meas,R2} + \frac{Q_{inf} \times (1+a)}{V_{R2}} \times (DO_{R1} - DO_{mid,R2}) + k_L a_{used,R2} \times (DO_{sat.,used} - DO_{mid,R2})]$ For AX-OX and AN-OX systems, $DO_{R1} = 0$	2.31
$FO_{OUR_{B,\ R1R2}}$ = Summation of equations (2.28) and (2.31) OX-OX system	2.32
$FO_{OUR_{B,\ R1R2}}$ = Summation of equations (2.29) and (2.31) AX-OX system	2.33
$FO_{OUR_{B,\ R1R2}}$ = Summation of equations (2.30) and (2.31) AN-OX system	2.34
$NO_3^- \rightarrow NO_2^- \rightarrow NO \rightarrow N_2O \rightarrow N_2$	2.35
$^1/_2\, NO_3^- + H^+ + e^- \rightarrow {}^1/_2\, NO_2^- + {}^1/_2\, H_2O$	2.36
$^1/_4\, O_2 + H^+ + e^- \rightarrow {}^1/_2\, H_2O$	2.37
$NO_2^- + 2\, H^+ + e^- \rightarrow NO + H_2O$	2.38
$^1/_3\, NO_3^- + {}^4/_3\, H^+ + e^- \rightarrow {}^1/_3\, NO + {}^2/_3\, H_2O$	2.39
$2\, NO + 2\, H^+ + 2\, e^- \rightarrow N_2O + H_2O$	2.40
$^1/_4\, NO_3^- + {}^5/_4\, H^+ + e^- \rightarrow {}^1/_8\, N_2O + {}^5/_8\, H_2O$	2.41
$N_2O + 2\, H^+ + 2\, e^- \rightarrow N_2 + H_2O$	2.42
$^1/_5\, NO_3^- + {}^6/_5\, H^+ + e^- \rightarrow {}^1/_{10}\, N_2 + {}^3/_5\, H_2O$	2.43
$FO_{NO3,denit} = 2.86 \times FN_{NO3,denit}$	2.44
$FN_{NO3,input\ R1} = a \times Q_{inf} \times N_{NO3,R2}$	2.45
$FN_{NO3,output\ R1} = (1 + a) \times Q_{inf} \times N_{NO3,R1}$	2.46
$FN_{NO3,denit} = a \times Q_{inf} \times N_{NO3,R2} - (1 + a) \times Q_{inf} \times N_{NO3,R1}$	2.47
$FO_{NO3,denit} = 2.86 \times [a \times Q_{inf} \times N_{NO3,R2} - (1 + a) \times Q_{inf} \times N_{NO3,R1}]$	2.48
$2\, NH_4^+ + 3\, O_2 \xrightarrow{Nitrosomonas} 2\, NO_2^- + 4\, H^+ + 2\, H_2O$	2.49

Table C. 1: List of reactions and equations (continued)

Reaction/equation	**No.**
$2\,NO_2^- + O_2 \xrightarrow{Nitrobacter} 2\,NO_3^-$	2.50
$2\,NH_4^+ + 4\,O_2 \rightarrow 2\,NO_3^- + 4H^+ + 2\,H_2O$	2.51
$FO_{nit} = 4.57 \times FN_{NO3,prod}$	2.52
$FO_{nit} = 4.57 \times (FN_{NO3,prod} + FN_{NO3,denit})$	2.53
$FO_{nit,\,R1} = 4.57 \times [(1+a) \times Q_{inf} \times N_{NO3,R1} - a \times Q_{inf} \times N_{NO3,R2}]$ For AX-OX and AN-OX systems, $FO_{nit} = 0$	2.54
$FO_{nit,\,R2} = 4.57 \times [\,Q_{eff} \times N_{NO3,eff} + Q_{WAS} \times N_{NO3,WAS} + a \times Q_{inf} \times N_{NO3,R2} - (1+a) \times Q_{inf} \times N_{NO3,R1}]$	2.55
OX-OX system: $FO_{nit,\,R1R2} = 4.57 \times [\,Q_{eff} \times N_{NO3,eff} + Q_{WAS} \times N_{NO3,WAS}]$	2.56
AX-OX and AN-OX systems: $FO_{nit,\,R1R2} = 4.57 \times [\,Q_{eff} \times N_{NO3,eff} + Q_{WAS} \times N_{NO3,WAS} + FN_{NO3,denit}]$	2.57
$^1/_8\,SO_4^{2-} + {}^{19}/_{16}\,H^+ + e^- \rightarrow {}^1/_{16}\,H_2S + {}^1/_{16}\,HS^- + {}^1/_2\,H_2O$	2.58
$FO_{SO_4,reduc} = 2 \times FSO_{4\,reduc}$	2.59
$FSO_{4\,input\,R1} = Q_{inf} \times SO_{4\,inf} + a \times Q_{inf} \times SO_{4\,R2}$	2.60
$FSO_{4\,output\,R1} = (1+a) \times Q_{inf} \times SO_{4\,R1}$	2.61
$FSO_{4\,reduc} = (Q_{inf} \times SO_{4\,inf} + a \times Q_{inf} \times SO_{4\,R2}) - (1+a) \times Q_{inf} \times SO_{4\,R1}$	2.62
Sulfide oxidized (mg S/d) = $(1+a) \times Q_{inf} \times (SO_{4\,R2} - SO_{4\,R1})$	2.63
$FO_{sulfide\,oxid} = 2 \times [(1+a) \times Q_{inf} \times (SO_{4\,R2} - SO_{4\,R1})]$	2.64
$FN_{TKN,inf} = N_{TKN,inf} \times Q_{inf}$	2.65
$FN_{TKN,WAS} = N_{TKN,WAS} \times Q_{WAS}$	2.66
$FN_{NO3,WAS} = N_{NO3,WAS} \times Q_{WAS}$	2.67
$FN_{NO2,WAS} = N_{NO2,WAS} \times Q_{WAS}$	2.68
$FN_{TKN,eff} = N_{TKN,eff} \times Q_{eff}$	2.69
$FN_{NO3,eff} = N_{NO3,eff} \times Q_{eff}$	2.70
$FN_{NO2,eff} = N_{NO2,eff} \times Q_{eff}$	2.71

Table C. 1: List of reactions and equations (continued)

Reaction/equation	**No.**
$FN_{TN,OUTPUT} = FN_{TKN,WAS} + FN_{NO3,WAS} + FN_{NO2,WAS} + FN_{TKN,eff} + FN_{NO3,eff} + FN_{NO2,eff} + FN_{NO3,denit}$	2.72
N mass balance (%) $= (FN_{TN,OUTPUT}/FN_{TN,INPUT}) \times 100$	2.73
P mass balance (%) $= \left[\left(FP_{TP,eff} + FP_{TP,WAS}\right)/FP_{TP,inf}\right] \times 100$	2.74
$FP_{TP,eff} = Q_{eff} \times P_{TP,eff}$	2.75
$FP_{TP,WAS} = Q_{WAS} \times P_{TP,WAS}$	2.76
$FP_{TP,inf} = Q_{inf} \times P_{TP,inf}$	2.77
$\frac{dDO}{dt} = k_L a \times (DO_{sat.} - DO)$	4.1
$\ln(DO_{sat.} - DO) = -k_L a \times t + const$	4.2
$\frac{f(\alpha,\beta)}{FCOD_{INPUT}} = \frac{24\, V_{R1}.\alpha.k_L a_{R1}.(\beta.DO_{sat} - DO_{mid,R1}) + 24 V_{R2}.\alpha.\ k_L a_{R2}(\beta.DO_{sat} - DO_{mid,R2})}{FCOD_{INPUT}}$	5.1
$\frac{f(\alpha,\beta)}{FCOD_{INPUT}} = 0.006\alpha \times (8.8\beta - 3.8)$	5.2
Oxygen consumption (% gCOD/gCOD) $= \frac{FCOD_{oxid}}{FS_{T,inf} - FS_{T,eff} - FS_{WAS}} \times 100$	B.1
Y_{OBS}(% gCOD/gCOD) $= \frac{FX_{WAS}}{FS_{T,inf} - FS_{T,eff} - FS_{WAS}} \times 100$	B.2
$FCOD_{INPUT,R1} = (Q_{inf} \times S_{T,inf}) + (Q_r \times S_{T,r})$	B.3
$FCOD_{OUTPUT,R1} = (Q_r + Q_{inf}) \times S_{T,R1} + FCOD_{oxid,R1}$	B.4
$FCOD_{oxid,R1} = FO_{OUR_{B,R1}} + FO_{NO3denit,R1} + FO_{SO4reduc,R1}$	B.5
$FCOD_{INPUT,R2} = (Q_r \times Q_{inf}) \times S_{T,R1}$	B.6
$FCOD_{OUTPUT,R2} = Q_{eff}S_{eff} + Q_{WAS}S_{T,WAS} + Q_r S_{T,r} + FCOD_{oxid,R2}$	B.7
$FCOD_{oxid,R2} = FO_{OUR_{B,R2}} - FO_{nit,R2} - FO_{sulfide\ oxid,R2}$	B.8